Seismic Interpretation and Depth Conversion of the Dinantian carbonates in the Dutch subsurface

Report by SCAN

September 2019

Ministerie van Economische Zaken en Klimaat
ebn
TNO
Interreg North-West Europe DGE-ROLLOUT

Seismic Interpretation and Depth Conversion of the Dinantian carbonates in the Dutch subsurface

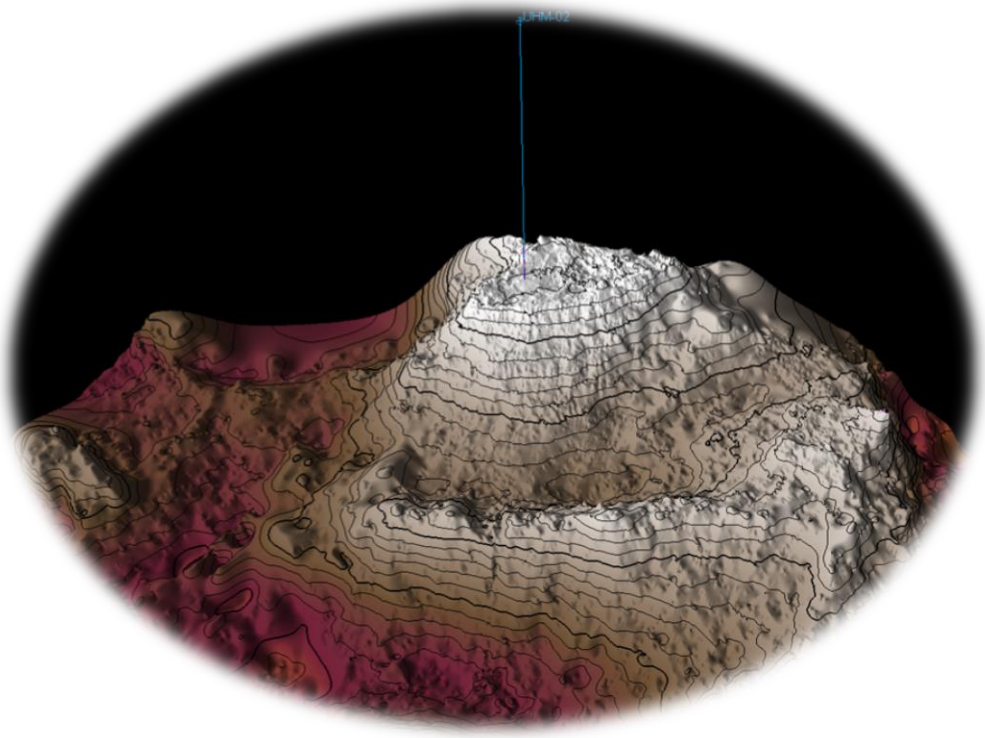

Report written by Johan ten Veen[1], Harald de Haan[1], Geert de Bruin[1], Nico[2] Holleman & Werner Schöler[2]

1. Geomodeling Group, Netherlands Organisation for Applied Scientific Research TNO, Princetonlaan 6, 3584 CB, Utrecht
2. Independent consultants at Energie Beheer Nederland B.V., Daalsesingel 1, 3511 SV Utrecht,

September 2019

Dit rapport is een product van het SCAN-programma en wordt mogelijk gemaakt door het Ministerie van Economische Zaken en Klimaat

Acknowledgements: We thank Bastiaan Jaarsma, Renaud Bourroullec, Kees Geel, Alberto Riva, Peter Gutteridge, Joanna Garland, Mahtab Mozafari, Marten ter Borgh, Henk van Lochem, Douwe Leverink, Susanne Nelskamp, Armelle Kloppenburg and many other colleagues at TNO and EBN for fruitful discussions and support throughout the project.

Table of Contents

List of Figures and Tables

1. Samenvatting

1.1 Doelstellingen

De identificatie van potentiële gebieden voor winning van diepe geothermische energie is vaak gebaseerd op de dieptekaart van de top van Dinantiën carbonaten. Tot nu toe was deze kaart nogal onnauwkeurig vanwege de slechte kwaliteit van onderliggende seismische data op de doorgaans grote diepte waarop deze carbonaten zich bevinden. Desalniettemin is deze dieptekaart vaak gebruikt om verdelingen van diverse afzetttingsmilieus aan te geven en om potentiële gebieden voor diepe geothermische energie af te bakenen. Informatie over de dikte van het carbonaatreservoir, een belangrijke vereiste voor het beoordelen van het geothermische potentieel, bestaat alleen voor het zuiden van Nederland, waar het Dinantiën minder diep begraven ligt. Het doel van deze studie is om de verdeling en dikte van de Dinantien kalkstenen in de Nederlandse ondergrond in kaart te brengen door middel van seismische interpretatie van de beschikbare seismische, gekalibreerd met putgegevens. De bruikbaarheid hierbij van verschillende geavanceerde seismische interpretatietechnieken is onderzocht, in de hoop op verbetering van het seismische beeld, en op extractie van geologische informatie, in het bijzonder breukzones. Dit rapport geeft talloze voorbeelden van de visualisatie van het Dinantien interval en doet aanbevelingen en “best practices” voor het verbeteren daarvan. Daarnaast richt deze studie zich op het analyseren van de snelheidsinformatie voor tijd-diepte-conversie van de seismische interpretatie.

1.2 Conclusies

1.2.1 Seismische interpretatie

- Vanwege de overwegend lage tot matige kwaliteit van de gebruikte seismische data, was de interpretatie van de bovenkant van de Dinantien carbonaten een grote uitdaging; die van de basis zo mogelijk een nog grotere uitdaging. Daarom is de resulterende informatie over de dikteverdeling tot op heden beperkt.
- De nieuwe interpretatie van de bovenkant van de Dinantien carbonaten resulteert in een, over het algemeen, diepere ligging dan de pre-SCAN TNO kaart van dit niveau.
- De studieresultaten tonen een eenvoudige, symmetrische horst en graben topografie met NNW-SSE georiënteerde grensbreuken, op sommige plaatsen gecompenseerd door een conjugaat breuksysteem met een WNW-ESE oriëntatie. De dieptekaart suggereert dat het West-Nederland Bekken, het Breeveertien Bekken en de Roerdalslenk onderdeel zijn van één gecombineerd (Vroeg Carboon) bekken dat twee structureel meer geaccentueerde gebieden in het noorden en zuiden scheidt.
- Een snelle, progressieve en gefaseerde verzakking van de zuidrand van dit grote West-Nederland Bekken kan afgeleid worden van het terug schreiden (“backsteppen”) van de jongere laagpakketen van de Dinantien kalksteen formatie. Dit is goed zichtbaar langs het London-Brabant Massief.
- In het nu diepere deel van het West-Nederland Bekken offshore, rond het Winterton High, zijn lokaal carbonaat mounds aanwezig die geassocieerd zijn met een overheersend laagfrequent en dun seismisch interval dat het Laagpakket van Beveland vertegenwoordigt. Deze interpretatie suggereert dat de Dinantien carbonaten in het grootste deel van het diepe vroege Carboonbekken van West-Nederland voorkomen.
- Het Mid-Nederland Hoog vormt een belangrijke grens tussen een diep marien bekken met een dun Dinantien interval en een gebied met meer uitgesproken paleo-topografie. Naast (bekende) prominente platformstructuren onthult de nieuwe seismische

interpretatie van deze studie enkele, voorheen onbekende, Dinantien kalksteen structuren. Deze structuren komen voor in een strook van Nagele tot Schagen, en op het Maasbommel Hoog en representeren mogelijke “mounds”.

1.2.2 Geavanceerde seismische interpretatietechnieken

- De seismische resolutie van de beschkbare data is laag. Dit komt enerzijds door de hoge seismische snelheden, anderzijds wordt de kwaliteit negatief beïnvloed wordt door het bovenliggende Zechstein-zout.
- Veranderingen in facies zijn niet zichtbaar in seismische data en verschillende kalksteen lithologieën zullen waarschijnlijk als één seismische eenheid verschijnen. *Spectral decomposition* and *waveform segmentation* geven de beste indicatie van de verdeling van facies (m.n. rond carbonaat platforms).
- Behalve de bekende indicaties voor dolines in de zuidelijke offshore zijn er voor midden en noord Nederland geen duidelijke indicaties van karst gevonden in de seismiek.
- Breuken vormen mogelijke zones met hogere porositeit. Voor het Uithuizermeeden platform is de *Thinned Fault likelihood* techniek gebruikt die een heldere beeld geeft van breuken in seismiek. Aan de noordoostelijke rand van het platform bevindt zich een grote NW-SE georiënteerde grensbreuk, terwijl het noorden begrensd wordt door W-E georiënteerde breuken. Waar deze breuken samenkomen, zijn ook een paar N-S georiënteerde breuken aanwezig. In dit gebied met verhoogde breukdichtheid vormt mogelijk een zone met hogere (breuk) porositeit en -permeabiliteit.

1.2.3 Tijd-diepte conversie

- Uit de beperkte dataset van putten die het Namurien doorboord hebben, blijkt dat dit interval vergelijkbare seismische snelheden heeft als het Westfalien. Dit is niet geheel onverwacht, daar de lithologieën van deze intervallen vergelijkbaar zijn. Daarom is het onnodig om de Top Namurien seismische te interpreteren en afzonderlijke snelheidsfuncties te gebruiken voor het Namurien en Westfalien.
- De verdeling van intervalsnelheden over structurele elementen (bepaald met behulp van de *Stratpiler*-benadering van Kombrink et al., 2012) laat zien dat putten in geïnverteerde gebieden vaak hogere intervalsnelheden hebben. Zowel de geïnverteerde en niet-geïnverteerde gebieden vertonen een lineaire snelheidstoename die beschreven wordt met de V_0, *k* methode.
- Lineaire regressie van de intervalsnelheid (V_{int}) tegen de gemiddelde diepte van het Carbooninterval voor alle gebieden tezamen resulteert in een waarde voor *k* van 0,2524 s^{-1} en een V_0 van 3448 ms^{-1}. Voor de geïnverteerde gebieden resulteert dit in een *k*-waarde van 0,3188 s^{-1} en een V_0 van 3213 $ms^{-1.}$
- In een regionale studie kan de eerste functie worden toegepast, terwijl in meer lokale studies in niet- geïnverteerde gebieden de tweede functie geschikter is. Als in een geïnverteerd gebied wordt gewerkt, is meer gebied-specifiek onderzoek nodig om het effect van de inversie op de snelheid te bepalen. Aangezien de mate van inversie lokaal sterk varieert, kunnen nog geen algemene regels en/of correcties worden gegeven.

- Een succesvolle tijd-diepte conversie van de seismische interpretatie van de bovenkant en basis van het Dinantien interval vereist (naast de snelheidsparameters, V_0 en k) dat de bovenkant van het bovenste Carbooninterval (de basis Rotliegend) beschikbaar is zowel in (seismische) tijd (TWT) als in diepte (TVD).
- Door het toepassen van een regionale V_0,k snelheids fuctie zijn de discrepanties ("misties") tussen dieptes van de top Dinantien uit putten en het geproduceerde diepte grid aanzienlijk (max. 272 m). Deze discrepantie wordt opgelost door het grid te corrigeren voor de diepte in de putten ("well-tying").

1.3 Algemene aanbevelingen

Verdere verbetering van de seismische interpretatie van het Dinantien interval is alleen mogelijk na verbetering van de nu beschikbare seismische gegevens (harmonisatie, re-processing, diepte migratie). Het zou ook profiteren van de (te schieten) 2D regionale lijnen. Dit geldt met name voor het centrale deel van Nederland. Voor meer gedetailleerde en technisch inhoudelijk aanbevelingen wordt verwezen naar de individuele hoofdstukken in dit rapport.

2. Executive summary

2.1 Aims and Objectives

Identification of potential areas for deep geothermal energy are often based on the depth map of the Dinantian top carbonate map. So far, this map has been rather inaccurate due to lack of quality of seismic data of this depth on which the depth map is based. This is largely due to the inability of the seismic data to properly display the targeted interval at larger depths. Nevertheless, this depth map has frequently been used to presume facies distributions (platform vs. basinal facies) and to delineate potential areas for deep geothermal energy. Information on the carbonate reservoir thickness, an important requirement for assessing geothermal potential, to date, only exist for the southern part of the Netherlands where the Dinantian is less deeply buried.

The objective of this study is to remap the distribution and thickness of the Dinantian carbonates in the Netherlands through ***Seismic Interpretation*** of the widely available seismic- and well data. The potential of several ***Advanced Seismic interpretation techniques*** has been explored that are focused either on enhancement of the seismic image or extraction of geological information (predominantly fractures) that may hint at reservoir conditions of the Dinantian carbonates. This report gives ample recommendations and best-practices for improving the visualisation of the Dinantian interval and provides numerous examples. Next to seismic mapping of the Dinantian target level, this study focuses on analysing the most appropriate seismic velocity information for ***Time-Depth conversion*** of the interpretation results.

2.2 Conclusions

2.2.1 Seismic interpretation

- In a setting of low to moderate data quality the interpretation of top Dinantian was challenging and that of the base even more challenging. Therefore, the resulting information on the thickness distribution, to date, is limited.
- The new interpretation of the top Dinantian mostly provides a deeper interpretation (both in TVD and TWT) than the pre-SCAN TNO map.
- The results show a simple symmetrical horst and graben topography with NNW-SSE trending margins/boundary faults, in places offset by a conjugate system of WNW-ESE trends. It combines the West Netherlands and Broad Fourteen Basin as well as the Roer Valley graben in one single (Early Carboniferous) graben domain that separated two structurally accentuated areas to the north and south.
- A continuous and at stages rapid subsidence of this enhanced West Netherland Basin can be deducted from the backstepping of Dinantian carbonate formation members as seen on along the London-Brabant High.
- The localized presence of mounds in the now deeper part of the WNB offshore towards the Winterton High is associated with a predominant low-frequency and thin seismic interval representing the Beveland Member in most of the Basin. This would suggest that carbonates occur in most of the deep Early Carboniferous basin of West Netherlands.
- The Central Netherlands High forms an important boundary between the thin basinal Dinantian interval and an area with more pronounced paleo-topography. Next to prominent platform structures, several previously unknown mound-like structures appear from the top Dinantian interpretation. These gentle mounds appear in a strip from Nagele to the Schagen area but are also suggested to occur on the Maasbommel High.

2.2.2 Advanced Seismic Interpretation techniques

- The seismic resolution is low, which is due both to the high seismic velocities and the fact that seismic data is very noisy due to the overlying Zechstein salt.
- Facies changes are not visible on seismic data and different carbonate lithologies will likely appear as one seismic unit. *Spectral decomposition* and *waveform segmentation* give the best facies image (especially around carbonate platforms)
- Apart from the known indications of the presence of dolines in the southern Dutch offshore, no clear indications of karst are found in the central and northern part of the country.
- Fault zones could have higher porosities. For the Uithuizermeeden platform, the *Thinned Fault likelihood* (ran on the Fault Enhancement Filtered seismic) was applied, which gives the sharpest and most continues image of faults. There is a major NW-SE trending bounding fault at the north-eastern edge of the platform, whereas W-E trending faults occur at the northern edge. At the junction of these faults a couple of N-S trending faults are present as well. This could be an area of increased faulting and possibly fracturing, which could be higher porosity/permeability zones.

2.2.3 Time Depth (TD) Conversion

- From the scarce dataset of wells that penetrate the Namurian it is found that the Namurian series shows similar velocity behaviour as the Westphalian series. This is not unexpected since lithologies within these series are quite comparable. Therefore, it seems unnecessary to pick the Top Namurian on seismic data and derive separate velocity functions for these intervals.
- Subdivision of the interval velocity data cloud into structural elements using the *Stratpiler* approach (Kombrink et al. 2012) shows that wells in inverted areas have elevated interval velocities. Both the inverted and non-inverted areas show a linear increase in velocity, which can be described with a $V_{0,}$ k velocity function.
- Linear regression of the interval velocity (V_{int}) against mid-depth of the Carboniferous interval for all areas combined results in a k of 0.2524 s^{-1} and a V_0 of 3448 ms^{-1}, while excluding the data of the inverted areas results in a k of 0.3188 s^{-1} and a V_0 of 3213 ms^{-1}.
- In a regional study the first function can be applied, while in more local studies in non-inverted areas the second function is more suitable. If working in an inverted area, more area specific research is necessary to estimate the effect of the inversion on the velocity. Since the amount of inversion is highly variable in inverted areas no general rules/corrections can be given yet.
- A successful TD conversion of the seismic interpretation results of the top and base of the Dinantian interval require (next to the velocity parameters, V_0 and k) the top of the Upper Carboniferous interval (the base Rotliegend) to be present both in TWT and TVD.
- Mis-ties between well- and grid depths can be considerable (max. 272 m) when applying regional values for the velocity parameters v_0 and k. Well-tying the grids does solve the mis-ties.

2.3 General recommendations

Further improvement of the seismic interpretation of the Dinantian interval is only feasible after seismic data improvement (reprocessing and harmonization) but would also greatly benefit from the (to be) acquired long and deep 2D regional lines. This holds especially for the central part of the Netherland. Please refer to the individual chapters in this report for more detailed and technical recommendations.

3. Introduction

Geothermal energy systems have been considered as a potential alternative for the fossil fuel heating. Currently, there are geothermal projects already functioning in the Netherlands. However, the application of geothermal energy in existing projects is not adequate for the provision of high-temperature heat for, as an example, the process industry. It is anticipated that Ultra Deep Geothermal (UDG) energy could potentially make a substantial contribution to the transition towards a sustainable heat supply. To reach sufficiently high temperatures in the Netherlands, geothermal reservoirs at depths over 4 km are required. The Dutch subsurface at these depths has not been explored extensively until now and is therefore relatively unknown. Based on the limited amount of subsurface data, the Lower Carboniferous Dinantian Carbonates were identified by Boxem et al., 2016 as the most promising target matching the initial requirements for UDG.
The studies reported in this document are a result of SCAN, a government funded, program to scope out the potential of geothermal energy, including the Dinantian Carbonates. This program includes a range of subsurface studies of the Dinantian Carbonates. The results of the SCAN studies will be released and become available via www.nlog.nl.
The objective of this study is to seismically map the distribution of the Dinantian carbonates in the Netherlands, using the readily available seismic- and well data and by incorporating gravity- and magnetic data. Next to seismic mapping of the Dinantian target level, this study focuses on analysing the most appropriate seismic velocity information for Time-Depth conversion of the interpretation results and modelling of gravity- and magnetic data to obtain insights into the depth to basement and composition of subsurface. The latter modelling efforts are useful where the penetration depth of the seismic data is not enough to image the Dinantian target level.

3.1 Background and Rationale

In few parts of the Netherlands the Dinantian rock formations are explored for hydrocarbons. However, as petroleum systems were never proven, the Dinantian was left relatively under-explored. Only limited well control exists and most of the wells are clustered around the margins of the Carboniferous basin (Kombrink, 2008; Van Hulten & Poty, 2008). Additionally, seismic coverage is poor because most seismic data were acquired and processed with a focus on the younger, shallower formations that are known to host significant amounts of hydrocarbon accumulations (Van Hulten & Poty, 2008).
Earlier activities by TNO to map the Dinantian resulted in a nationwide top carbonate map that has many uncertainties due to the inability of the seismic data to properly display the targeted interval at larger depths. Nevertheless, this depth map has frequently been used to presume facies distributions (platform vs. basinal facies) to delineate potential areas for deep geothermal energy. Information on the carbonate reservoir thickness, an important requirement for assessing geothermal potential, to date, only exist for the southern part of the Netherlands where the Dinantian is less deeply buried.
The drilling of the geothermal well CAL-GT-01 near Venlo (Fig. 4) in the Dutch southern onshore in 2012 revealed the presence of Dinantian carbonates with better than expected reservoir properties (Jaarsma et al., 2013). Based on the analysis of drill cuttings these increased reservoir properties probably can be attributed to hydrothermal karstification (Poty, 2014) due to the flow of fluids with temperatures higher than the ambient matrix temperature, so-called hypogene karst processes following Klimchouck (2017). In several wells and in seismic data along the London Brabant Massif, evidence for major karst features (intra- and top platform) was also found (Jaarsma et al., 2013). In Belgium, Dinantian carbonates with good reservoir properties are known from the underground gas storage (UGS) facility near

Loenhout and the Merksplas–Beerse geothermal doublet (Fig. 4). All sites utilize a karstified Dinantian reservoir with porosities up to 20% and 2 Darcy permeabilities (Vandenberghe et al., 2000, Jaarsma et al., 2013). The occurrence of locally improved reservoir properties contrasts the notion of the generally tight character of the Dinantian carbonates in the Dutch subsurface.

Despite these local successes, various important questions need to be answered in more detail:

- Is the entire Dinantian succession (as embodied by the Zeeland Formation) present, or only specific members? This is relevant because the various members are different in lithology, which has an influence on the geothermal potential.
- How are the different facies (platform top / slope / basin) that are known from the cored wells distributed? What is the distribution of the Kulm basin facies? This is relevant as the Kulm is presently considered to have less potential.
- Different parts of the Dinantian platforms may have different burial and diagenetic histories. For instance, the platform top is the first part of the platform that is exposed during a sea level drop, and therefore has the largest potential for the presence of meteoric karst.
- The platform slopes may be dissected by faults, which is important for predicting the presence of fractures and predicting the potential for hydrothermal karst.

3.2 Research approach

This task starts with an inventory, QC and of existing interpretations and maps (in TWT) of top and base Dinantian, (expected) and intra-Dinantian boundaries (e.g. member level, platform-slope-basin boundaries). This information was subsequently used to improve and refine the seismic interpretation of horizons and faults that resulted in an improved perception on the lateral distribution of rocks of Dinantian age. The latter includes both deeper basement faults that may have determined the platform initiation and growth as well as faults that are considered to define the current platform-slope-basin boundaries. The latter faults, which may be younger extensions of the basement faults, may have been active during the platform formation, and may also play a role in post-depositional diagenesis. Therefore, they are important for the prediction and mapping of lateral facies and reservoir quality changes. As faults are often less visible in deeper seismic sections, gravimetry and (aero)magnetics data was used for giving constraints on the deep structure of sedimentary basins and the underlying crust where possible. This will be reported in a separate report. The basin scale interpretation of fault systems was linked to recent insights in the Devono-Carboniferous structural development of the area and be linked to shallower fault systems. A parallel project within the SCAN Dinantien program focused on the burial and structuration of the Dinantian carbonates in the Dutch subsurface, see Bouroullec et al., 2019.

3.3 Deliverables

Next to this report, the seismic interpretation results are delivered as grids (zmap) and maps in both PDF and GIS formats. These maps include two-way travel time (TWT) maps, depth (TVD) maps, and thickness maps of the Dinantian carbonates, difference maps with previous interpretations. The results are also combined with the facies maps from Mozafari et al., (2019)

4. Databases, literature and information available

This chapter describes data(bases), literature, and other types of information available. There is a vast amount of relevant data and information about the Dinantian in de the public domain. All data that is required to perform the seismic interpretations task is collected in the UDG Master project, a data structure that contains all available subsurface data concerning the Dinantian and Namurian i.e. seismic surveys, seismic interpretations, layer models, well data (logs, stratigraphy, etc.).

4.1 2D and 3D Seismic data

The selection of seismic 2D data with focuses on imaging the Dinantian, i.e., shallow seismic surveys were excluded (Figure 1). Potentially this includes all exploration seismic data with penetrations depth down to 4 km or more. An inventory list can be found in the Appendix 9.5. For each survey, the number of lines, depth (ms) and type are given. Next to this onshore 2D seismic data, a selection of near-coastal offshore lines was added to the project as they often allow for a better visualization. The offshore S, O and P blocks have been included as well, because the high-quality seismic data, in combination with good well data, allows for detailed interpretations of the Dinantian. All offshore data has been included in the folder "offshore".

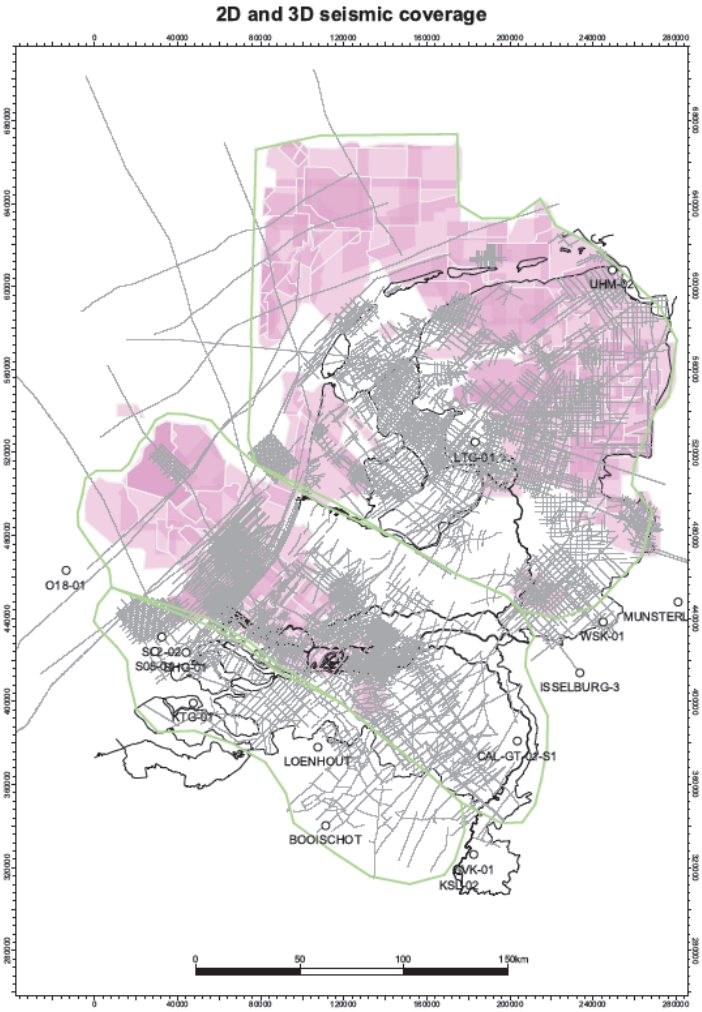

Figure 1: Overview of all the available and consulted 2D (grey lines) and 3D (pink polygons) seismic data. The three outlines indicate the areas of different data quality as discussed in the text.

Public 3D seismic cubes can be found and requested via NLOG.nl. For the seismic interpretation that took place at the EBN premises, the CGG Meg Merge cube was used (see section 4.3)

4.2 Belgian data

In this folder Belgian seismic and well data can be found. There are two 2D seismic surveys available, several composite well logs, one .Las file of Merkplas-01 and one file with well-tops of MER-01. This data is publicly available through the Geological Survey of Belgium (GSB) and needs to be referenced when used. This data is also available in Petrel. Other Belgian data can be found on: https://www.dov.vlaanderen.be.

4.3 Non-public data

The 3D dataset used for the largest part of the study area is the MegaMerge cube. This cube is a merge of all publicly available 3D surveys and is a product commercially available with CGG. An exact fit of existing interpretations based on individual surveys and those made from the MegaMerge survey lay-out is not always possible, since the latter survey only uses exact N-S and E-W in-lines and cross-lines, respectively. Individual survey lay-out were rotated to achieve this.
The Advanced Seismic Interpretation was applied on a recently re-processed and depth imaged seismic dataset from the Groningen area, see Chapter 4.2 for details.

4.4 Assessment of Seismic Data Quality

The quality of the seismic data can be described in terms of four properties a) data coverage, b) penetration depth, c) seismic reflection quality and d) seismic resolution. Whereas the first term affects the precision of constructed/modelled/interpolated surfaces in between data covered areas, the other terms affect the accuracy at the seismic data locality (to what extent are individual objects detectable and how good is the interpretation). The available seismic data have a reasonable amplitude scaling and phase consistency between surveys, although some conversion toward zero-phase, SEG-polarity had to be performed. Nevertheless, individual 2D seismic lines may show mis-ties that are either inherent to 2D seismic surveys or exist because of differences in acquisition and processing parameters between 2D surveys.

4.4.1 Data coverage

2D seismic coverage is sparse, i.e. not designed for cross-line verification. Furthermore, key wells often have no seismic line attached. For example, well WSK-1 is positioned 800 m from the nearest line, the highly deviated well CAL-1 has a significant angle with the seismic tie lines in the area, well KTG-1 does not have any seismic lines nearby and well S05-01 is positioned just next a seismic line.
Another issue is that there are large areas without well calibration and that wells often do not have an adequate log suite for well calibration. In many cases density logs, checkshots or VSP's are missing or have bad quality. Also calliper logs needed for QC of synthetic seismograms are often not available. Hardly any well has good quality shear sonic logs. This hampers the calibration of the AVO response, which can be crucial in separating the impedance responses of limestone, dolomite and volcanic/intrusive rocks and would be a necessity for (future) calibration of seismic inversion.

4.4.2 Penetration depth

Almost all available 2D seismic data has been cropped at 4 seconds TWT, whereas most 3D has been cropped at 5 seconds TWT. Note that (almost all) seismic data were acquired for

hydrocarbon exploration and the cropping was done with the depths of the targeted reservoirs in mind. Penetration depths, in general, are not enough to capture an image of the base and top reflections of the Dinantian interval. For instance, in the West Netherlands Basin the top Dinantian is for a large part deeper than 5 seconds TWT. In these cases, it might be worthwhile to get hold of the original, i.e. pre-stack seismic data, to explore for larger trace depths.

4.4.3 Seismic reflection quality

At larger depths multiples and interbed multiples are frequently observed, illustrating that trace stacking focused on shallower intervals (i.e. the traditional target reservoirs for oil and gas exploration and production). Sometimes it is difficult to separate primary reflections from multiples. See section 0 for examples.

4.4.4 Seismic resolution

When using advanced techniques for the seismic interpretation of geological intervals (tops and bottoms) or for the detection of specific geological features (channels, slumps, faults, karst, facies, etc) it is paramount to understand the scale of features the interpreter is after and whether the seismic resolution is sufficient to record these.
The resolution of 3D seismic data can be expressed in a horizontal (or lateral) resolution and two vertical resolutions. The vertical resolutions result from the interaction of the top and bottom reflection of a geological layer (Brown, 2011). When a geological layer is thick the top and base reflector are separated and do not interfere. The limit of separability is the thickness at which both top and base reflectors of a geologic layer are at the closest separation, though still discernible.

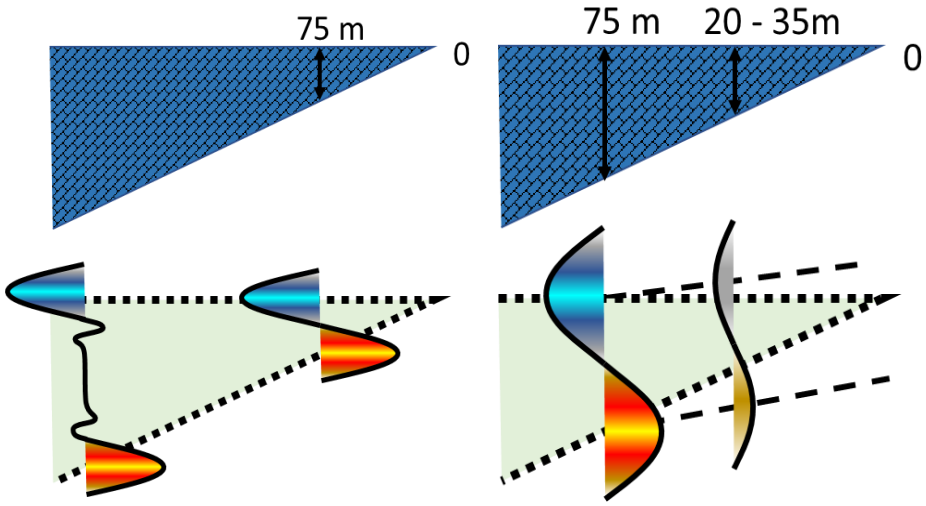

Figure 2: Left: The limit of separability is the limit at which the top and base reflectors of a geologic layer are at the closest separation. Right: If a geological layer becomes thinner than $\frac{\lambda}{4}$ (75m) the top and base reflectors are interfering, and tuning occurs.

The limit of separability is defined as ¼ of the wavelength that corresponds to the dominant frequency and seismic velocities of an interval considered and is calculates as follows:

$\lambda = \frac{v}{F}$ (eq. 1) and the limit of separability: $\frac{\lambda}{4}$ (eq. 2)

Where: λ = wavelength, v = Velocity (m/s) and F = Dominant Frequency (Hz)

The limit of separability at the Dinantian level is about 75 meters (see Figure 2), since the (dominant) frequency (F) is about 20 Hz and the seismic velocities of the Dinantian is about 6000 m/s.

If a geological layer becomes thinner than $\frac{\lambda}{4}$ the top and base reflectors are interfering, and tuning occurs (Figure 2). The reflectors are still visible, but the reflector strength progressively attenuate as the geological layer becomes thinner. Also, the seismic thickness, i.e., the distance between top and base is not representative of the true thickness. The limit of visibility is the point at which the seismic reflectors is obscured by background noise. The limit of visibility is therefore greatly dependent on the data quality (signal to noise ratio) and is given below for several cases:

Poor S/N	$\frac{\lambda}{8}$
Moderate S/N	$\frac{\lambda}{12}$
High S/N	$\frac{\lambda}{20}$
Outstanding S/N	$\frac{\lambda}{30}$

The limit of visibility is in the order of 25 to 38m (λ/8 to λ/12) and the lateral resolution is about 150 m (λ/2). The horizontal resolution or lateral resolution is the limit at which two points can be recognized as two separate points. The post-migration horizontal resolution is $\frac{\lambda}{4}$ for perfectly migrated seismic data, but in practice it is in the order of $\frac{\lambda}{2}$ (Brown, 2011), which is ~150 m for the Dinantian level. These resolutions issues put important limits to the ability to map thin beds and make inferences on the thickness.
Based on the first three properties, the Netherlands can be divided in three parts: 1) a strip along the London Brabant Massif (LBM) towards the southern boundary of the RVG. Here, 3D seismic data is absent and 2D data coverage onshore is low. Only part of the 2D seismic lines has enough penetration and reflection quality is generally poor. For reference, the offshore area is included because here 2D data density is much higher. 2) a central part from the RVG to and including the Mid Netherlands High (MNH, see Figure 1). Here, both 2D and 3D data have too low penetration depths. Only few regional deep lines with moderate reflection quality are able to image the Dinantian below 5 seconds TWT. Due to limited coverage at depths >3-4 km, the 3D seismic data from the WNB is hardly useable, because the Dinantian interval is here located at greater depths. Reflector quality at the Dinantian and deeper levels, generally improves further to the south, along the LBM, where these units are less deeply buried. 3) Apart from the IJsselmeer and Wadden Sea areas, the northern domain that has almost full 3D coverage and penetration depths and reflector qualities of the surveys allow for a readily reflector interpretation down to the base of the Devonian. At depths > ~4 km, the data suffers from various migration- and other processing artefacts that relate back to the individual seismic surveys
The data coverage and quality are shown in Figure 1 which give a general, qualitative indications of the ability to pick the top Dinantian and deeper horizons. Conditioning of the seismic data, in some cases, results in data improvement (see next section).

5. Methodologies and workflows applied in the project

5.1 The Seismic interpretation workflow

5.1.1 Interpretation Strategy

The seismic interpretation strategy largely corresponds to that standardly used in the hydrocarbon E&P industry. However, the regional aspect, the large amount of data and huge variation in data quality, sometimes calls for a more pragmatic approach towards data conditioning, the use of seismic attributes and tying and correlating data.
Seismic conditioning was focused at removal of noise and enhancement of the often-weak seismic responses at depth. The seismic attributes *Dominant Frequency* and *Sweetness* were used to help detection of carbonates as these have a tendency for stronger absorption of higher frequencies than the surrounding clastics. For key wells with suitable well logs a seismic-to-well tie study was performed that gives information on how and if lithological boundaries show up as reflectors in seismic data.
The seismic interpretation was further supported by previous interpretations of the Dinantian interval, for instance made by TNO (available at www.nlog.nl), Reijmer et al., 2017, Hoornveld, 2013 and Panterra, 2012. Long regional seismic lines were used to tie the data dense areas in the south and north. Also composite seismic lines were constructed if regional lines were not available. One such line is situated along the coast, connecting (offshore) Zeeland across the WNB to the Schagen and Sloten 3D area in the northern part of North Holland. A central line coincides with the 1984 NAM deep line that runs from western Brabant to Groningen. The third line, in the east, connects the Californië geothermal development with Winterswijk and the Central Netherlands High.
Next to regional lines, the solution of the Depth to Magnetic Source (see separate reporting) is often used as guidance for interpretation. Locally, this solution represents the top of clastic formations of Devonian age (magnetic conglomerates) and can thus guide the interpretation of the corresponding base Dinantian carbonates. Even though the depths do not closely correspond, the DTMS solution gives a glimpse of the structuration, i.e. the presence of structural highs and lows.

5.1.2 Data conditioning

Petrel incorporates data conditioning tools and filters in the ‘Volume Attribute’ domain. Data conditioning is discussed first here. Frequency analysis of the interpretation target level using the ’inspector’ tool of Petrel indicates a predominance of higher frequencies that ‘rained down’ from the better resolved near surface. Noise -and multiples- are a common problem in seismic data. Data conditioning is geared to improve detection and auto-tracking by a combination of removing high redundant frequencies and enhancement of signal continuity. Above 40Hz (sometimes even 25Hz) no signal was encountered at target levels. Therefore, filter parameters need to be adjusted according to target levels. Petrel’s Graphic Equalizer attribute was used to detect useful frequency sub-bands. A subtle lift of the lower frequencies can sometimes be beneficial; however, the 10 and 20 Hz bands should be left untouched (or perhaps supplied with a little ‘lift’). It often pays to reduce the 30 and or 40 Hz band somewhat for a balanced filtered result. Over the Brabant High the Dinantian target can be shallow and higher primary frequencies do occur in the 2D seismic. In the Rijnmond area, the Dinantian drops to below 4 seconds TWT, and 25 Hz could be the maximum primary frequency.
Petrel’s *’Structural Smoothing’* gives also a powerful and quick improvement of Dinantian seismic reflectivity (see Figure 3) and was used prior auto-tracking. Because of its relatively

inaccurate algorithm, i.e., Gaussian trace smoothing, it also tends to reduce mid and high frequencies, and hence can sometimes make frequency filtering redundant.

5.1.3 Seismic-to-well tie

To understand the reflective character of the Dinantian carbonates, both in platform and basinal settings, well ties have been created for wells WSK-01, CAL-GT-01-S01 S2-02 (shown in Figure 4), P18-01, BHG-01, LTG-01. It should be noted that interpreter-oriented well ties are performed that are focused on seismic loop level calibration ("tying reflectors to lithological transitions"). These can differ somewhat from well ties focused on generation of calibrated time depth tables to serve time-to- depth conversion. The interpreter-oriented well ties often use filtered (conditioned) seismic data in the comparison with synthetics from a lower frequent wavelet and rely on some 'stretching and squeezing' of the synthetic for optimal loop correlation.

From the well tie analysis, it follows that the strongest acoustic impedance response in the seismic is that of basalt intrusions, followed by that of platform carbonates. Top and Base carbonates are generally seen as strong to medium-strength reflections of low frequency content.

The ~150 m of basinal carbonates encountered in WSK-01 have many shale intervals and are capped by a fining upward sequence that does not show any acoustic impedance contrast. Here, the most dominant reflectors correspond to the top and base of the overlying basalts in the overlying Namurian succession. Dinantian carbonates in WSK-1 are not visible in the seismic data. Interestingly, the California well (CAL-GT-01-S1) tie shows a similar fining upward pattern, but show one or two hard interbeds that, unlike in well WSK-01, do generate a good acoustic impedance contrast.

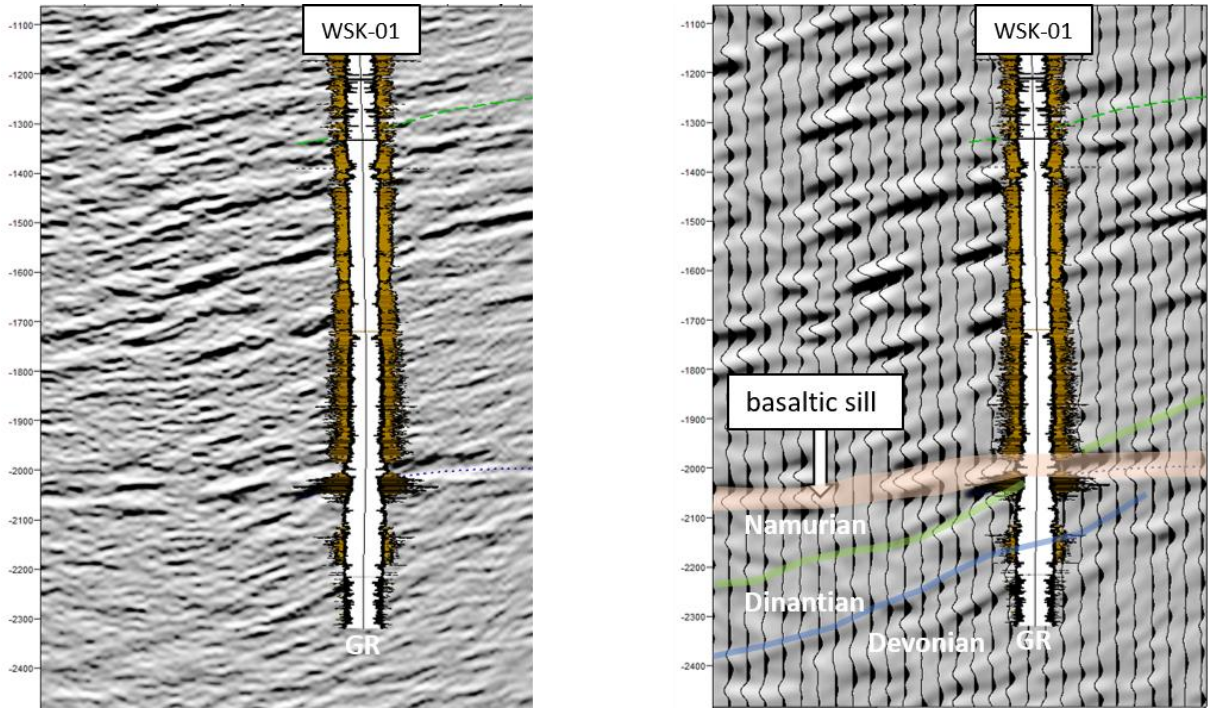

Figure 3: Seismic-to-well tie of well WSK-01 showing the colour-filled Gamma-Ray (GR) log. Left: unfiltered; Right: Dip-guided filtering and lift of lower frequencies reveals the sub-horizontal basaltic intrusion (sill?) cutting through dipping reflectors representing the Carboniferous strata.

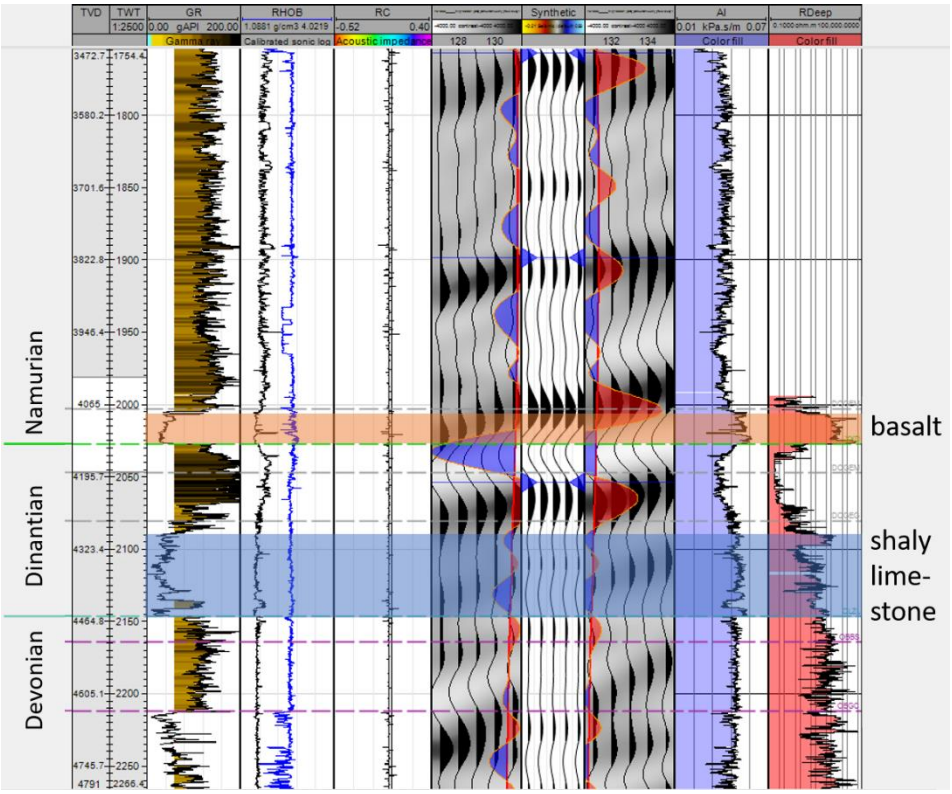

Figure 4: Seismic well tie of well WSK-01. Logs shown: Gamma-ray, Density, Sonic, Reflection Coefficient (RC), Synthetic reflection and amplitudes (red/blue wiggles) vs. original seismic reflection (black/white wiggles). Here it shows the strong acoustic response of basalt (pink band) and the weak acoustic response of basinal, shaly limestones (blue band)

The base of the Beveland Member –with dolomitization prevalent in most wells: is represented as a seismic doublet of a uniform thickness of >100, as can be seen in wells O18-01 and S-02-02. The middle Schouwen Member represents the carbonate level where most of the (Walsortian) mounds are found on regional seismic lines connecting the well ties. These mounds create mild relief of up to 100-250 ms as can be seen in seismic data around wells LTG-01, S02-02, and BHG-01. In seismic data, the uppermost Goeree Member is seen as a reflective drape on top of the mound-prone Schouwen Member, filling in topography and exhibiting a backstepping reflection pattern onto the Brabant.

The zero-phase synthetic appears to not always do full justice to the real seismic response in amplitude and phase detail. This might be due to lack of AvO reflection components that can be considerable given the strong contrasts in shear moduli of carbonates and clastics. Unfortunately, none of the wells had shear logs to create an AvO synthetic.

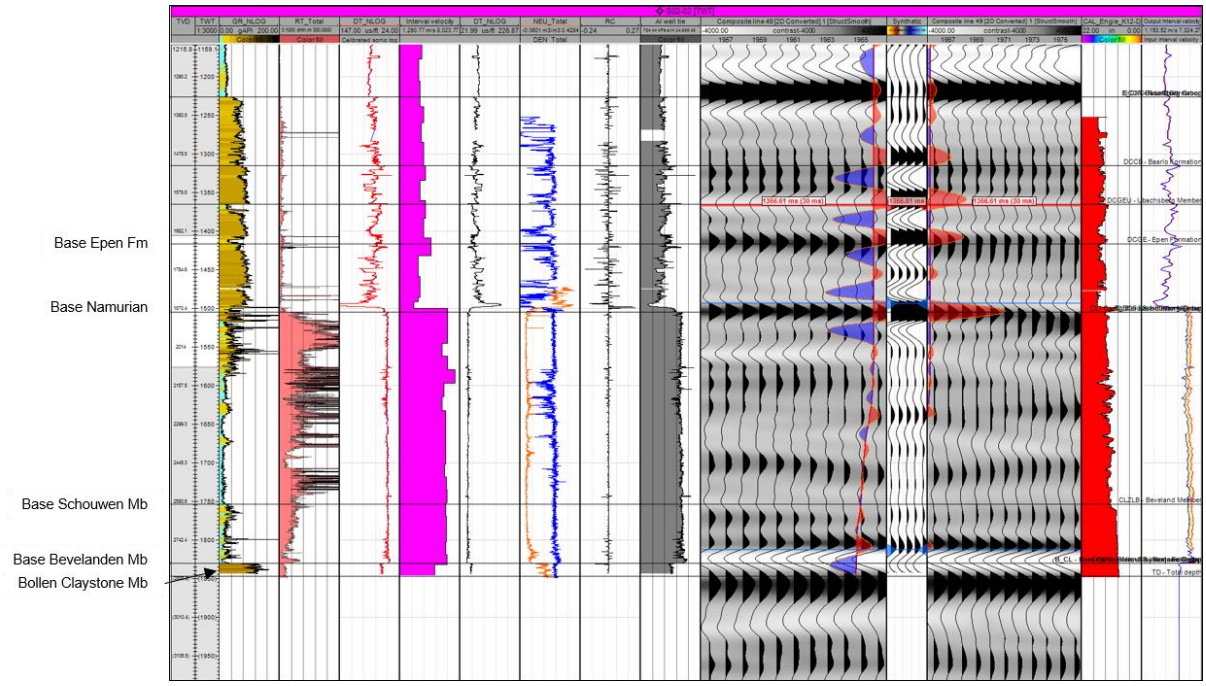

Figure 5: Seismic-to-well tie of well S02-02. Here the base of the Dinantian interval is represented by a seismic doublet explained by the transition from the dolomitized Beveland Member to fine-grained clastics of the Devonian Bollen Claystone Formation. Well tops (bases) are displayed at the left side of the panel.

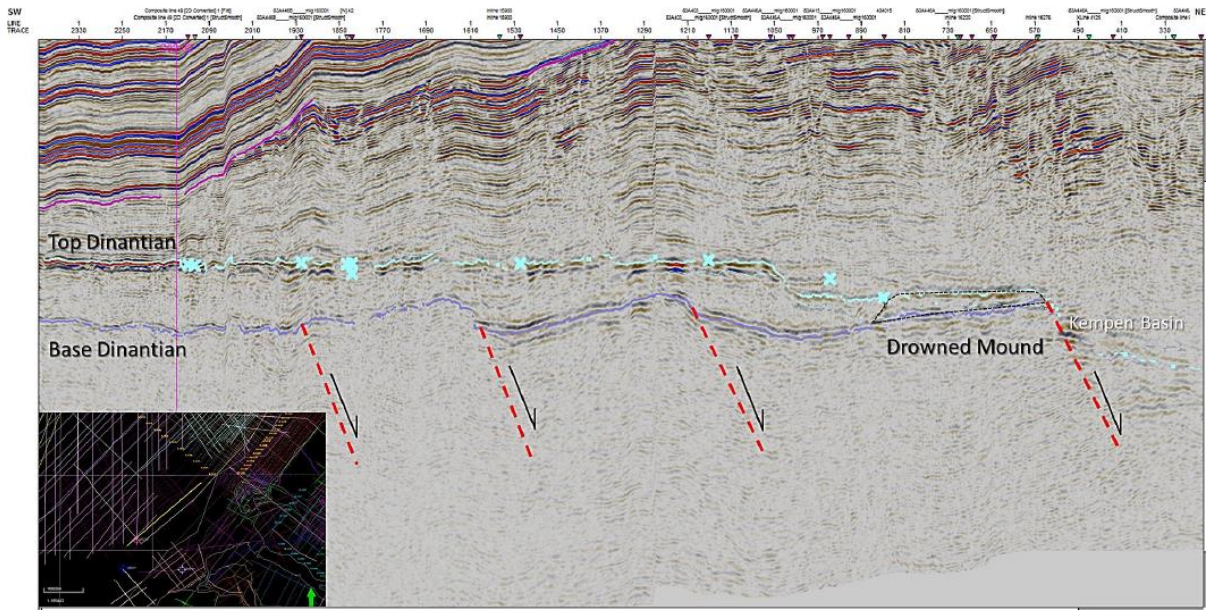

Figure 6: Interpreted line 83a446, crossing well S02-02 flattened on top Dinantian sea level, showing the clear tectonic control on the development of the Brabant carbonate platform. The same features have been interpreted by Reijmer et al. (2017) as the shelf step back sequences due to sea-level rise.

5.1.4 Interpretation of regional lines

From the seismic dataset a couple of regional lines have been constructed and interpreted that form the basis for further horizon interpretations.

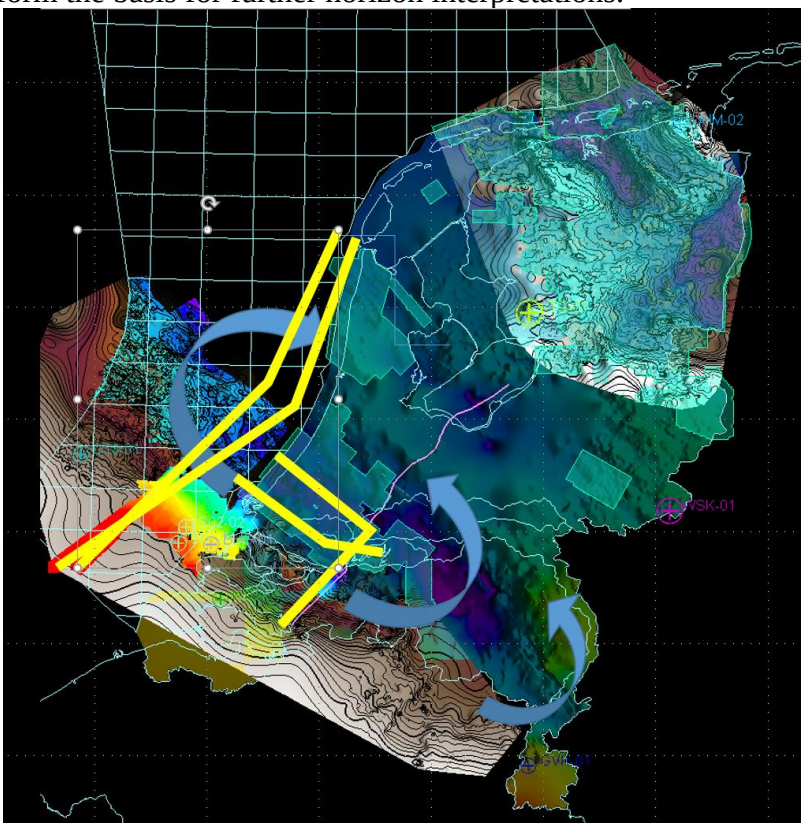

Figure 7: Locations of regional 2D lines

Coastal 2D line 1024002_MPNI-9101 2d line (RGD deep Z2 1991A)

This line (Figure 8) has 8 seconds TWT reach and has potential to cover the Dinantian interval. Quality below 4 s is low. Applying the dominant frequency attribute reveals the presence of several seismic reflectors. Especially the Dinantian carbonates stand out because of the low frequency content. The Dinantian interval is especially clear in the southern part of the section, whereas below the WNB and further north no reflection is inferred.

Central Netherlands SW-NE NAM84

The NAM84 central Netherlands also reaches 8 s TWT and ties the Brabant High near well RSB-1, to LTG-1. This line allows a reasonably good interpretation by applying a low pass filtering at ~ 30 Hz and a dip-guided structural smoothing- and overlaying with the Dominant Frequency attribute. In the southern part of the section, the very low-frequency reflection character of the Dinantian on top of the Brabant platform can be readily identified.
The regional NAM84 continues northward from Flevoland into the southern Groningen area through line 821005R, a version with 10 seconds TWT cover and full overlap with the NAM84 line.
The LTG-1 well shows a Dinantian carbonate mound of similar thickness and extent as do the BHG-1 and S02-02 wells near its southern end. The RSB-1 well penetrates an almost full Namurian sequence and TD'd just above the Dinantian.

Petrel composite lines

Several composite semi-regional lines were created that contain the better quality 2D and 3D seismic elements and are of value in creating an overview of stratigraphic and structural developments that the individual short 2D sections lack. For example, the composite of Figure 10 strikes SW-NE through well SO2-02 and is calibrated with synthetic seismic. Note the different stratigraphic character on either side of the hinge line in the centre picture. Going basinward, the upper Dinantian carbonate Goeree and Schouwen Members wedge out in a down-lapping fashion. In contrast, the lowermost Dinantian Beveland Member doublet continuous into the centre of the West Netherlands Basin, and forms the basis of the deep Dinantian carbonate interpretation.

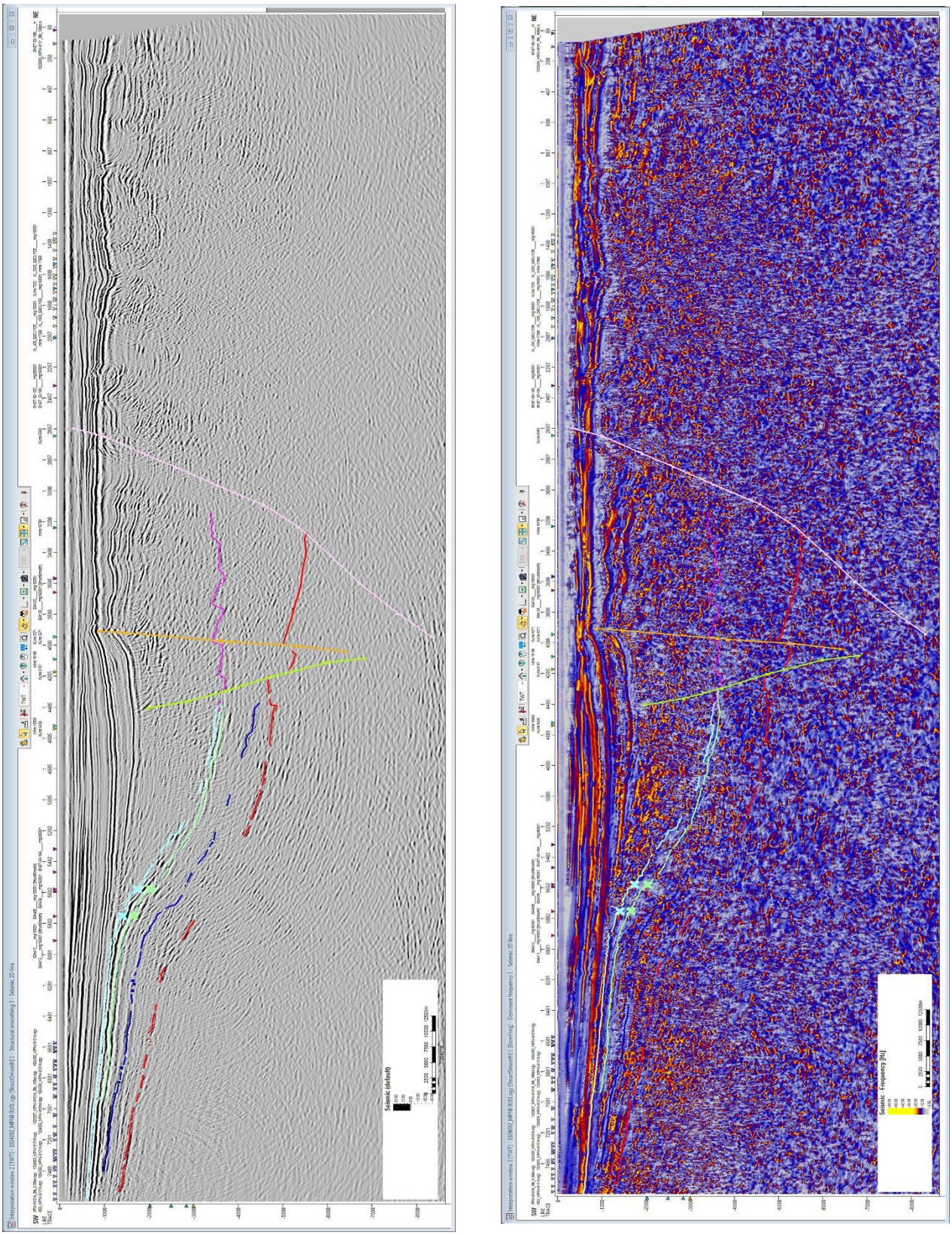

Figure 8: Coastal 2D line Z2 1991A, represented as B/W amplitudes (upper) and dominant frequency (below). See Figure 7 for location

.

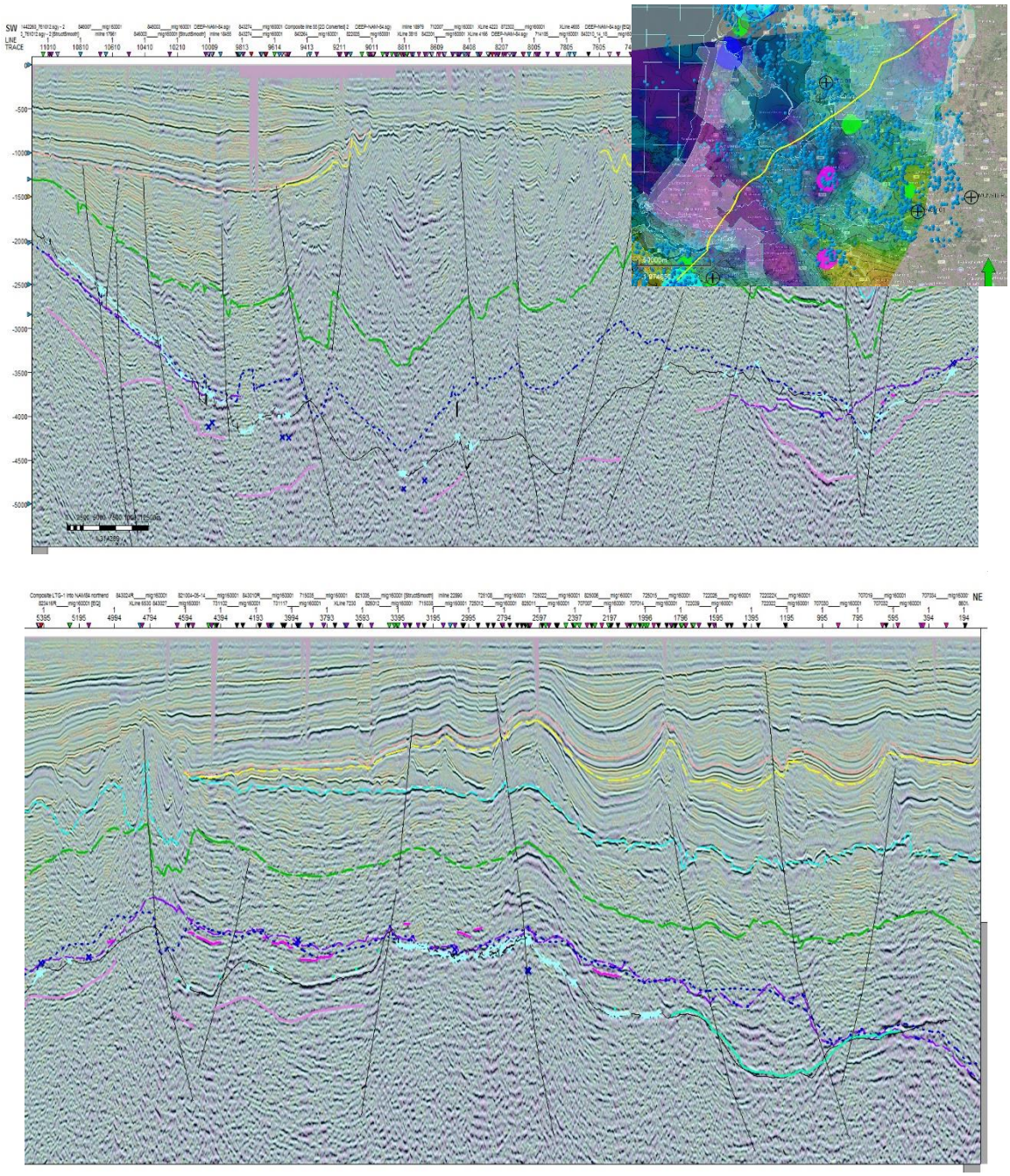

Figure 9: Southern (above) and northern (below) parts of the regional 2D tie line NAM1984A- 821005R (see inset for locality), represented as B/W amplitudes with dominant frequency overlay. The newly interpreted top Dinantian horizon in light blue and exisiting TNO-2014 interpretation is in dark blue, showing the shallower solution of the latter in large parts of the profile.

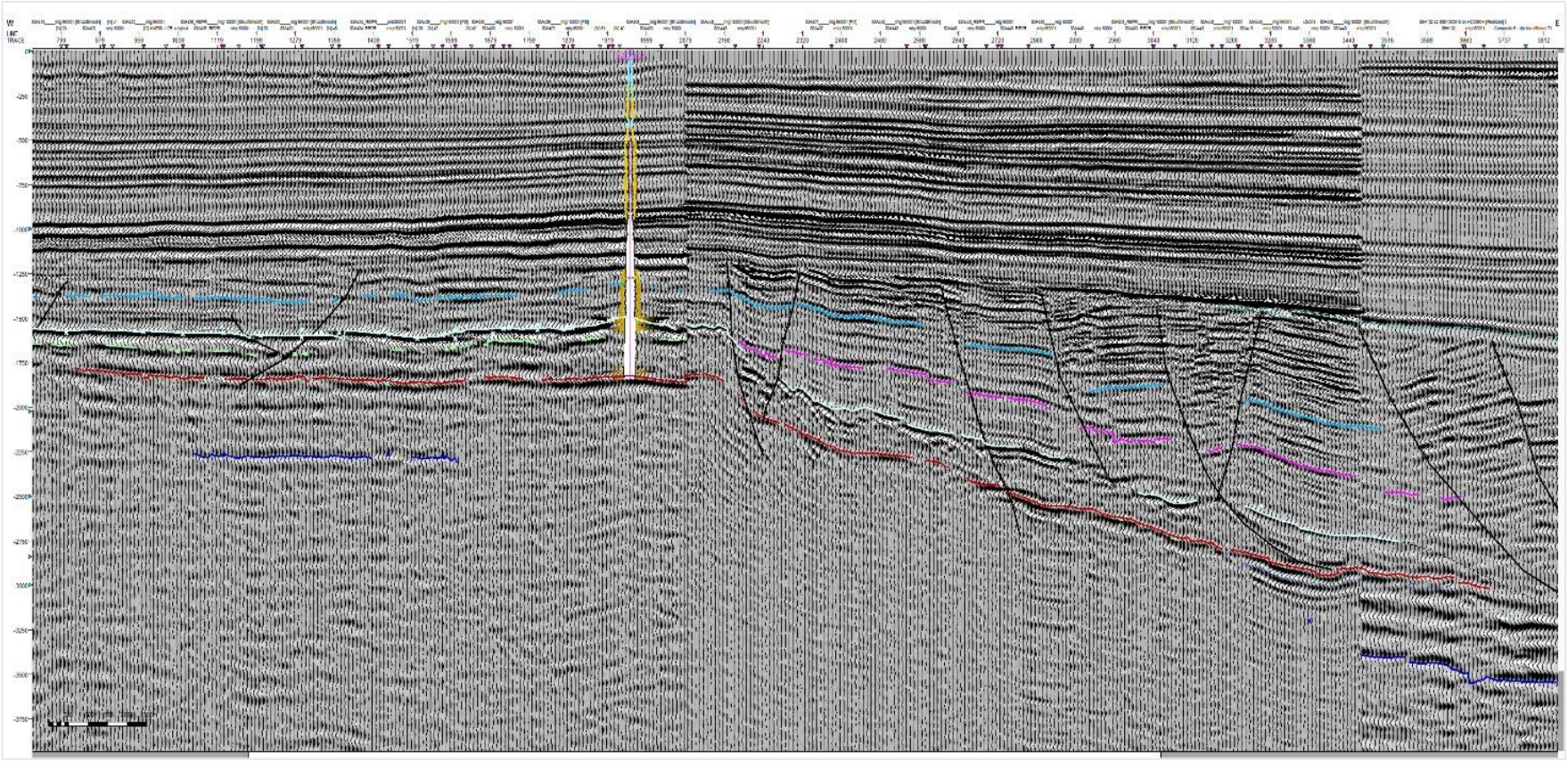

Figure 10: Figure: composite W-E seismic line in the coastal waters of the Goeree island, calibrated by well S02-02.Base Dinantian = orange, top Dinantian, light pale green, intra Namurian = cyan, base Westphalian = blue)

5.2 Advanced SI

The ‘Volume Attribute’ domain of Petrel contains the more conventional seismic attributes. With low quality 2D and 3D data, attributes must be treated with caution, or are even outright useless, giving credit to the adagio of ‘rubbish in, rubbish out’. A few attributes such as Dominant Frequency and Sweetness are more robust and could add a hint of enhanced continuity -in reflections, faults, and stratigraphic units- to the input seismic. In good quality 3D seismic data, coherency/semblance attributes are useful for structural grain analysis. Finding high porosity zones is paramount for geothermal exploration. Here, it is investigated if seismic attributes and advanced seismic interpretation techniques can delineate facies with higher porosity or predict the presence of karst and faults.

5.2.1 Data selection and quality

Four seismic volumes of the Groningen area were made available by NAM for the purpose of advanced seismic interpretation techniques. These include recently reprocessed data in two sets that have both a time and depth version:

- R3136_15UnPrDMkD_Full_D_Rzn_RMO_shp_vG_16bit
- R3136_15UnPrDMkD_Full_T_Rzn_RMO_shp_vG_16bit
- R3136_RTM_vG_depth_16bit:
- R3136_RTM_vG_16bit

The first two surveys did not show reflections for deep strata and only show the top part of the Uithuizermeeden platform (Figure 11). The latter two run deeper and are therefore better suited for this study (Figure 12). The depth survey has a large mis-tie at the well location, which indicate that the velocity model used for the depth conversion was not good enough. Therefore, the R3136_RTM_vG_16bit (time) survey was selected for testing the advanced interpretation techniques. This also enables the use of mapped TWT horizons from the other work packages. Nevertheless, the data contains several phenomena that hamper the quality. First, the data is whitened at a shallower interval, secondly the data has vertical noise zones and lastly, the data contains multiples.

Spectral whitening

The amplitude spectrum shows a flat spectrum between 8 and 48 Hz (Figure 13). A normal amplitude spectrum has an asymmetric bell shape, and therefore it is safe to assume that the data at hand is whitened. This means that the amplitudes of the higher frequencies are boosted. This is fine when the original seismic response is larger than the background noise. However, at the target depth, it is highly unlikely that such high frequencies are present (i.e. that these high frequencies are signal) and that boosting these frequencies results in boosting noise. The amplitude spectrum for the deepest section (below 2500 ms) shows a dominant frequency of roughly 14 Hz (Figure 14). Above 26 Hz, the spectrum becomes flat, and appears boosted.

Vertical noise

Vertical noise streaks are present in the data. The ‘Simple Chimney’ attribute was applied to detect these vertical noise zones (

Figure 15). This attribute observes a 200 ms window to detect zones that have a consistently low similarity (lateral discontinuity attribute). By comparing a time-slice through this ‘simple chimney attribute (Figure 16) with the top of the Zechstein (Figure 17) it becomes clear that the noise zones are positioned directly below the steep parts of the Zechstein zones that represent structured salt. Here, the salt and overlying strata are (too) steeply dipping such that

the energy of the seismic waves is likely deflected sideways or dispersed, causing a vertical noise zone below.

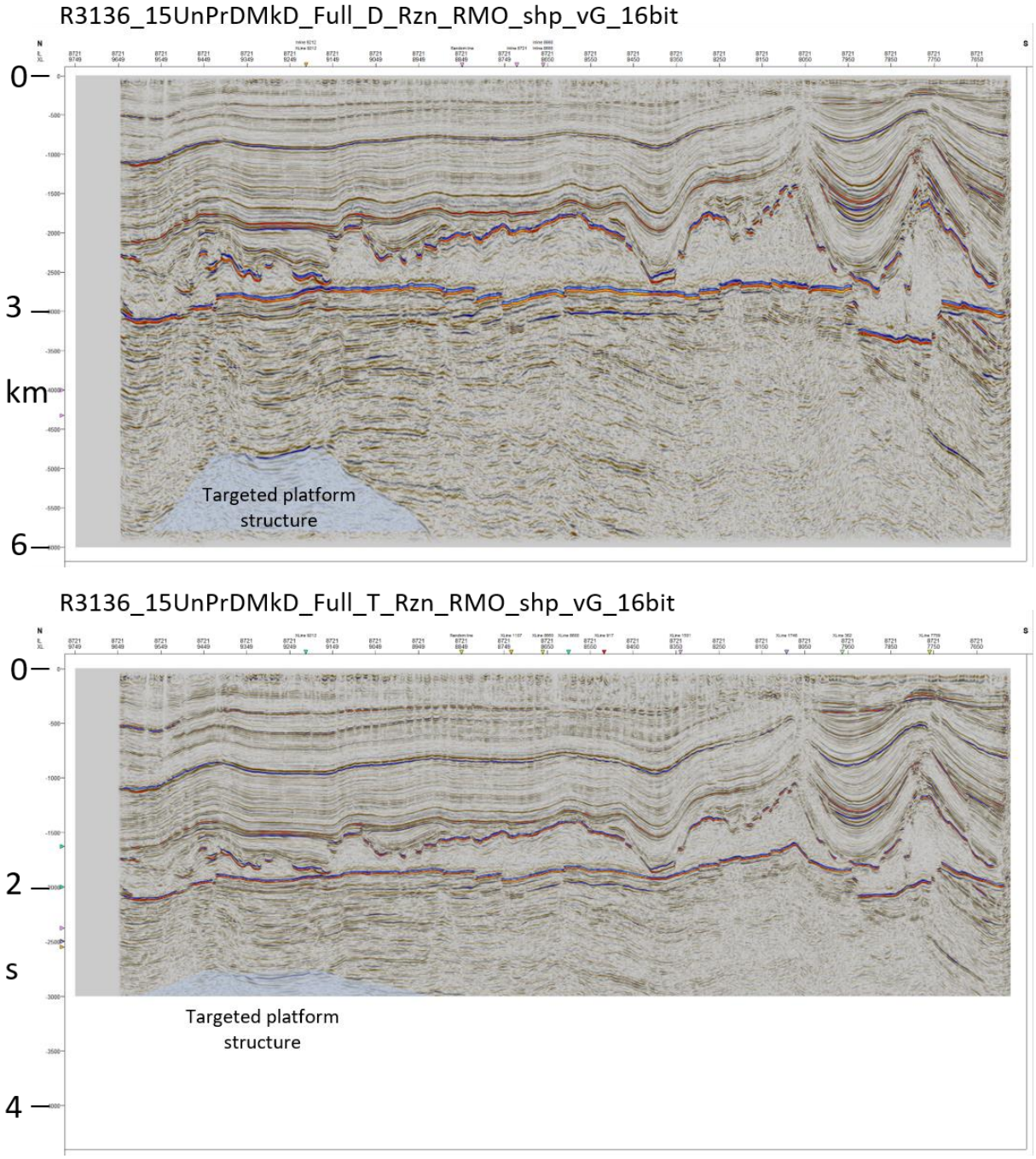

Figure 11: Available seismic data: this set (time and depth surveys) was not used.

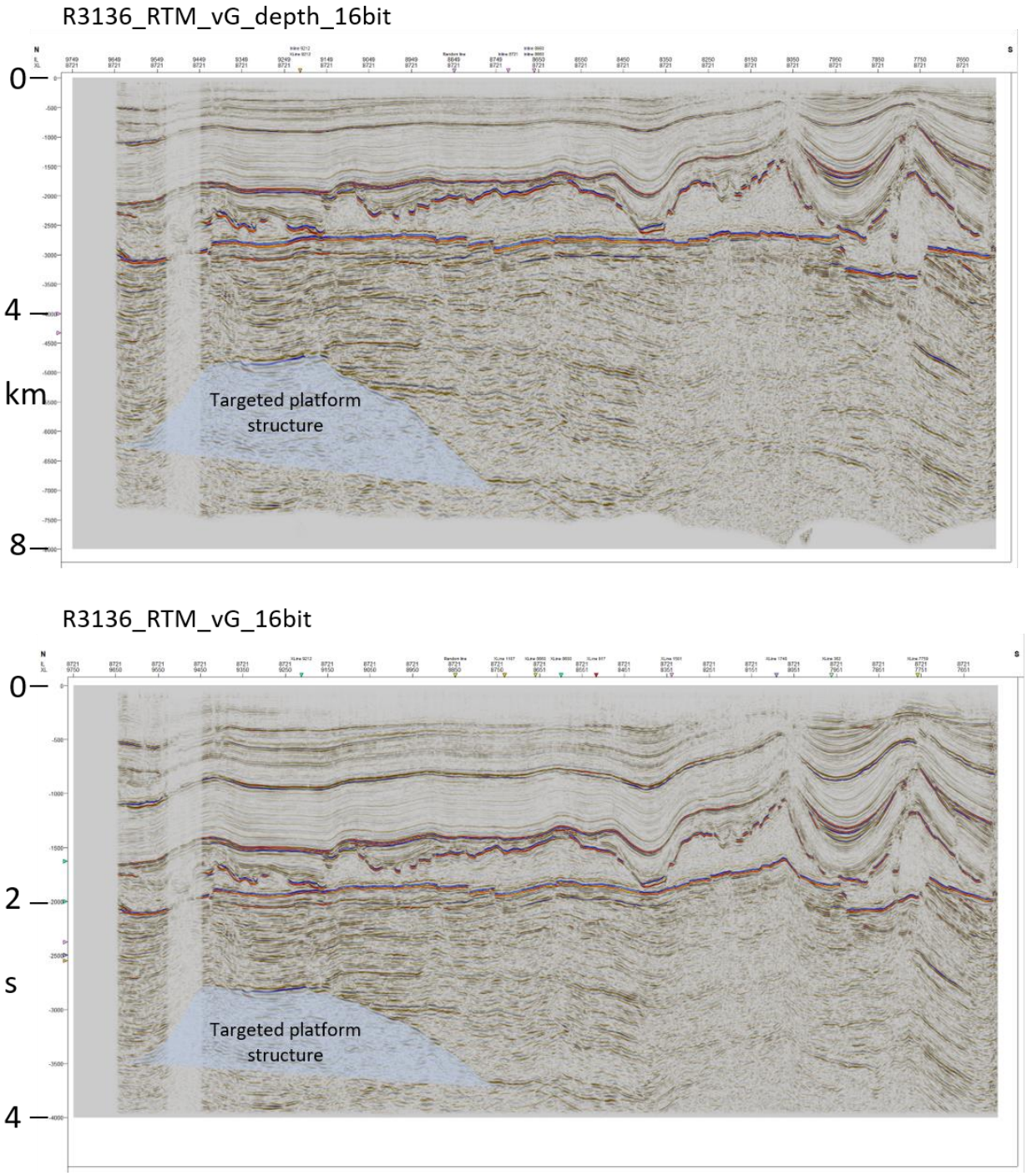

Figure 12: Available seismic data. These surveys run deeper and depict more of the Uithuizermeeden platform. Since the depth survey was not depth converted properly for larger depths (below the Rotliegend level), it has a large offset at the target interval. Therefore, we used the Time survey (bottom), even though penetration is less.

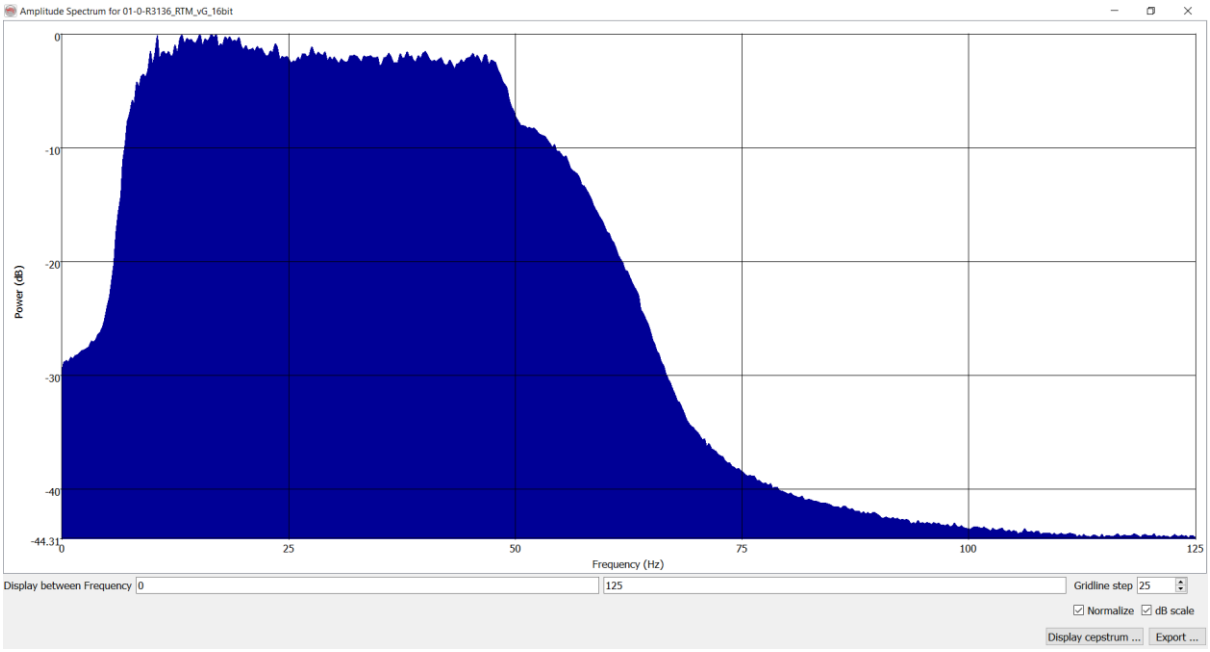

Figure 13: Amplitude spectrum over entire depth range of inline 8721.

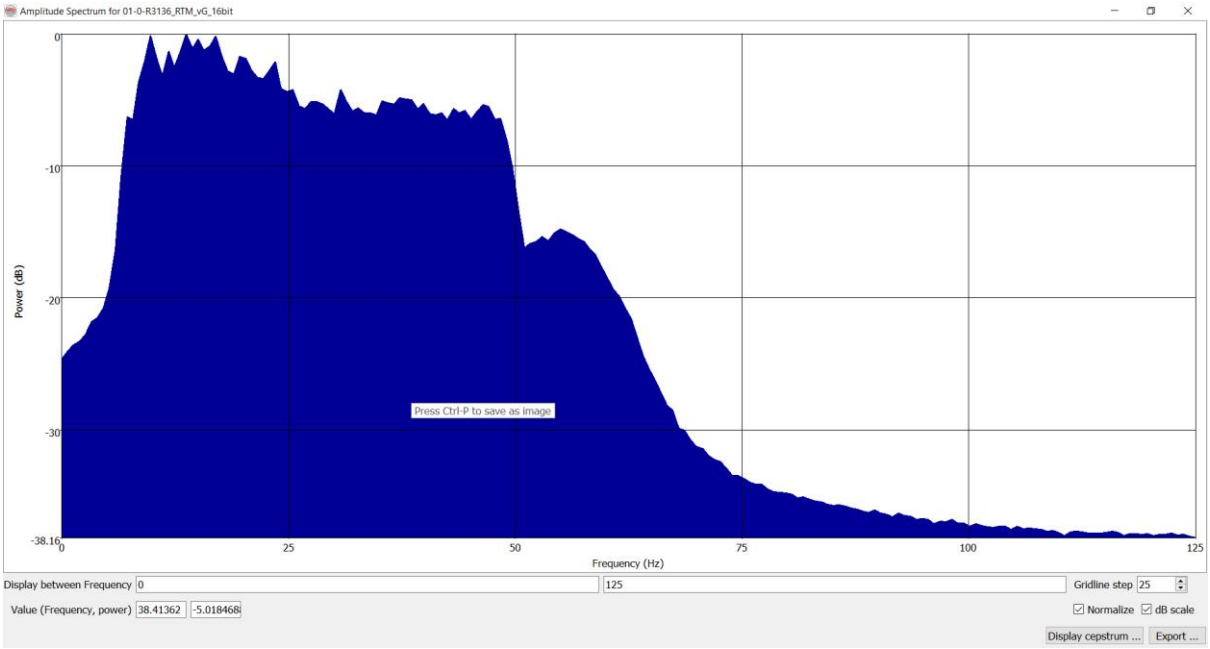

Figure 14: Amplitude spectrum of the target interval (below 2500 ms) of inline 8721.

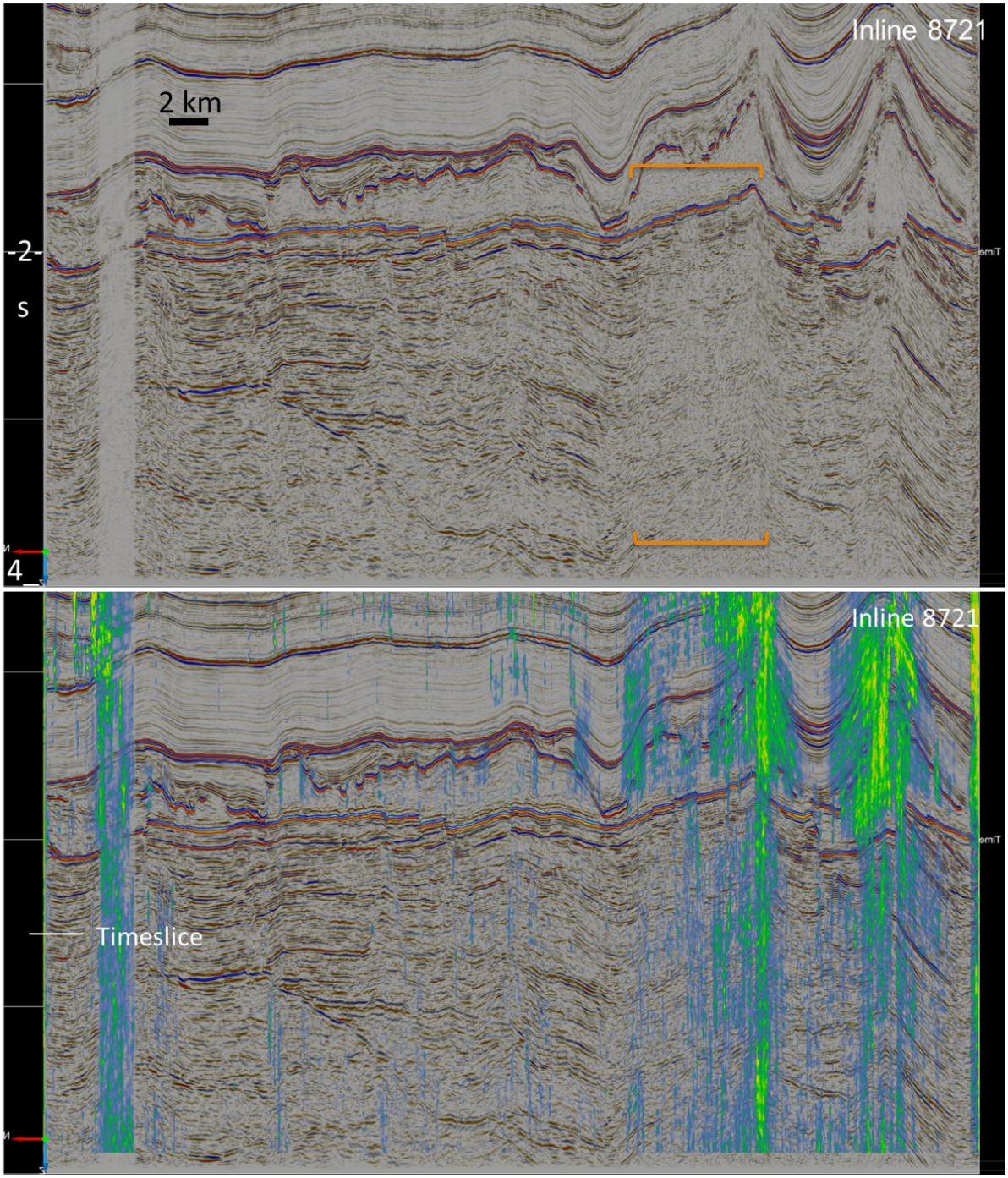

Figure 15: Seismic section (inline 8721) showing the seismic data and the seismic data with a ‘simple chimney attribute’ overlay. Level of the time slice shown in Figure 16 is indicated.

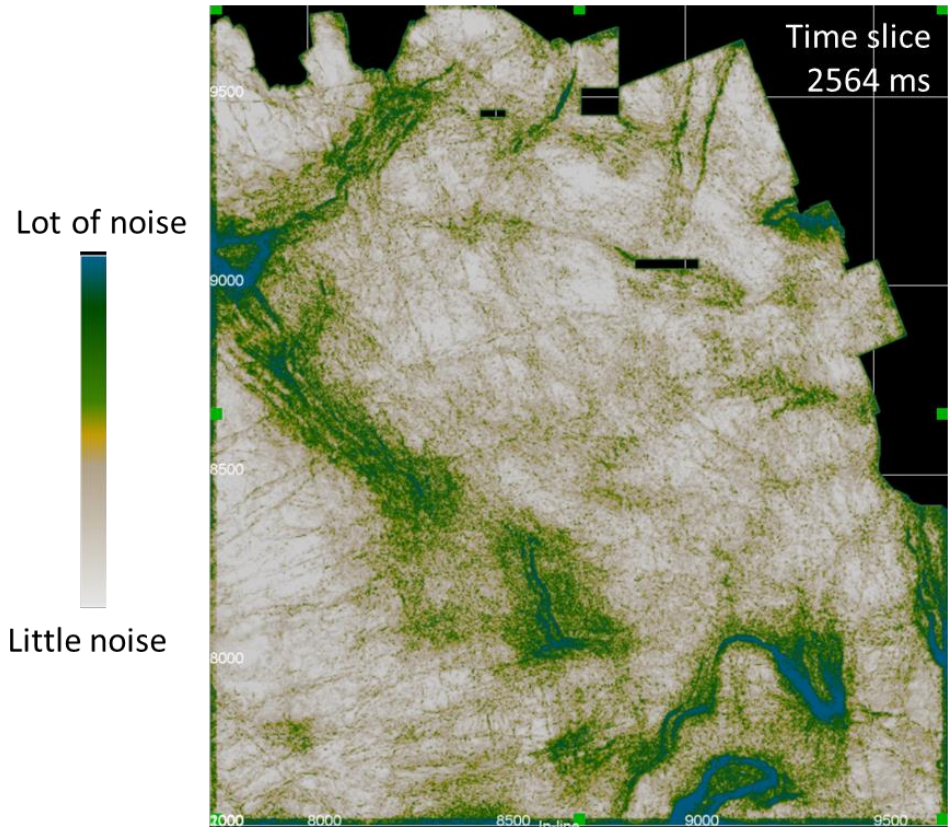

Figure 16: Time slice of the ‘simple chimney attribute’

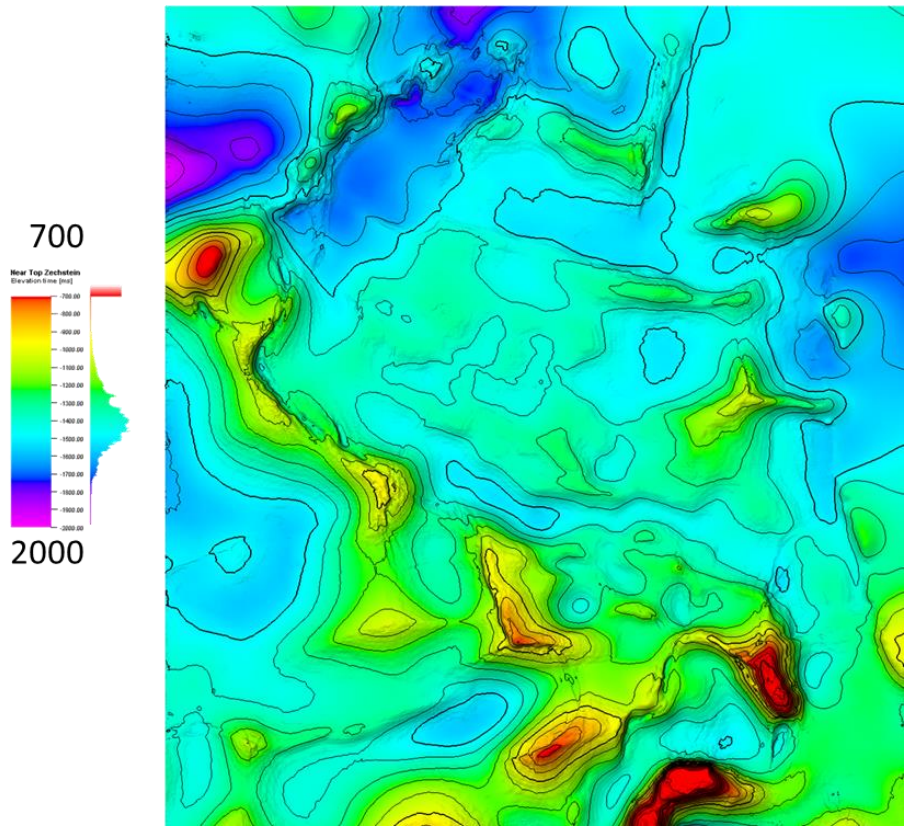

Figure 17: Time-structure map of the near top Zechstein showing the distribution of steep-walled salt structures

Multiples

The R3136_RTM_vG_16bit data-set contains several multiples. One clear example is given Figure 18 showing a cross-cutting event in the Westphalian, that looks like a deep-cutting erosional feature. In fact, this event is caused by seismic rays bouncing between the base Zechstein and the anhydrite stringers in the salt, causing an interbed multiple at larger TWT depth.

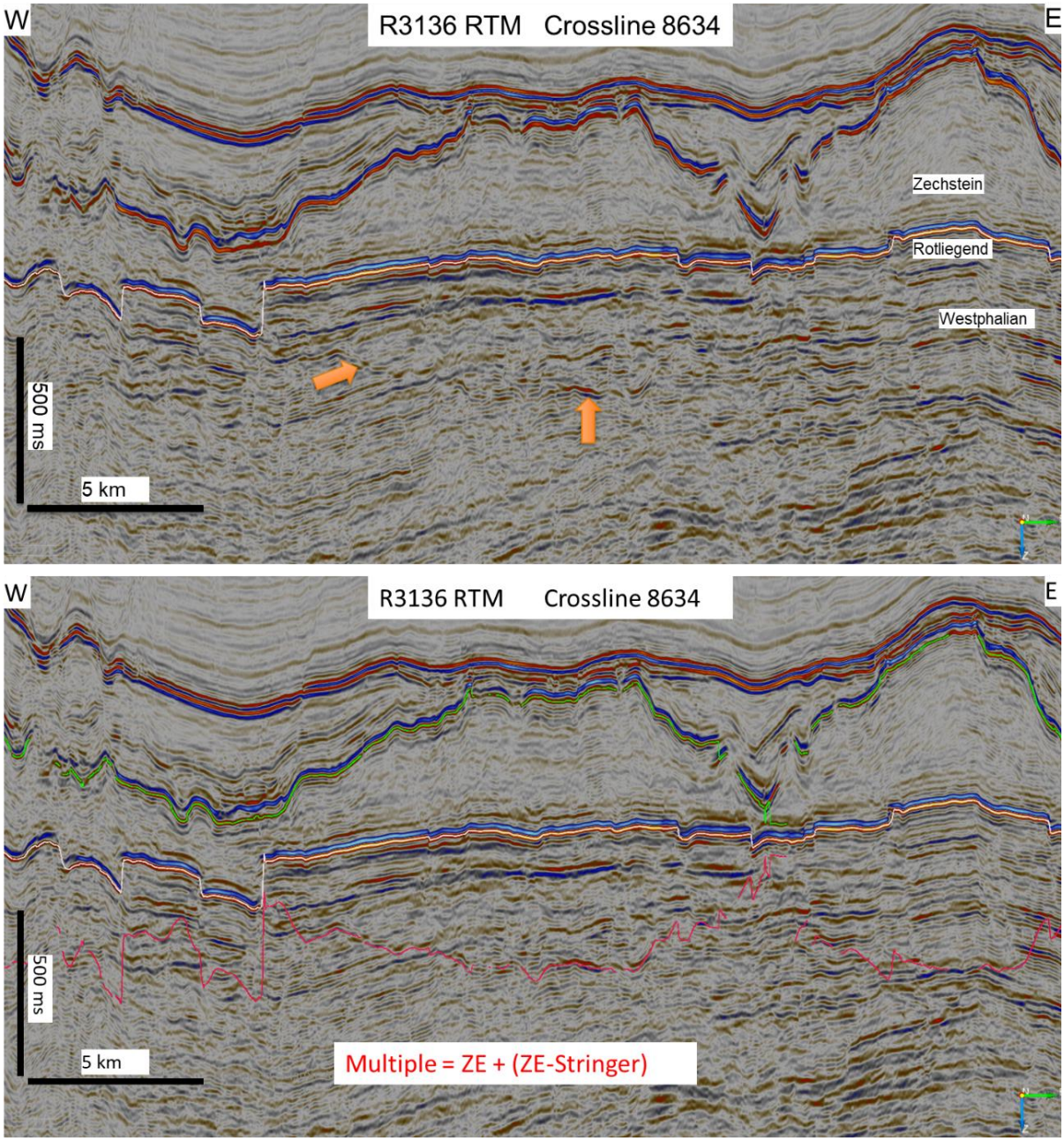

Figure 18: Multiple (red) caused by the base-Zechstein (light pink) and intra salt stringers (green). The multiple was computed by adding the thickness between the stringer and the base Zechstein to the Base Zechstein time-structure map.

5.2.2 Methodologies and workflows applied in the project

The advanced seismic interpretation is focused on post-stack seismic attributes, that are computed on horizons. The horizons used are conventionally mapped as well as automatically

tracked. The latter are part of relatively new interpretation software packages (OpendTect HorizonCube and PaleoScan) that automatically map all seismic reflectors simultaneous.

OpendTect SteeringCube

In the OpendTect workflow, many multi-trace attributes, filters, and the HorizonCube rely on a SteeringCube. This is a seismic volume that contains the dip and azimuth at each seismic sample. This dip and azimuth information are used to guide (steer) multi-trace attributes along a seismic event, which improves their performance. Furthermore, it is used to create the HorizonCube (see below). SteeringCubes are made for the original data, as well as the filtered cubes (see below).The first SteeringCube that was made is the 'PCA 225' SteeringCube (see Figure 19). A large step out of 2x2x5 (5 samples in X direction, 5 samples in Y direction and 11 samples vertically) was chosen to get the general dip of the seismic. The SteeringCube that was used for the HorizonCube was computed from a structure-oriented cube (Dip Steered Median Filter) and a slower, more precise algorithm (Fast Fourier Transform) was used. The SteeringCube has more detail than the previous cube although it is computed with a larger step-out (3x3x7). This is related to the difference in algorithm.

OpendTect data optimization and filtering

Many attributes and horizon tracking algorithms perform better when the data is filtered. For that reason, several different filtering methods are used that are specifically designed for different purposes; the dip steered median filter is a structure-oriented filter that increases the lateral continuity of seismic events, which improves auto-trackers and cleans up multi-trace attribute results. The Fault enhancement filter is a structure-oriented filtering increases the sharpness of faults, which improves fault detection.
Both the Dip Steered Median Filter and the Fault Enhancement Filter were applied with a step-out of 4x4. This produces a horizontal disc of 69 samples that follows reflectors around each seismic sample; all samples are used for the computation. The Dip-Steered Median filter results in more continuous events and reduces noise, while the Fault enhanced Filtered data has sharpened faults (see Figure 19).

OpendTect Attributes

Several seismic volume attributes are used to visualize lateral facies variations and faults. The best way to visualize these features is to compute the attributes on horizons. There are many possible horizon-extractions of attributes; here we list the ones examined:
Amplitude is a great attribute to visualize lateral variability, however it requires a very accurate horizon pick. Where the horizon-pick is not accurate, the amplitude map shows the mapping error instead of a lateral variation. When the mapped horizon is of a lower quality, the Energy attribute or RMS amplitude is a useful attribute since it averages the amplitude information over a (used defined) time window. Energy is the squared sum of the sample values in the specified time-gate (-20,20ms) divided by the number of samples in the gate.

Frequency attributes are used to determine the vertical resolution (see above) and is related to bed thickness, depth and noise. Dominant Frequency is the frequency with the highest amplitude.

Spectral decomposition is used to visualize sedimentary features together with faults. Spectral Decomposition is the amplitude at an iso-frequency. The amplitudes of 3 different iso-frequencies (low, mid and high) are colour blended into one colour display. First, an amplitude spectrum is made to establish the low, mid and high frequencies. Next the amplitude map at the low frequency is depicted in a red colour (red to black), the amplitude

map at the mid frequency is depicted in green colours, while the amplitude map at the high frequency is depicted in blue colours.

Waveform segmentation or clustering is used to visualize variations in bed thickness and seismic facies. Relative to the mapped horizon the waveform is extracted and sorted based on its shape. Next similar waveforms are put together in a class or group. The waveform that is most representative for that class is called the class centre.

Similarity, and Semblance attributes are discontinuity attributes used to highlight faults. They are all multi-trace attribute that returns how similar (or different) neighbouring trace-segments are within a time-gate. The actual algorithms vary but all are excellent tools for structural analysis. Since we have a dipping geology, the algorithms that compensate for structural dip give the best results. Furthermore, since the faults are steep, the best parameter settings are a small horizontal step-out and a large vertical window. In order to highlight faults that are close to visible limit, an edge detection filter is applied to the similarity output. This Ridge Enhancement Filter computes the largest horizontal difference in 4 directions. This boosts the small-scale faults.

Thinned Fault likelihood is also a filter that is run over a discontinuity attribute and produces accurate and sharp faults. The algorithm scans a discontinuity volume within a range of fault dips to identify maximum likelihood of faults. The Thinned fault likelihood attribute provides razor-sharp fault images on horizontal slices as well as on vertical sections.

Sweetness has been found to be useful in detecting stratigraphic features as well as enable a semi-quantitative evaluation of thickness. Sweetness is the instantaneous amplitude divided by the square root of the instantaneous frequency.

Seismic Chimney attributes are used for detecting vertical noise. Their intended purpose is to detect vertical hydrocarbon migration. When hydro-carbons migrate through the sub-surface connate gas stays behind, causing vertical noise trails in seismic data. Such trails are known as chimneys and they reveal where hydro-carbons originate, migrate and accumulate.

The Simple Chimney attribute is designed to detect chimneys, but it is also an excellent attribute to visualize vertical noise zones.

OpendTect HorizonCube and Elliis Paleoscan

Conventional interpretations are only performed on a fraction of the available data (e.g. not every line is interpreted) and only a handful of 3D horizons are mapped. This means that a lot of information remains unused and that models derived from these products rely on limited data constraints. Using new and advanced software tools, all stratigraphic events (horizons) within the seismic cube can be auto detected and placed into stratigraphic order. These horizons have many applications. They can be used to unravel the sedimentary evolution, construct high resolution geological models (e.g. low frequency models for AI inversion), map internal events and to perform advanced horizon-based attributes. It enables the interpreter to perform true stratigraphic slicing through seismic volumes e.g. by removing and adding each 3D seismic event one at the time the depositional development in time and space is visualized.
We used two different software packages; the OpendTect HorizonCube developed by dGB Earth Sciences and PaleoScan of Elliis. Both provide similar functionalities to automatically map seismic events that are placed into stratigraphic order; the technical approach and the

underlying algorithms, however, are different. The HorizonCube is based on the dip information of the SteeringCube, while PaleoScan is based on horizon tracking (amplitude based). Consequently, the results, in theory, are dissimilar.

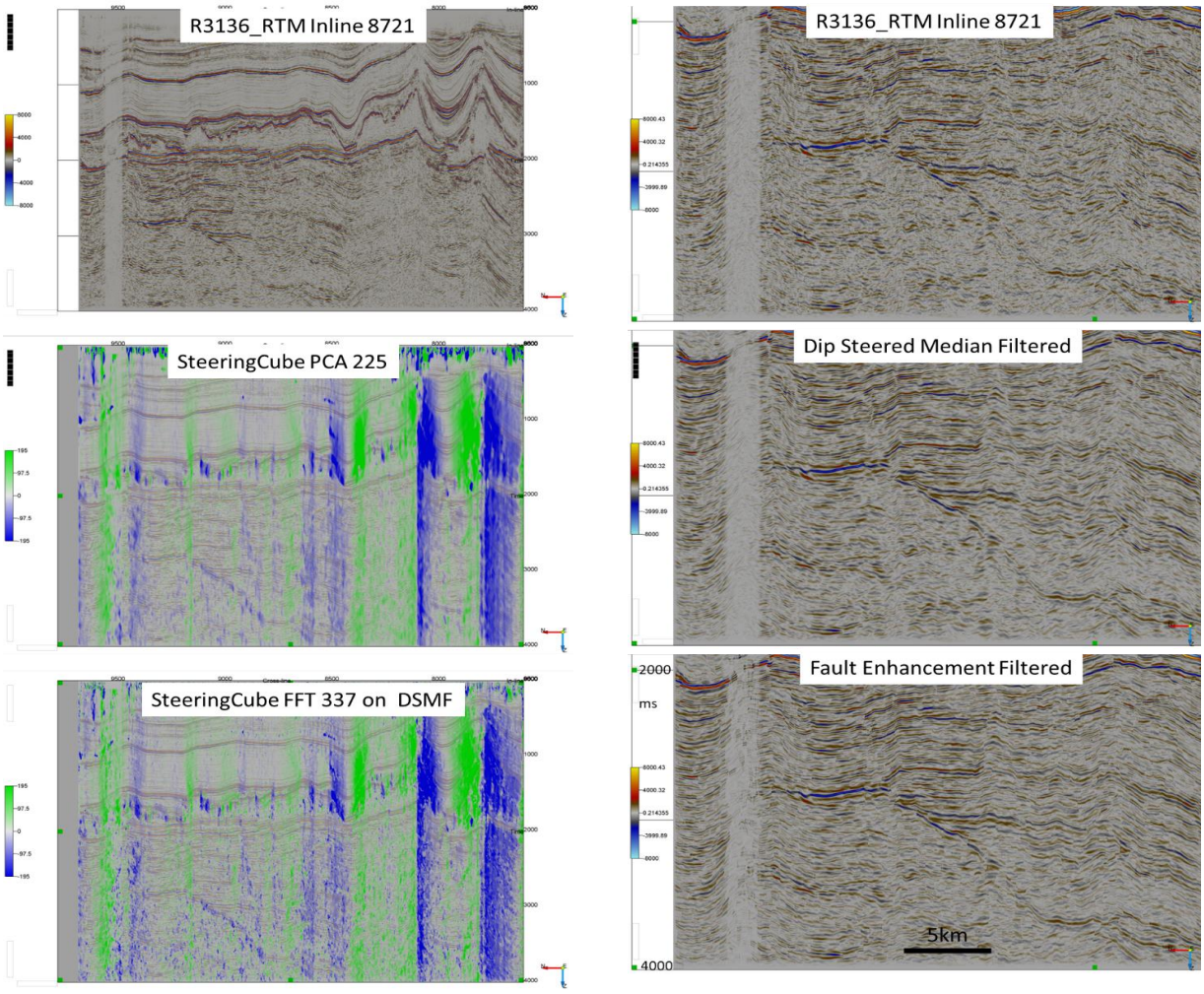

Figure 19: Left: Several Steering Cubes are computed. The PCA 225 is used for structure-oriented filtering and to improve multi-trace attributes. The FFT 337 was used for the HorizonCube. Right: Top: unfiltered seismic data, Middle; Dip steered median filtered seismic, Bottom; Fault Enhancement Filtered seismic

5.2.3 Facies, faults and karst

Facies distribution from geometry

Many seismic attributes were applied and tested. Here, only a selection is presented of those that adequately link to facies and faults. The time structure map of the Uithuizermeeden Platform (Figure 20) seems to consist of a flat-top, raised rims and a slope. Based on these initial observations a map was drawn that show the distribution of several sub-environments (Figure 21).

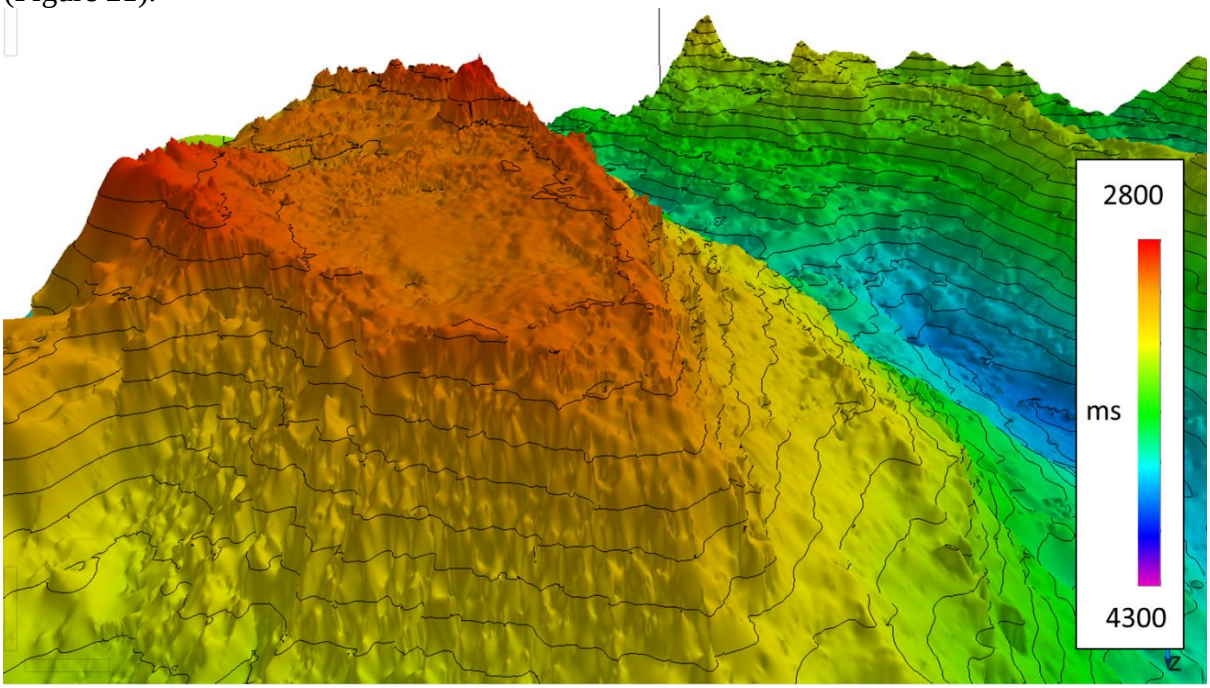

Figure 20: Birdseye view of the top of the Uithuizermeeden platform. The present-day time structure map shows a rim at the edge of the platform.

A clear platform rim is visible on the present-day topography in TWT. However, vertical "pulled up" features are seen above the platform, all-the way up to the base Zechstein and coincide with thick salt structures above. Also, in map view these pull-up zones line up with the rim of the platform (Figure 22). This suggests that the rim could be caused by a velocity pull-up caused by the high velocity Zechstein salt. It is safe to assume that the Zechstein salt was deposited flat, and therefore we flattened the seismic section on the Base Zechstein. The pull-up disappears after flattening, and the rims of the Uithuizermeeden platform also largely disappear (see Figure 23). However, the remaining relief of ~20-40 m is too much to exclude the presence of a rim constructed by reef builders completely.

The updated preliminary facies distribution map predominantly consists of a 'slope' and 'platform interior' facies after removing the velocity effects. Please note that the slope of the platform is only about 8 degrees. It appears much steeper, since many seismic images are vertically exaggerated. The slope is fairly low for a carbonate build-up and supports the theory that there are no reef building organism at this geologic time. Moreover, the question remains if on seismic data a slope facies can be differentiated from a platform interior facies.

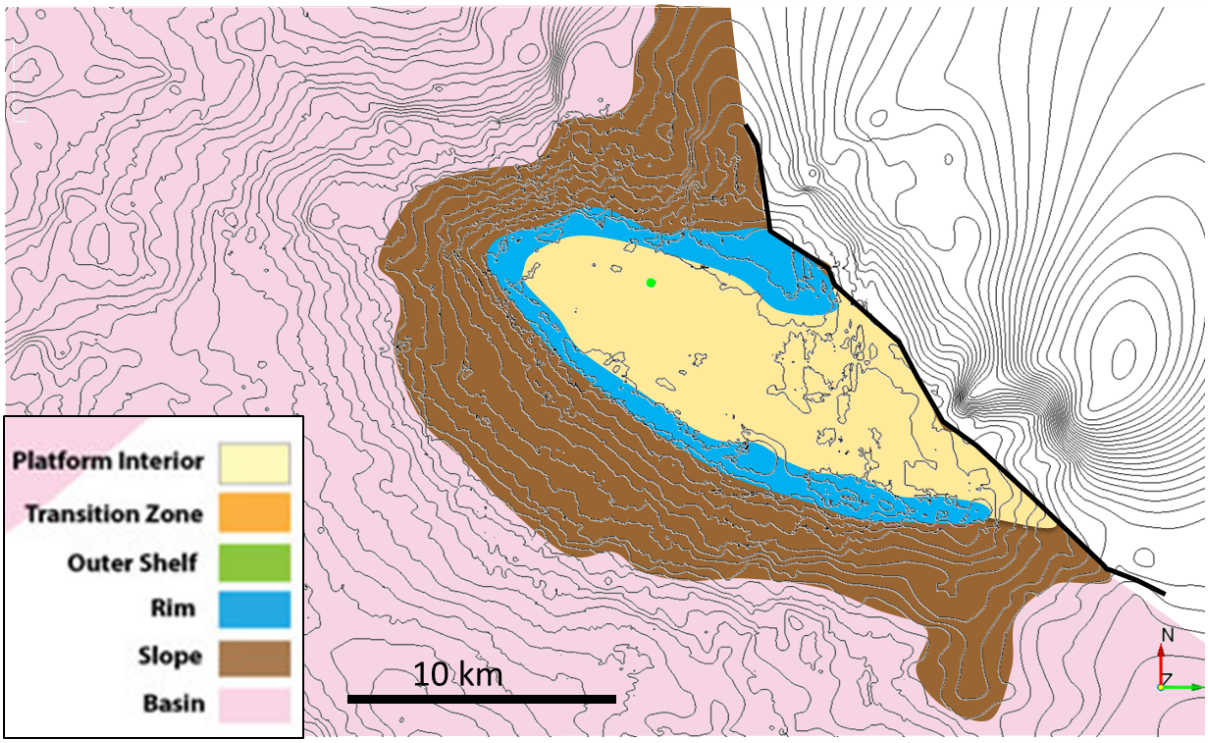

Figure 21: Initial facies distribution map around the Uithuizermeeden platform

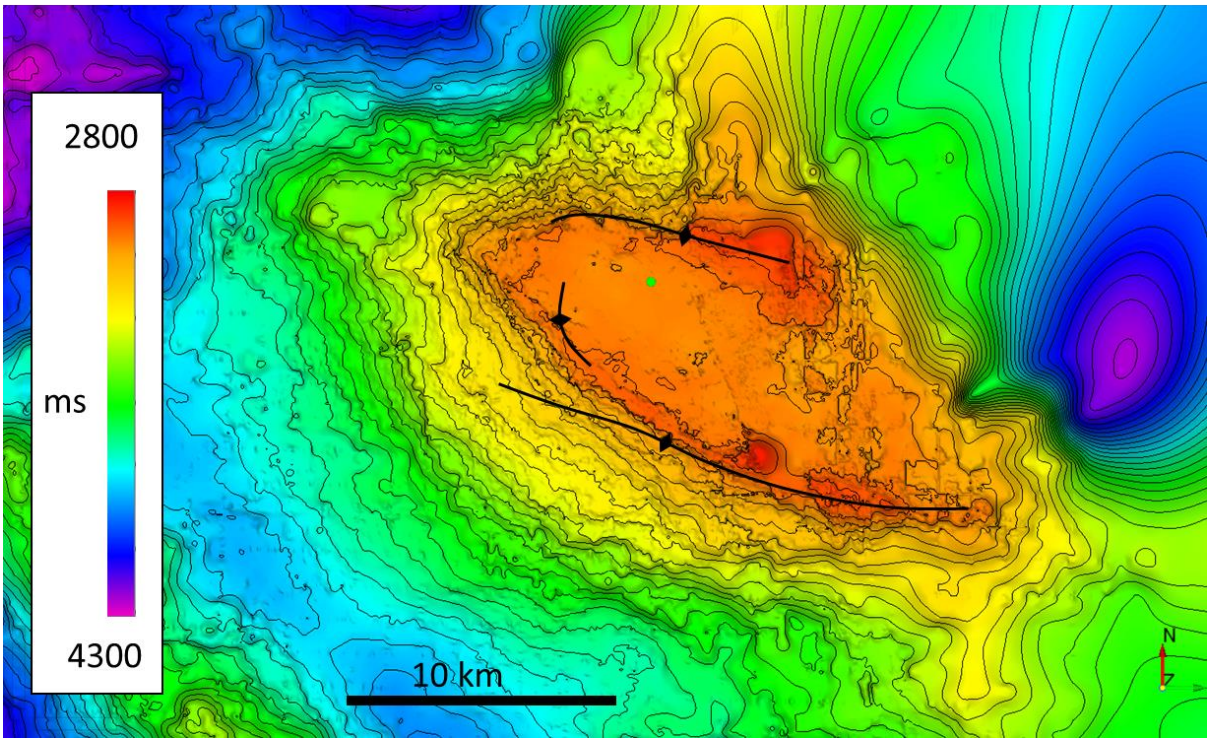

Figure 22: Time structure map of the Uithuizermeeden platform with the axis of structured salt superposed.

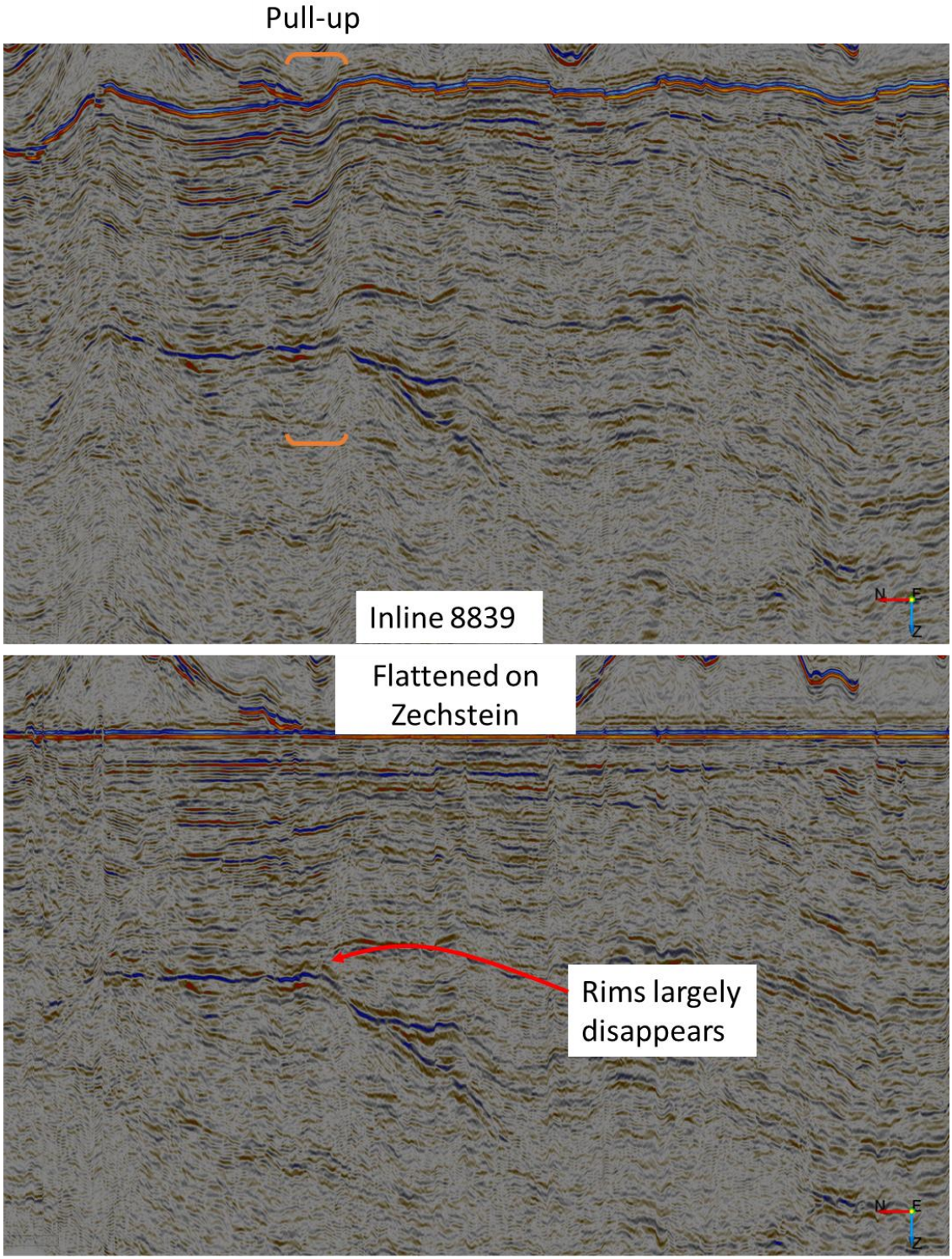

Figure 23: Top; Seismic cross-section showing a pull-up below the salt. When the seismic is flattened according to the base Zechstein, the pull-up disappears, as well as large part of the rims.

Spectral decomposition and waveform segmentation

Spectral decomposition (Figure 24) and waveform segmentation show that the seismic signal is similar for the top of the platform and the slope of the platform. Well UHM-2 shows the presence of tight packstones with high velocities (> 6000 m/s) at the top of the platform. From the sonic log it can be deduced that there is almost no difference in the velocity of the

different lithologies (e.g. dolomite and limestones.). Consequently, a lateral facies change at the top of the carbonates would not be visible on seismic data because it has the same seismic expression. The slope and top of the platform likely appear as one seismic facies (Figure 25).

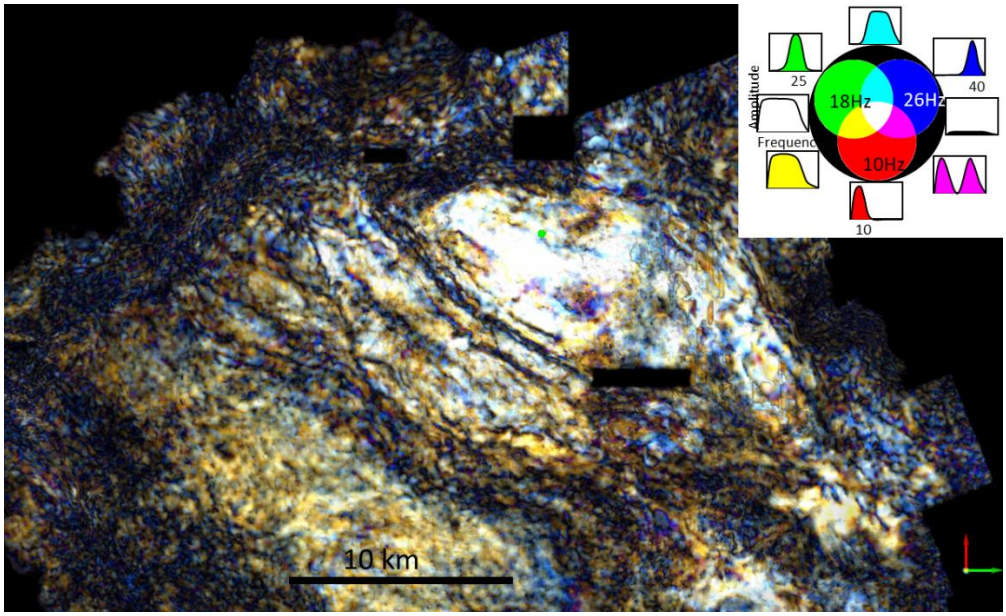

Figure 24: Colour-blended image of three Spectral decomposition results shown on the top Dinantian. The red channel represents a low frequency (10Hz), the green channel represents a mid-frequency (18Hz), and blue is a high frequency (26Hz). The top of the platform and the slope are characterized by 'white' which indicate that all frequencies have a high amplitude response. Faults show-up in black and noise as blue-purple colours.

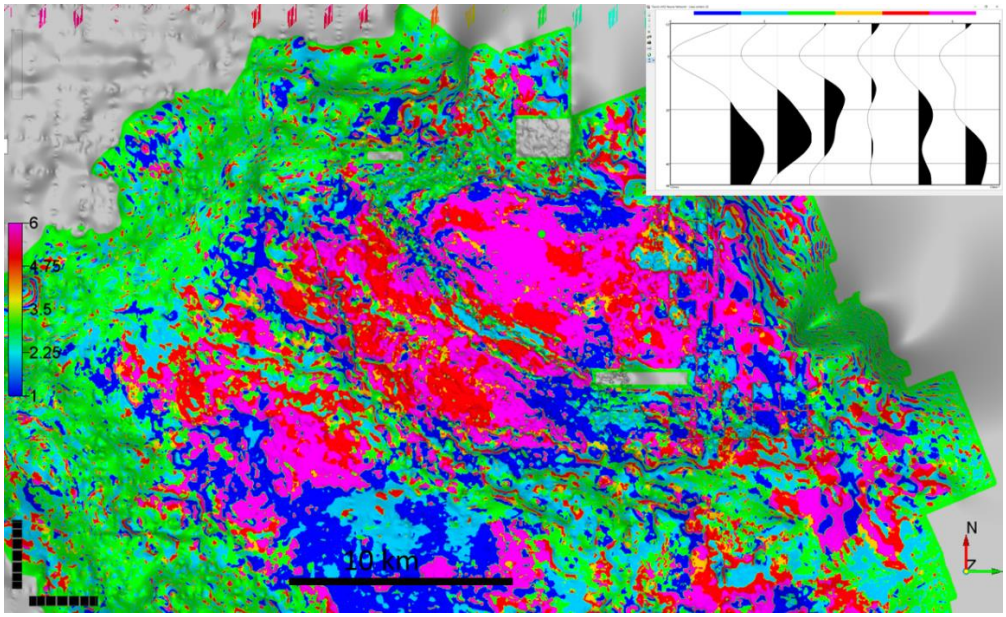

Figure 25: Waveform segmentation on the Top Dinantian horizon. In a short time-window relative to the top Dinantian (12 ms above to 40 ms below) all waveforms are extracted and categorized in six different classes. Similar waveforms are grouped (into a class) and the class-centre is depicted in the insert. Again, the top of the platform and the slope have similar colours, hence they have similar seismic facies.

Karst

The seismic response of karst was modelled (see Jaglan, 2012) and it appears as clear bright events; peak over through. There are many small bright events below the top of the platform, however in combination with the observed lateral brightening of these seismic events, it is more likely that they are caused by tuning. Moreover, the lack of a clear peak over through signature is missing. This leads to the conclusion that no clear indications of karst were found.
.

Faults

Several attributes were applied to the Top Dinantian horizon. Similarity and Semblance (Figure 26) gave similar results and highlight large scale faults. Ridge enhancement filter shows smaller faults. The Thinned Fault likelihood (run on the Fault Enhancement Filtered seismic) gives the sharpest and most continues faults (see Figure 27).

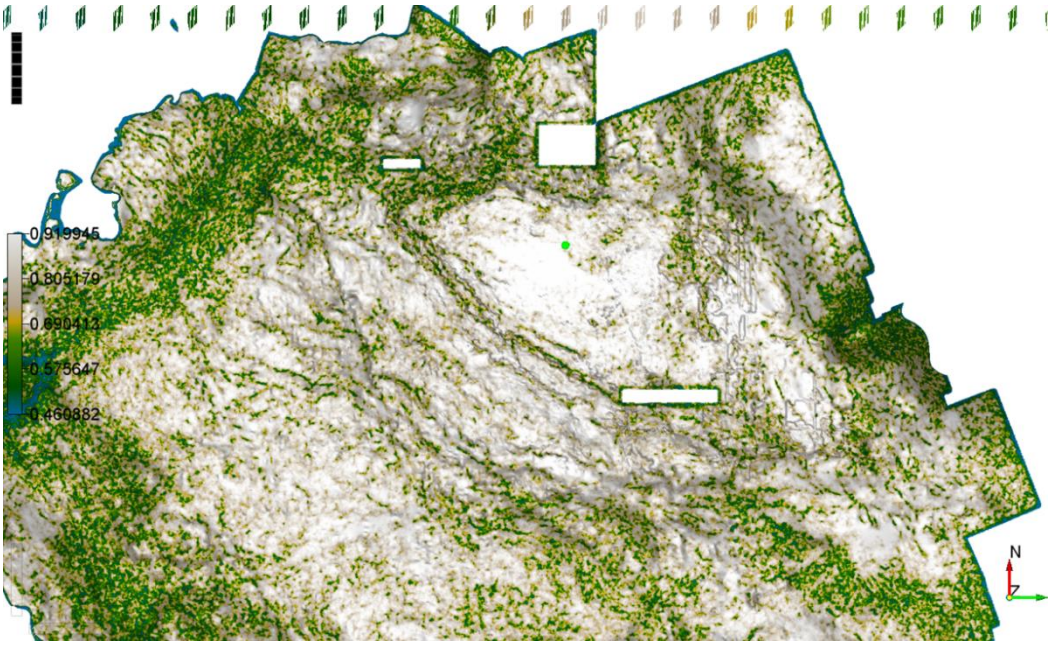

Figure 26: Semblance shows large scale faults that are mainly present around the edges of the platform

There is a major NW-SE trending bounding fault at the north-eastern edge of the platform, whereas W-E trending faults occur at the Northern edge. Where these faults meet there are a couple of N-S trending faults present as well. This could be an area of increased faulting and possibly fracturing. We manually mapped these faults to highlight this zone (Figure 28).

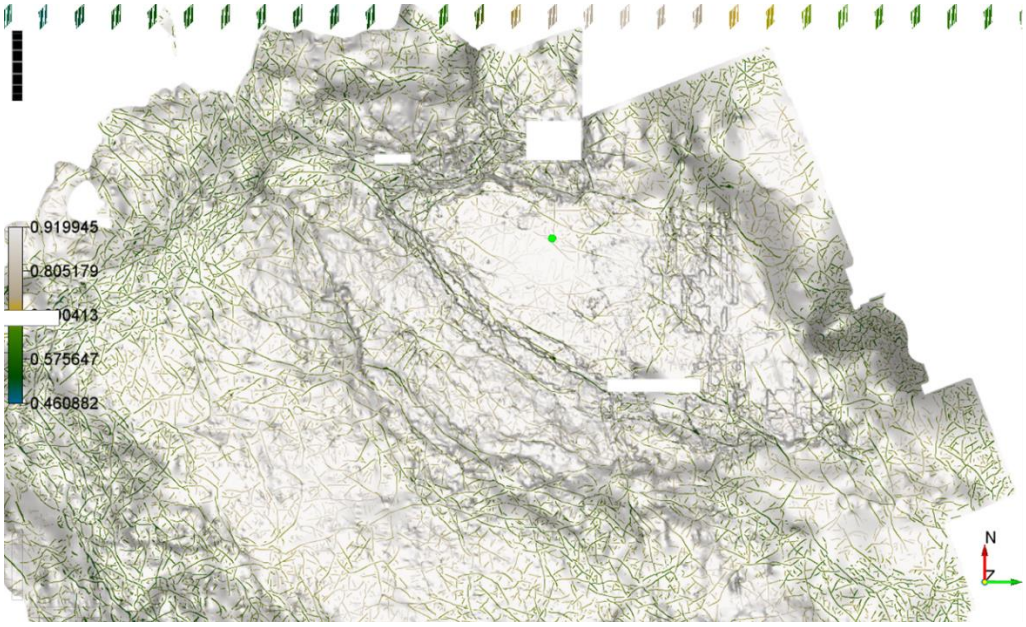

Figure 27: Thinned Fault likelihood on Fault Enhanced Filtered seismic. This attribute gives the best results

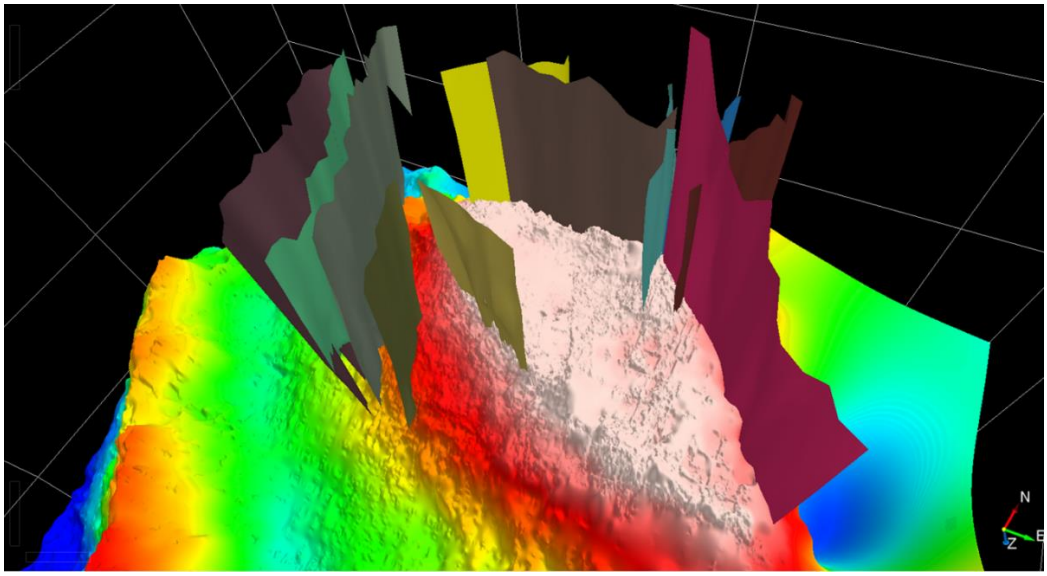

Figure 28: Manually mapped faults. Note the crossing of several faults in the north-eastern part of the platform that could indicate a zone with higher porosity/permeability.

5.2.4 HorizonCube and Paleoscan

The HorizonCube and PaleoScan results show a similar depositional development. The base of the Dinantian is southward sloping, and the platform starts growing in the south (see Figure 29 and Figure 30). Note that this build-up is vertically exaggerated by a pull-up caused by the Zechstein salt (see before). It remains unclear whether the base of the Dinantian was indeed dipping and that the platform grew onto it (onlapping, backstepping system), or that the base was flat, and it was tilted.

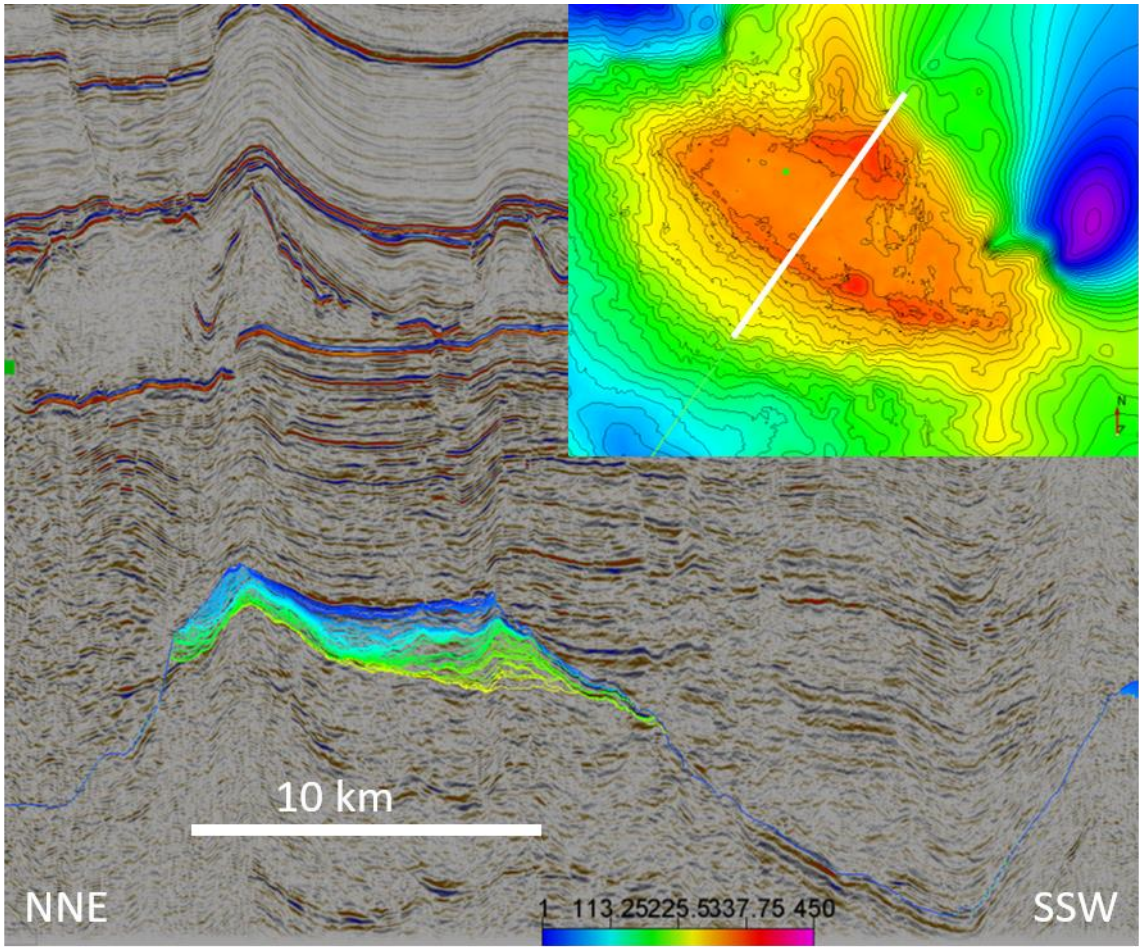

Figure 29: The HorizonCube shows a south sloping Base Dinantian and an initial growth of the platform in the south.

5.2.5 Conclusions

- The seismic resolution is low due to the high seismic velocities, while the seismic data is noisy due to the overlying Zechstein salt.
- Facies change is not visible on seismic data and different carbonate lithologies will likely appear as one seismic unit. *Spectral decomposition* and *waveform segmentation* give the best facies image.
- No clear indication of karst is found.
- Fault zones could have higher porosities. The *Thinned Fault likelihood* (ran on the Fault Enhancement Filtered seismic) gives the sharpest and most continues faults. There is a major NW-SE trending bounding fault at the north-eastern edge of the platform as well as on W-E trending faults at the Northern edge. Where these faults meet there is also a couple of N-S trending faults present as well. This could be an area of increased faulting and possibly fracturing, which could be higher porosity zones.

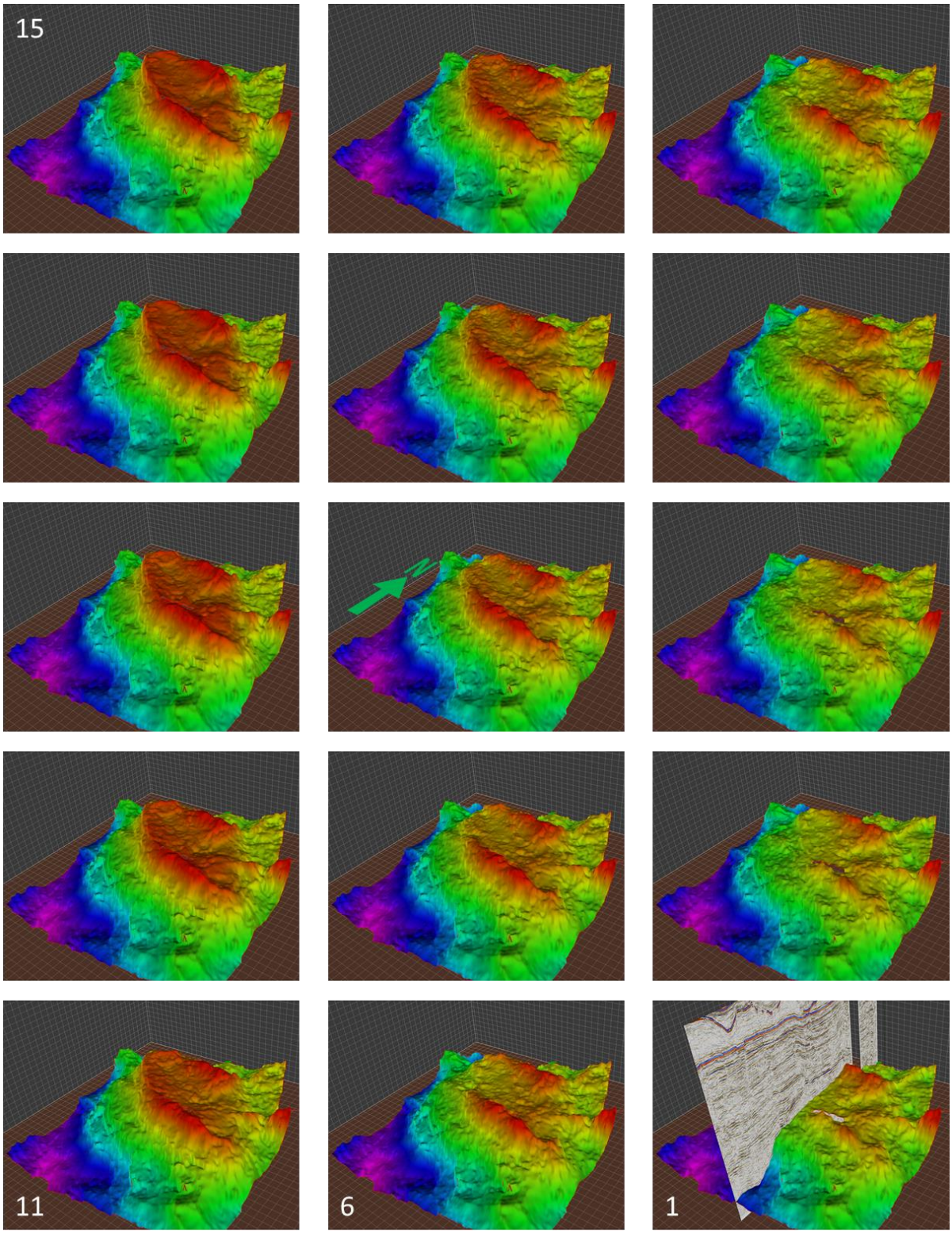

Figure 30: Bird-eye view of the growth of the Dinantian platform (from PaleoScan). Horizon 1 is close to the base of the Dinantian and horizon 15 is near the top of the Dinantian

5.3 Velocity modelling & depth conversion

5.3.1 Introduction

Predicting the depth of the top Dinantian after mapping this event on time seismic data requires a velocity model. The P-wave velocity behaviour of the Cenozoic and Mesozoic strata are well described by the velocity model *VELMOD 3* made by TNO. The velocity behaviour of the Palaeozoic strata is less well-known. The availability of well-based velocity data is ample in the upper part of the Silesian (Westphalian/and, if present, Stephanian) but is scarce for the older strata. The Namurian interval is drilled only by a few wells. In this study an analysis was made of the velocities of both the Westphalian and Namurian strata (Silesian or Limburg Group (DC) according Dutch Nomenclator of Van Adrichem Boogaard, 1992) to be able to establish a best practice approach for time-depth conversion of top Dinantian.

5.3.2 Data

The database of velocity information consists of both seismic velocities and well velocities. Seismic velocities can be stacking velocities or tomographic velocities derived in velocity model building exercises prior to migrating seismic data. TNO has a database of stacking velocities for most seismic surveys and the availability of these data has led to the integration of well velocities and stacking velocities in the *VELMOD 4* project.
More important are the velocities measured in wells which are derived either from borehole measurements using the sonic tool or from first arrivals from check-shot/VSP data. Sonic data are high resolution data of the velocity directly around the borehole and are sensitive to the condition of the borehole. The check-shot/VSP data are data collected by an array of geophones in the borehole and sources at the surface. This velocity data source has a lower resolution compared to the sonic data but has a frequency content that is more like the seismic data and is theoretically more comparable to the velocity of the ray-paths in the seismic data. Most boreholes have sonic data while checkshot/VSP data are scarcer. For some boreholes the two sources of velocity information are integrated by calibrating the sonic log with check-shot data.
The well database consists of 780 boreholes that have velocity information in the DC interval. There are 9 wells that contain velocity information in the Namurian interval in the *VELMOD 3* project. Three wells (LTG-01, UHM-01 and TJM-02-S1) with velocity information in the Namurian were not present in the VELMOD 3 dataset and added to the current study. Sonic data were calibrated with VSP/check-shot data and synthetics were generated to arrive at an optimal Time-Depth curve that was input to the interval velocity determination of these wells.

5.3.3 Velocity analysis

Seismic velocities

Two seismic velocity datasets were available:

1. A migration velocity dataset from the reprocessing of a large 3D dataset consisting of several vintages of 3D data in the area of the Groningen field
2. The VELMOD 4 dataset built by integrating well velocities with stacking velocities covering the entire Dutch subsurface. Stacking velocities are derived from 3D and from 2D data and are therefore variable in density of spatial sampling. From the well velocities and this variable stacking velocity dataset a 3D dataset with instantaneous velocity information is derived at a vertical sampling rate of 40 ms and a horizontal grid distance of 1000 m.

From the reprocessing report of the first dataset there has been no velocity picking in the Carboniferous interval. A flood of constant velocities has been applied to the Carboniferous

series and no velocity information has been derived in this interval. The second dataset contains velocity information in the Carboniferous. Analysing the derived velocities in this stacking dataset shows that there is not a lot of variation in velocity at this depth. Plotting well velocities on the VELMOD 4 data cube indicates that the resolution in velocities at this depth is very low. It can be questioned whether the input data of the VELMOD 4 model has long enough offsets (and big enough angle) to be able to estimate the move-out velocity in an adequate way. The conclusion from the analysis of the VELMOD 4 dataset that it is not suitable to build velocity models for depths at which the Carboniferous series normally resides. Possible exception could be in the south close to *the London-Brabant massif* where the Carboniferous series is at a shallower depth.

Well-based velocities

Clastic and carbonate sediments in the Dutch subsurface have been subject to considerable compaction due to sediment loading during burial phases. This compaction resulted in an increase of compressional wave velocity of sediments with burial depth. Therefore, for the compacting layers, model velocities are adopted that increase linearly with depth and which are described by:

$V=V_0+k* Z$ (eq. 1)

Where V [m/s] is the instantaneous velocity, V0 [m/s] the normalized velocity (at depth = 0), k [m/s/m] the velocity-depth gradient and Z [m] the depth.
The V0 and k model parameters are determined according to the Vint: Zmid method that describes a linear relationship between interval velocity (Vint) and the mid-depth of a lithostratigraphic unit (Zmid). For lithostratigraphic units separated by velocity breaks, individual parameters are derived to achieve a best fit between well velocities and mid-depth of the form:

$Vint = V_0 + k* Zmid$ (eq.2)

In case of a normally compacted unit this V_0 should be around the water P-wave velocity (1500 m/s), but a complex burial history potentially in combination with diagenetic processes can lead to a velocity that is significantly higher than that of water. This approach works reasonably well up to depths of 5000-6000m; at deeper levels compaction may slow down and a linear increase of velocities is not applicable. Plotting the interval velocity of the Limburg Group (DC) against Z_{mid} and plotting a regression line through it gives the result shown in Figure 31.

If the Namurian interval (DCG) is analysed separately, the number of data points in the data cloud is reduced drastically. In Figure 32 the interval velocities of the DCG interval are plotted against mid-depths. The regression line (blue) of the scarce DCG dataset does not differ much from the regression line from the entire DC interval (green). Based on this (limited) dataset it can be concluded that for a regional (or national) mapping of the top Dinantian, there is no need to make a distinction between the Westphalian (and younger Carboniferous sediments) and the Namurian. This also implies that for time-depth conversion no TWT depth of the top Namurian is required, i.e., the difficult seismic interpretation of the top Namurian can be avoided

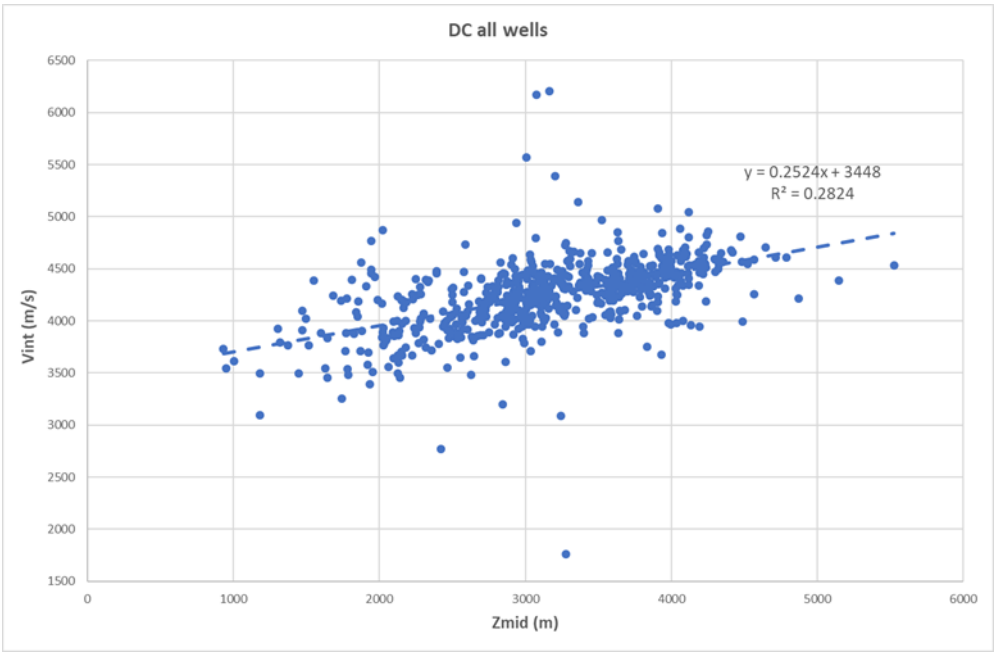

Figure 31: V_{int} versus Z_{mid} plot of all wells through the Carboniferous (CD) interval and the derived linear regression line

.

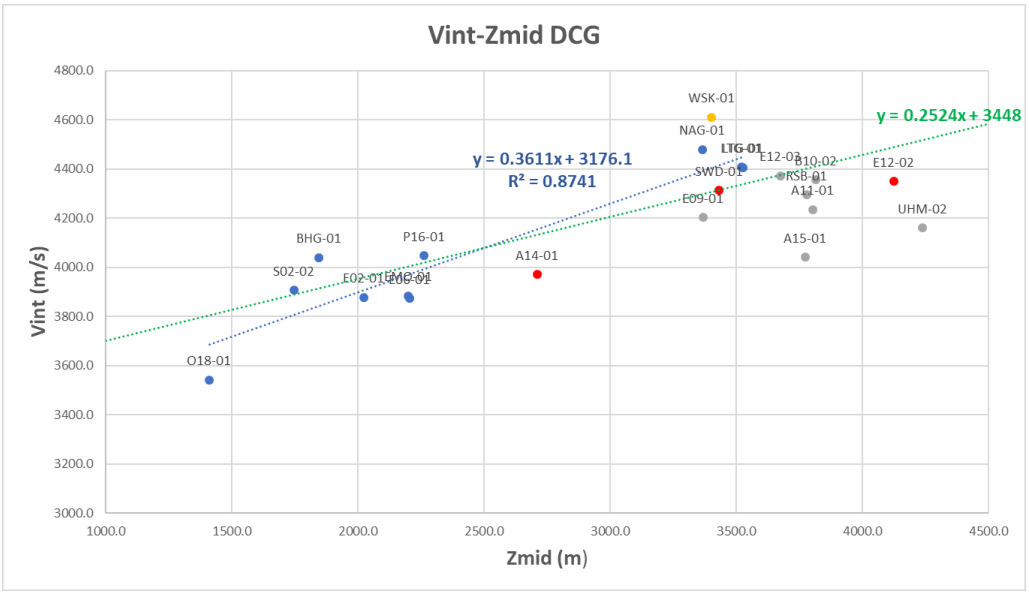

Figure 32: Vint versus Zmid plot of wells through the Namurian (DCG) interval and the derived linear regression line

For local time-depth conversion possibly a more optimal velocity function can be found. This will be investigated in the next section. The local parameter V_0 can be determined at borehole locations by the following calibration formula (Japsen, 1993):

$$V_0(X,Y) = k \bullet [Z_b: Z_t \bullet \exp(k \bullet \Delta T)] \bullet [\exp(k \bullet \Delta T): 1]^{-1} \quad \text{(eq.3)}$$

This formula uses the traveltime (ΔT) according to the V_{int}: Z_{mid} and a global k value.

Velocity dependency on area

In a paper by Kombrink et al. (2012) a classification for the sequence of stratigraphic units in the Netherlands is introduced. The methodology in the paper is named *Stratpiler*. The method results in 10 classes that each have a distinct sequence of stratigraphic units (Figure 33). For this evaluation some of the Stratpiler classes are combined resulting in a simpler subdivision in order to prevent a low number of velocity data points per class. Subsequently the DC Vnt-Zmid data cloud is subdivided according to the Stratpiler classification scheme depending on the location of the wells.

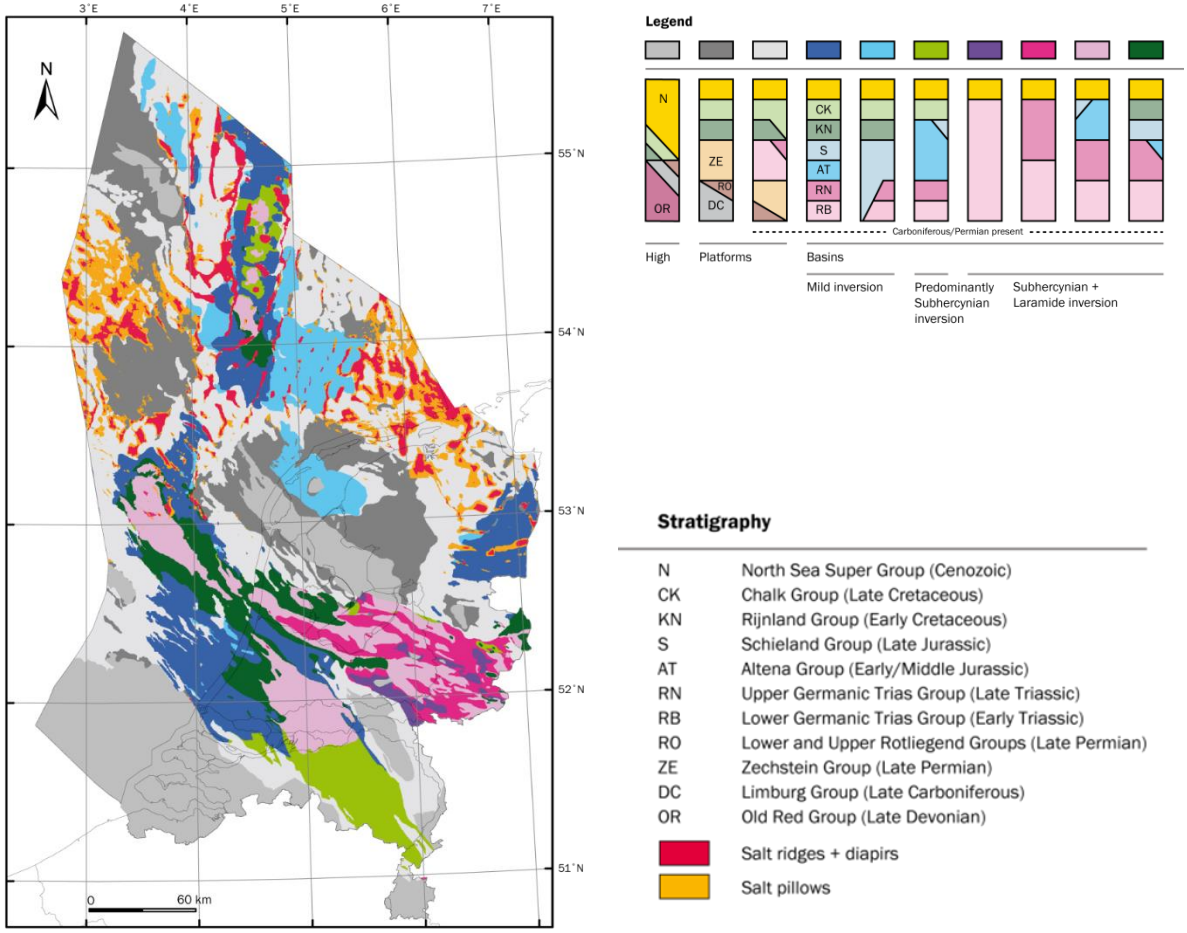

Figure 33: Map showing the distribution of (Mesozoic) structural elements based on the Stratpiler analysis. The degree of degree of inversion that took place in Late Cretaceous: Paleogene times is indicated with different colours.

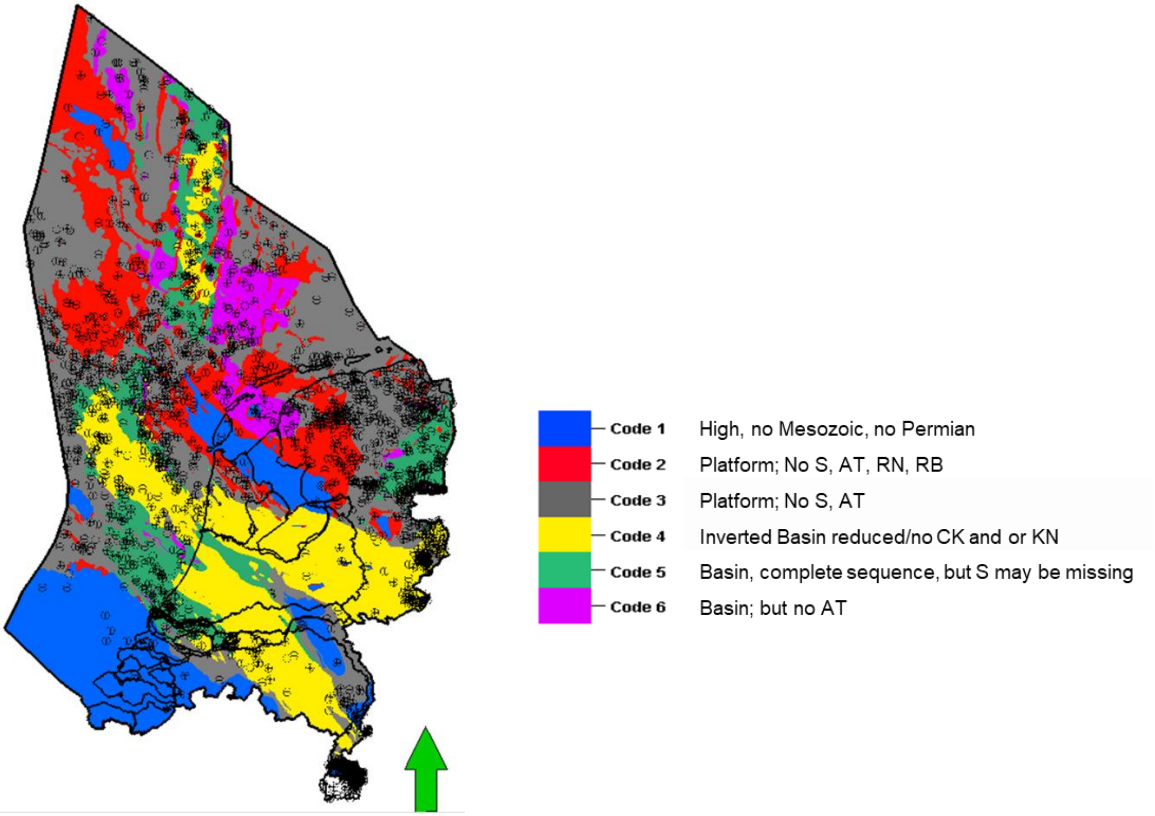

Figure 34: Generalization of the map shown in Figure 33 with inverted areas (Code 4) in yellow

A generalized map (Figure 34) of the Stratpiler maps was used to group the velocity data. It shows that especially velocity data points in class 2 areas (red) have a relatively strong correlation with depth, while the class 3 area points (grey) show a similar trend but with a larger velocity spread. Class 1 points are only sampling the lower range of the depth spectrum, but are generally in line with the other points, though with quite a big spread.

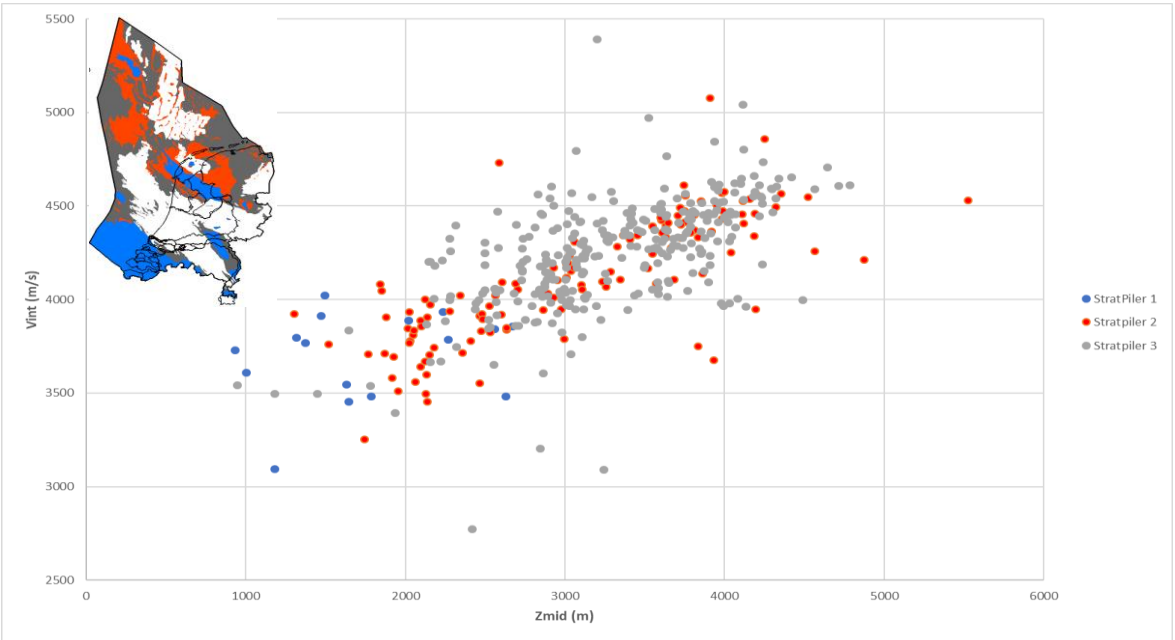

Figure 35: Velocity data points Stratpiler areas 1, 2 and 3 (see Figure 34 for legend) for all wells through the Carboniferous (CD) interval

The class 4 interval velocity points (yellow) plot distinctly different compared to the relatively well behaving class 2 (Figure 35). Apart from a few exceptions the wells in this class have higher interval velocities than what would be expected based on the current burial depth, implying that a substantial part of the wells in this class is currently not at maximum burial depth, i.e. were uplifted in later period(s) of inversion.
In areas of mild inversion (class 5 wells, green, in Figure 36) velocity data plot on the class 2 trend, while other wells in this class show somewhat higher interval velocities. This means that some wells in stratpiler class 5 are probably not at maximum burial depth at this moment, while others are. Data in class 6 areas, representing non-inverted basins (pink, Figure 36) is not too different from class 2 and 3.
The conclusion is that variability of velocities in the dataset is quite big. Class 4 and class 5 data are the datasets that have a centre of gravity of the datacloud plots distinctly at higher velocity than the derived V0-k function (Figure 36). If all area's are combined the V0-k is a bit different from the regression if class 4 and 5 points are left out. The regression functions through the DC velocity data points in all areas and in non-inverted areas only are displayed in Table 1.

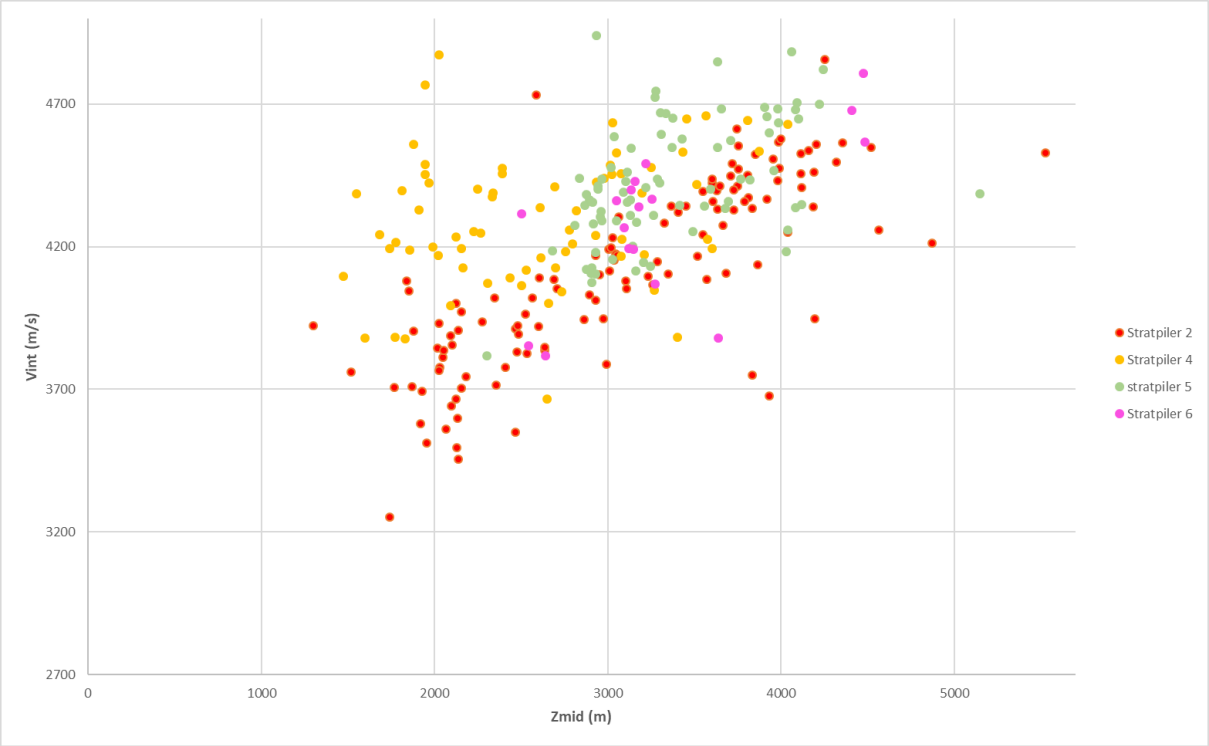

Figure 36: Velocity data points of Stratpiler areas 2, 4, 5 and 6 compared (see Figure 34 for legend) for all wells through the Carboniferous (CD) interval.

Table 1: Best fit V0, k values obtained after analysis

	k (1/s)	V0 (m/s)
All areas	0.2524	3448
Non-inverted areas (excluding stratpiler classes 4 and 5)	0.3188	3213

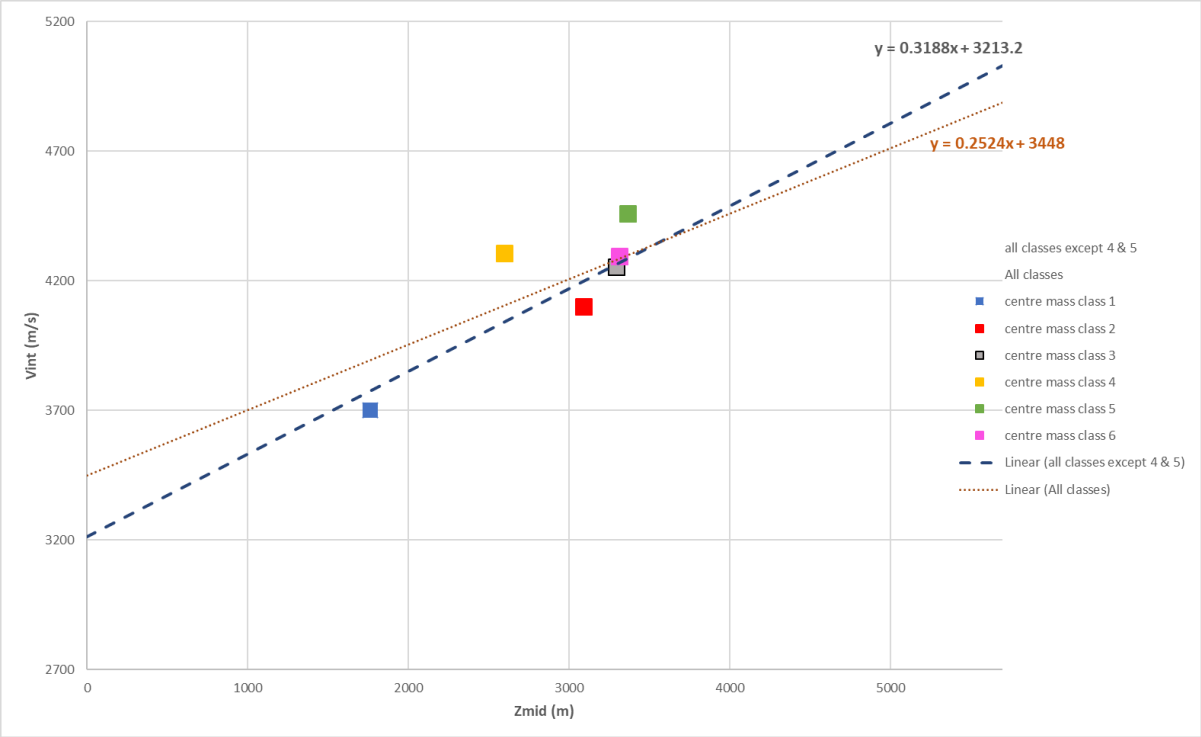

Figure 37: Mass centres of the individual classes relative to the V0, k regression lines for all areas (dashed blue line) vs. non-inverted areas (stippled orange)

5.3.4 Uncertainty velocity

From Figure 31 it is clear that the scatter in the Carboniferous interval velocity is considerable. To estimate uncertainty the difference in Interval velocity (Vint) measured in wells and predicted velocity by the linear velocity function is calculated for each Stratpiler class. For classes 4 and 5 the difference is calculated with the velocity function Vint = 0.2524*Zmid + 34448 (being the velocity function based on wells including from the uplift areas). For the other classes the non-uplifted area function was applied (Vint=0.3188*Zmid + 3213). Table 2 shows the average (bias) and standard deviation of well interval velocities around the linear functions for all wells and each class separately.

Table 2: Statistics of V_{int} around the two velocity functions for non-inverted (blue) and inverted (pink) areas

w.r. regression	All wells	Class 1	Class 2	Class 3	Class 4	Class 5	Class 6
Average (m/s)	0	-76	-99	-11	203	163	26
StDev (m/s)	294	264	297	261	255	305	207

The average is indicative of the position of the mass centres of the classes in Figure 37 with respect to the regression line. The standard deviation (Stdev) is in the range of 200-300 m/s for all classes. The standard deviation for all wells of 300 m/s is representative for regional studies. As an illustration of the uncertainty one and two standard deviation lines (using 300 m/s as 1 Stdev) around the regression line for non-inverted areas is plotted in Figure 38. Using this linear relationship, there is 67% change that the DC interval at any place falls within 1 SD and 95% change that it falls within 2SD (assuming a normal data distribution).

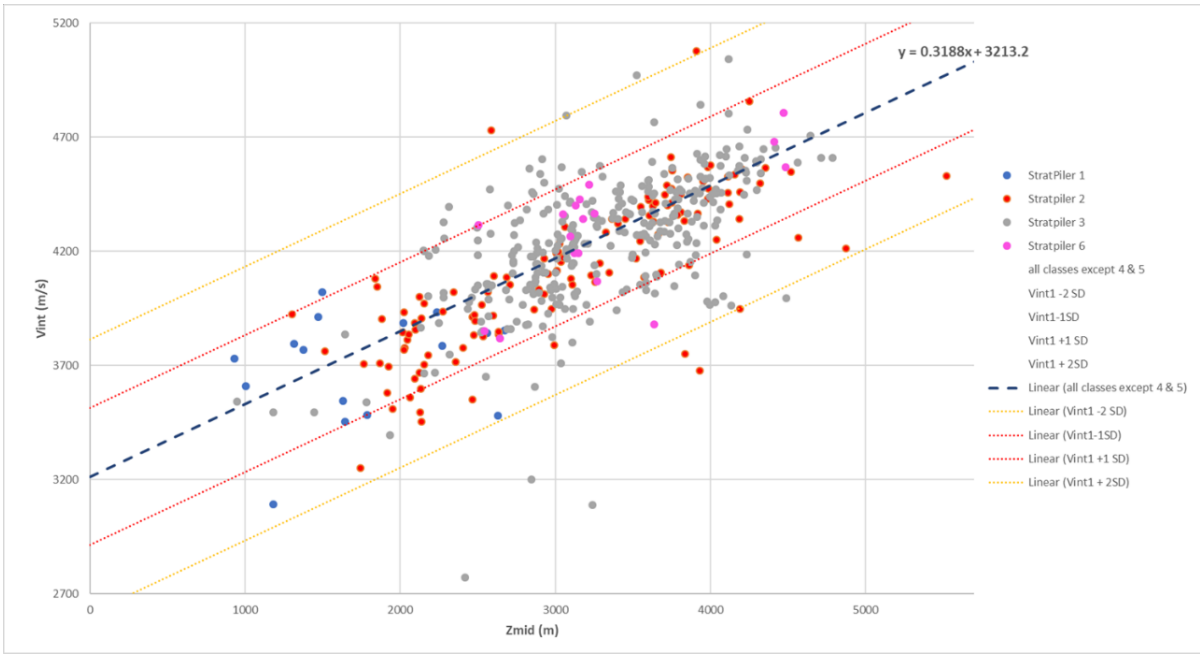

Figure 38: Linear regression and +/- 1 and 2 StDev lines for interval velocities of non-inverted area

A standard deviation in interval velocity in the Carboniferous interval of 300 m/s will give after time-depth conversion of this interval considerable uncertainty in depth. In Table 3 an indication of this uncertainty in depth is calculated for an interval velocity of 4300 m/s and various (time) thicknesses of the DC interval. It is obvious that an uncertainty of several 100's of meters is inevitable if there is a thick Upper Carboniferous interval above the targeted top Dinantian.

Table 3: Indicative uncertainty in depth resulting from uncertainty in Vint for several DC thicknesses

TWT (ms)	Vint - 2StDev	Vint - 1StDev	Vint	Vint + 1StDev	Vint + 2StDev	
	3700	**4000**	**4300**	**4600**	**4900**	**Velocity (m/s)**
250	463	500	538	575	613	**Thickness (m)**
500	925	1000	1075	1150	1225	
750	1388	1500	1613	1725	1838	
1000	1850	2000	2150	2300	2450	

5.3.5 Uplift analysis

To investigate the difference between current dept and maximum burial depth an attempt was made to estimate the magnitude of post-burial uplift from velocities of the Lower Triassic Main Claystone Member. These estimates are subsequently used to correct the Upper Carboniferous velocities.

Van Dalfsen et al. (2005) estimated the magnitude of apparent uplift of the Main Claystone Member based on its interval velocity interval. In this study it was assumed that the P-wave velocity increases linearly with burial depth and once compacted the velocity remains the same during later uplift and renewed subsidence, unless the previous maximum burial depth is exceeded. Apparent uplift is therefore defined as the actual, net result of all phases of uplift, erosion, subsidence and sediment deposition since maximum burial. A "normal" compaction line was defined based on the lowest interval velocities, after removing the wells which have a certain degree of overpressure (see next section).

Based on the same dataset as used in Van Dalfsen et al. (2005) a comparable "normal" compaction function relating Vint and Zmid was derived: Vint = 0.78* Zmid + 1560. For each well the apparent uplift was calculated. The DC dataset was limited to those wells for which an apparent uplift could be calculated. Subsequently, the apparent uplift was added to the Zmid to arrive at the maximum burial depth. This procedure is valid under the assumption that maximum burial of the Carboniferous strata was post early Triassic, thus at the same time as the maximum burial of the Main Claystone Member. This assumption holds as the thickness of removed Carboniferous material below the Early Permian Saalian unconformity is less than the post Main Claystone present day thickness in most of and probably in all of areas where the Main Claystone is present today.
In Figure 39 the original data cloud (blue) can be compared with the apparent uplift corrected points (grey). The expectation was that the original DC Vint points would collapse to a position close to a line that would represent the Carboniferous compaction line. This effect is not recognizable, the effective R^2 is even smaller after the apparent uplift correction. It can be concluded that a well by well uplift correction does not give a better compaction line. To estimate the uplift from the Triassic Main Claystone velocity on a well by well basis is probably pushing the data too much, ignoring other factors that influence the velocity besides uplift. Therefore, this approach and the suggested correction for data points from the inverted areas was not pursued. A better way to do the uplift correction might be to isolate the inverted areas and define an "average" uplift for these areas. Subsequently the velocity data could be corrected to help and define the compaction line. It is therefore suggested that leaving out the velocity data from inverted areas and define the velocity linear regression on non-inverted area data points only (as was described in the previous paragraph) is the best. In parts of the inverted areas where the maximum burial depth exceeds present day burial depth the velocity for time-depth conversion should be increased with respect to the velocity function derived from data points from non-inverted areas. Local analysis of wells will be needed to make a local estimate.

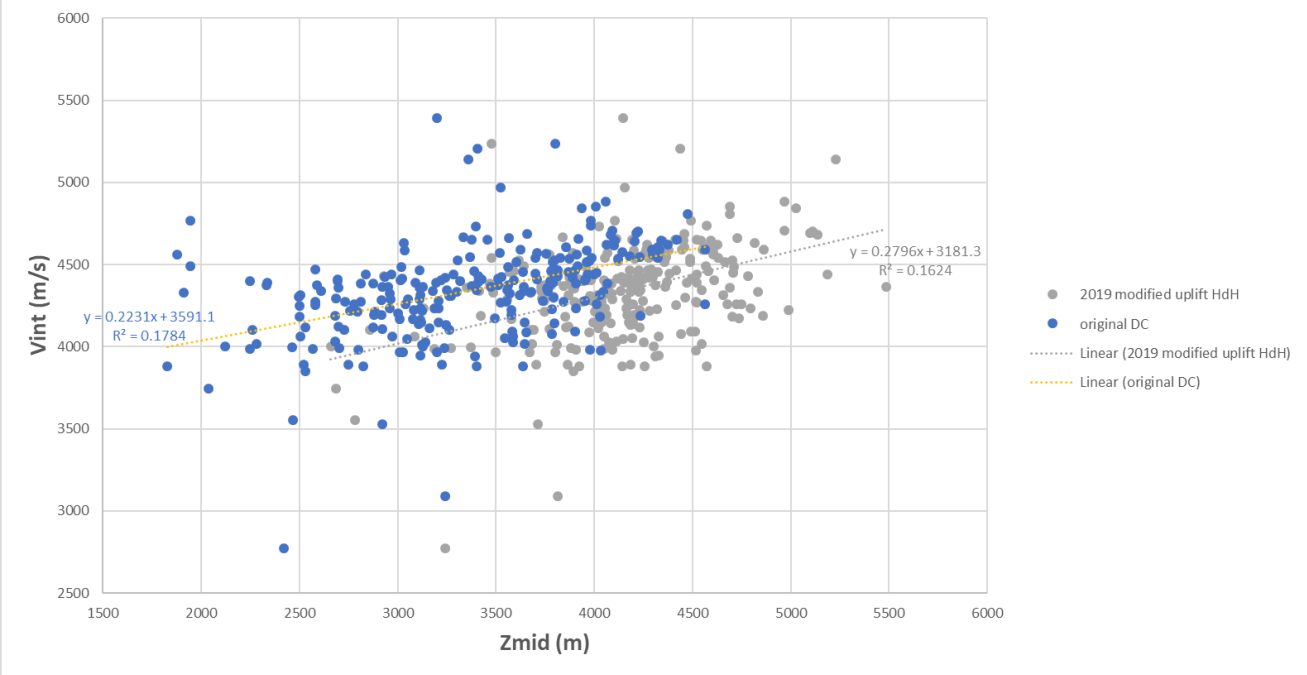

Figure 39. Comparison of original V_{int}-Z_{mid} data (blue) of the upper Carboniferous interval with data that was corrected for apparent uplift (grey).

5.3.6 Overpressure

The effective pressure is the difference between confining pressure and pore pressure and decreases with increasing pore pressure. Increasing effective pressures result in increasing P-wave velocity to an asymptote at high pressure. Consequently, P-wave velocities go down with increasing pore pressure and wells with overpressures at the upper Carboniferous interval should not be considered to derive a general velocity-depth trend. TNO holds a pressure database (the pressure SNS database, see www.nlog.nl/en/pressure-data) from which well wells were selected that have overpressures in the Limburg Group interval. For these wells the Vint-Zmid was plotted (Figure 40). Wells UHM-02 and LTG-01 show an overpressure of 187 and 140 bar, respectively. From the velocity cross-plot it is clear that the well UHM-02 plots distinctly below the regression line, while LTG-01 does not. The plot further shows that most interval velocities of the over-pressured Limburg Group intervals plot close to the regression line of all wells, i.e., including the normal-pressured wells. The overpressures are mainly in the order of 10-100 bar, and significantly lower than the overpressure in UHM-02. Possibly this relative low overpressure compared to the confining pressure is the cause for the fact that no lower velocities were found. The dataset is also relatively small and no quantification of the uncertainty in the over-pressure estimate is given (only qualitative uncertainties in the form of reliability (low, high) of the pressure measurements are present in the database).

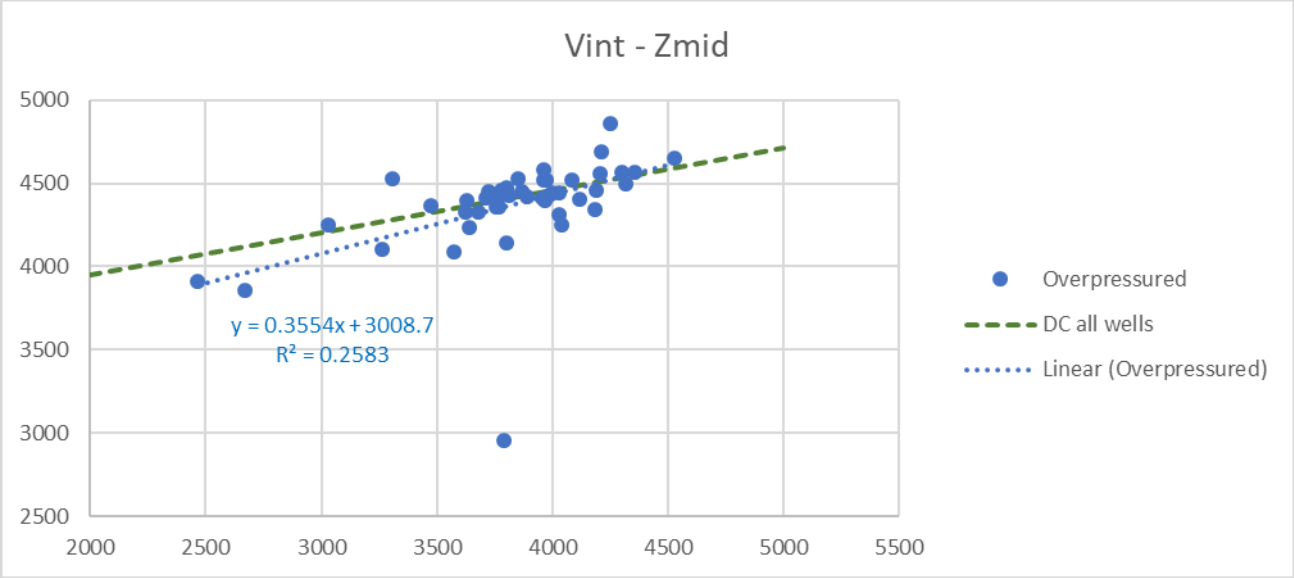

Figure 40. Carboniferous Vint (m/s) vs Zmid (m) of wells in which overpressure has been determined. The green dashed line represents the regression line of all Carboniferous wells, the blue dotted line the regression line of only the over-pressured wells

5.3.7 Execution of the time-depth (TD) conversion

The seismic interpretation results of the Lower Carboniferous Limestone Group (CL, i.e., the Dinantian below the DC interval) where first converted to point data, then time-depth converted using the V0,k method with the here- derived values k = 0.2524 s^{-1} and V_0 = 3448 ms^{-1}. After obtaining the interpretations points in depth (TDV) surfaces where generated using Petrel's convergent gridding algorithm. This sequence of seismic-interpretation data treatment was chosen to make sure that data density would remain equal and that the interpolation procedure would not affect the intermediate TD conversion results.

TD conversion Top Dinantian

For the conversion of the top Dinantian, the base Rotliegend (RO) from TNO's DGM-deep v5.0 model was chosen as reference. The depth of this surface was obtained using layer-cake velocity modelling using Velmod 4. it further requires this reference surface to be available in time (TWT) because time-thickness (ΔT_{DC}) between top Dinantian and the base RO reference is an input requirement. The true vertical depth of RO (Z_{RO}) is the second requirement. These parameters are input for the layer cake TD conversion formula, which calculates the depth (Z_{DC}) of the base of the DC interval (top Dinantian):

$$Z_{DC} = \left(\frac{v_0}{k} + Z_{RO}\right) \cdot e^{k \cdot \Delta T_{DC}} - \frac{v_0}{k}$$

TD conversion Base Dinantian

After the afore-described first conversion step, the top Dinantian interpretation points are available both in time (TWT) and depth (Z_{DC}). Where the base of the Dinantian is interpreted, the thickness is available in TWT. The same TC conversion formula is now used to obtain the depth of the CL interval (Z_{CL}), of the base Dinantian:

$$Z_{CL} = \left(\frac{v_0}{k} + Z_{DC}\right) \cdot e^{k \cdot \Delta T_{CL}} - \frac{v_0}{k}$$

Since an interval velocity of V_{int} = 6000 ms^{-1} for the Dinantian carbonates appears most representative, the thickness ΔZ_{CL} can (more) easily be obtained by multiplying the ΔT_{CL} with a factor 3 (in ms):

$$\Delta Z_{CL} = 3\Delta T_{CL}$$

Residuals and well-tying

By applying regional V0, k values as listed in Table 1, the calculated depth (Z) may deviate from the True Vertical Depth (TVD) observed in wells. This mis-tie is indicative for the goodness of the applied TD conversion. Table 4 lists the mis-ties between wells and the non well-tied grid of top Dinantian gridded surface (see section 6.7). Mis-ties are both positive and negative and the average mis-tie is 69 m. The use of one single velocity function, knowing that there is considerable spread in velocity information, importantly contributes to the mis-tie at well location. With a ~1000 m thickness of the overlying Limburg Group (DC), 1 SD of the velocity data corresponds to +/-150 m depth variation for the top of the Dinantian (Table 3). This value is in general agreement with the calculated mis-tie values. Moreover, mis-ties might be related to inaccuracies in the seismic interpretation as well.
Note that, subsequently, the generated maps for the base, top and thickness of the Dinantian interval were well-tied to the corresponding information in the wells. In other words, the well information was considered dominant over the TD conversion and the mis-tie at well location becomes zero.

Table 4: Listing of top Dinantian depths from wells (Z_{well}) and grid and their mis ties. Red and blue colours indicate where the well depths is greater, respectively, less than that of the depth grid. All depths in meter

well	Z_{well}	non-well tied top Dinantian grid	Mis tie
WSK-01	-4225	-4065	-160
KTG-01	-937	-805	-132
S02-02	-1847	-1818	-29
BHG-01	-2009	-2009	0
GVK-01	-885	-884	-1
LTG-01	-4304	-4345	41
UHM-02	-4670	-4718	48
P16-1	-2416	-2524	108
S05-01	-1158	-1281	123
CAL-GT-02	-1161	-1320	159
O18-01	-1552	-1727	175
CAL-GT-01	-1422	-1694	272
Average			**69**
Stdev			**112**

5.3.8 Discussion

Velocity in sediments are dependent on many parameters. Making a velocity model is a simplification of the variations in velocity that are present in the subsurface. The Carboniferous strata covering the Dinantian limestones consist of shales, sandstones and coals. The coals have a significantly lower P-wave velocity than the sands and the shales that show to a large extent overlapping velocities. The presence or absence of coal rich intervals like the Maurits Formation will have an impact on the interval velocity of the Carboniferous. To incorporate this in a velocity model requires detailed mapping of this interval. This could be done in areas of good quality 3D seismic data but is deemed to be unsuccessful in other areas. Apart from the coals also variations in porosity, lithology/mineralogy, diagenetic processes like dissolution and/or precipitation of minerals, fracture density, weathering surfaces, fluid content, will have an influence on velocity and can only be captured in (local) velocity models if sufficient knowledge about these variations/processes is available. In a mapping exercise on national scale these effects can't be incorporated resulting in a velocity model that is fit for purpose but has significant uncertainty values attached.

5.3.9 Conclusions and recommendations

- From the scarce dataset of wells that penetrate the Namurian it is found that the Namurian series shows similar velocity behaviour as the Westphalian series. This is not unexpected since lithologies within these series are quite comparable. Therefore, it seems unnecessary to pick the Top Namurian on seismic data and derive separate velocity functions for these intervals.
- Subdivision of the interval velocity data cloud into structural elements using the *Stratpiler* approach (Kombrink et al. 2012) shows that wells in inverted areas have elevated interval velocities. The non-inverted area shows a linear increase in velocity.
- Linear regression of the interval velocity (Vint) against mid-depth of the Carboniferous interval for all areas combined results in a *k* of 0.2524 s^{-1} and a V_0 of 3448 ms^{-1}, while excluding the data of the inverted areas results in a k of 0.3188 s^{-1} and a V0 of 3213 ms^{-1}.
- In a regional study the first function can be applied, while in more local studies in non-inverted areas the second function is more suitable. If working in an inverted area, more area specific research is necessary to estimate the effect of the inversion on the velocity. Since the amount of inversion is highly variable in inverted areas no general rules/corrections can be given yet.
- A successful TD conversion of the seismic interpretation results of the top and base of the Dinantian interval require (next to the velocity parameters, v0 and k) the top of the Upper Carboniferous interval (the base Rotliegend) to be present both in TWT and TVD.
- Mis-ties between well- and grid depths can be considerable (max. 272 m) when applying regional values for the velocity parameters v_0 and k. Well-tying the grids does solve the mis-ties.

6. Results

6.1 Seismic interpretation of the top and base Dinantian

Given the great variation in seismic data quality (see section 4.1) and the fact that a large number of data was cropped at 4000 ms, not at all available lines and surveys provided an interpretation of the top Dinantian level (see Appendix 9.7). Not surprisingly, the depth issue is of even greater impact for the interpretation of deeper levels, i.e., interpretation density of the base is even smaller (see Appendix 9.8). The interpretation density maps show that especially in the southern half of the Netherlands (where 2D data prevail), the results are patchy. The seismic interpretation coverage rapidly decreases going from the Brabant high northward into the West Netherlands and Roer-valley grabens and gets sparser in the central part of the Netherland, i.e., around the Central Netherlands High. This is largely due to the depth position of the Dinantian interval in combination with structural complexity of the area under investigation.

6.1.1 Rijnmond to coastal Zeeland

Long, regional lines and composites form the basis (framework) for the seismic interpretation in the data-poor southern half of the Netherlands. Here the solution of the Depth to Magnetic Source is often used as guidance for interpretation as it is inferred to locally represent the top Devonian (base Dinantian) level. The followed approach is that the Rijnmond 3D survey, via the Maasvlakte, is calibrated to coastal wells off Zeeland using a number of good 2D lines. For the Rijnmond 3D area this correlation resulted in a top Dinantian up to 600 ms deeper than the existing TNO map of that area. The Zeeland and Rijnmond interpretation were further checked and matched with the existing offshore 3D top Dinantian interpretation from EBN/Panterra. Although the Dinantian is improperly imaged in onshore Zeeland, the coastal interpretation could be connected to the LBM platform edge using several of the better lines. Around well RSB-01 interpretation focused on connecting the Roer Valley Graben to the LBM via a single 2D line (#7013). This worked out well as significant faults are absent here.

6.1.2 Basalt sills around Bronkhorst 3D and WSK-01

The basalt sill observed in WSK-01 (see section 4.1) sub-horizontally crosses the lower Namurian sequence and appears to have an equivalent 20 km to the west in the Bronkhorst 3D survey (Figure 42: Left: Seismic profile (B/W/ wiggle display)through the 3D Bronkhorst survey showing a strong reflective doublet that might be comparable to the situation around well WSK-01. Right: 3D view of the same seismic section with auto-track result of amplitude mapping (auto-track) of the basaltic sill. The fault planes (blue) might have acted as conduit for the intrusion. Amplitudes of this reflection show a strong correlation with, and appear to radiate from a strike slip fault that also trends along dyke intrusions calculated from the magnetic data.

6.1.3 The Sloten-Schagen 3D area

This area is isolated and hard to calibrate with other areas. Apart from seismic data that is hardly useable for deeper event interpretation this area shows significant structural deformation. Without further reprocessing and additional seismic lines for accurate well ties, the degree of freedom in interpretation remains large here. The slightly concave downward structure? of the interpreted top Dinantian just north of a complex fault zone (continuation of the Raalte FZ?) give some vague indications of mounds (Figure 43). Note that this situation is comparable to the setting near the Luttelgeest mound/platform structure.

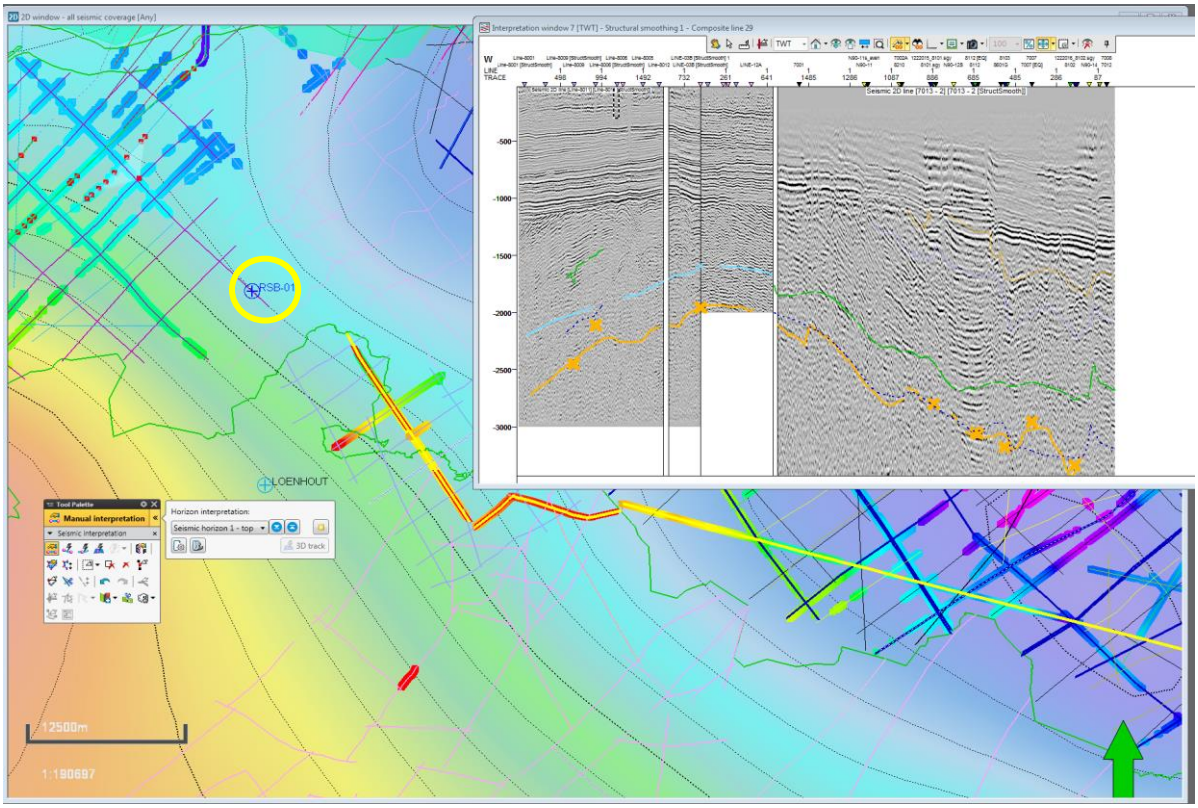

Figure 41: Connection from RSB-01 (encircled) with the RVG area basinward to the E.

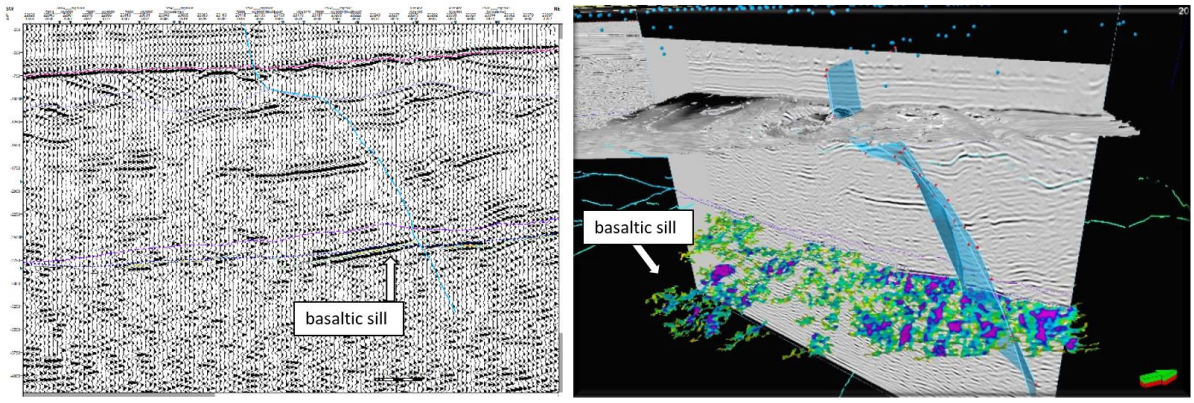

Figure 42: Left: Seismic profile (B/W/ wiggle display)through the 3D Bronkhorst survey showing a strong reflective doublet that might be comparable to the situation around well WSK-01. Right: 3D view of the same seismic section with auto-track result of amplitude mapping (auto-track) of the basaltic sill. The fault planes (blue) might have acted as conduit for the intrusion.

6.1.4 The Californië area

A flattened (on top Dinantian) seismic section (Figure 44) suggests the presence of a large half graben since at least Devonian times. This graben shows westward thinning sediments and westward increase in thickness and reflection strength of the Dinantian and Devonian sequence. The Dinantian carbonates appear to thin on the east, provide a final phase basin fill west of the California wells. However, the German well Wachtendonk-1 on the eastern fault block in the line, is reported to have a few hundred meters of dolomites under this top

Dinantian reflector. These dolomites have apparently no seismic response, and their dating as Dinantian might not be correct.

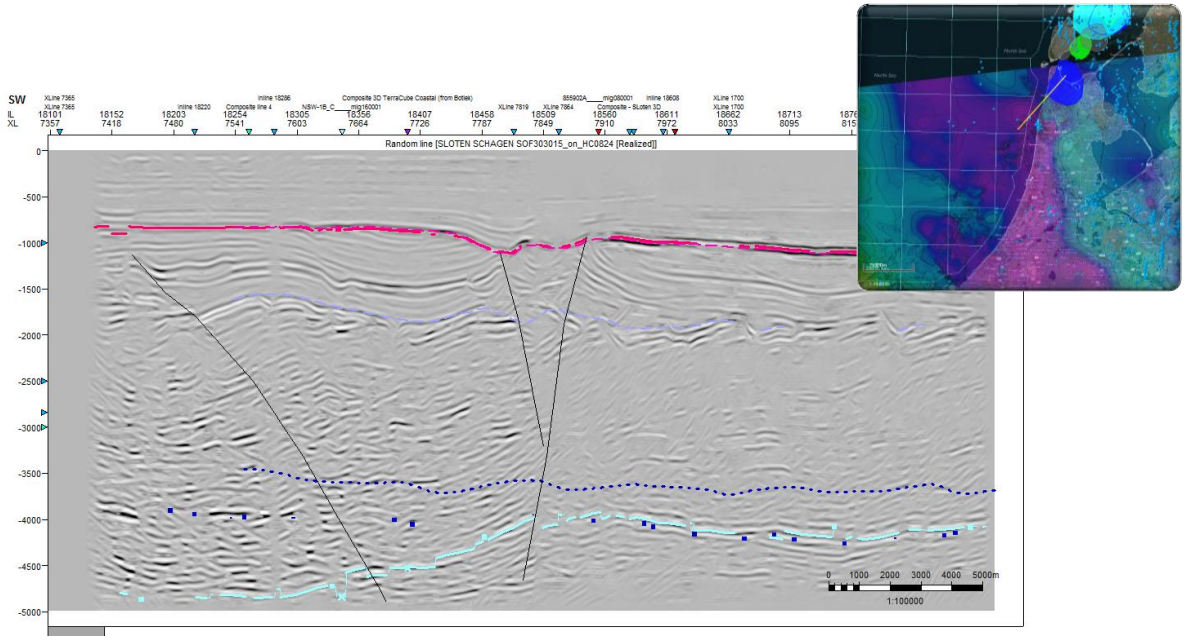

Figure 43: SSW-NNE seismic section through the Sloten-Schagen 3D survey showing mound-like structures in the top Dinantian horizon (light blue). See inset for locality. Older TNO interpretation in dark blue squares. Blue square dots:

6.1.5 The Maasbommel High

The Maasbommel High between Venray and Wijchen in general has (very) poor seismic coverage. After data conditioning a weak carbonate mound emerges with a signature comparable to mounds observed in Luttelgeest and offshore Zeeland.

6.1.6 Central Netherlands

The 2D seismic cover in the Central Netherlands area (the strip from Zaandam-Amsterdam-Utrecht-Utrechtse Heuvelrug-Amersfoortse Vallei-Veluwe) is extremely low and the available data is generally of poor quality. With data being cropped at 4 seconds TWT most data is not suitable for interpretation of the Lower Carboniferous. Indications from the Deep NAM 84 line supported by fragments of Rijnmond 3D and some of the 2D on the Maasbommel High suggest that the top Dinantian is here well below the maximum trace depth of the 2D data. This depth range is generally consistent with the depth estimated from the low-pass filtered versions of the- total magnetic intensity map of the Netherlands (results from WP 2.1.3). Older interpretations, such as the pre-SCAN TNO top Dinantian map are not supported and appear to be often inspired by a phantom (multiples) of the inverted Mesozoic horizons. The 2D density slightly improves on either side of the Central Netherlands seismic data gap, i.e., south of the Oude Rijn and Waal rivers and north in the Markermeer to West Flevoland area. However, the cropping at about 4 s TWT here also impeded interpretation of the deep Dinantian.

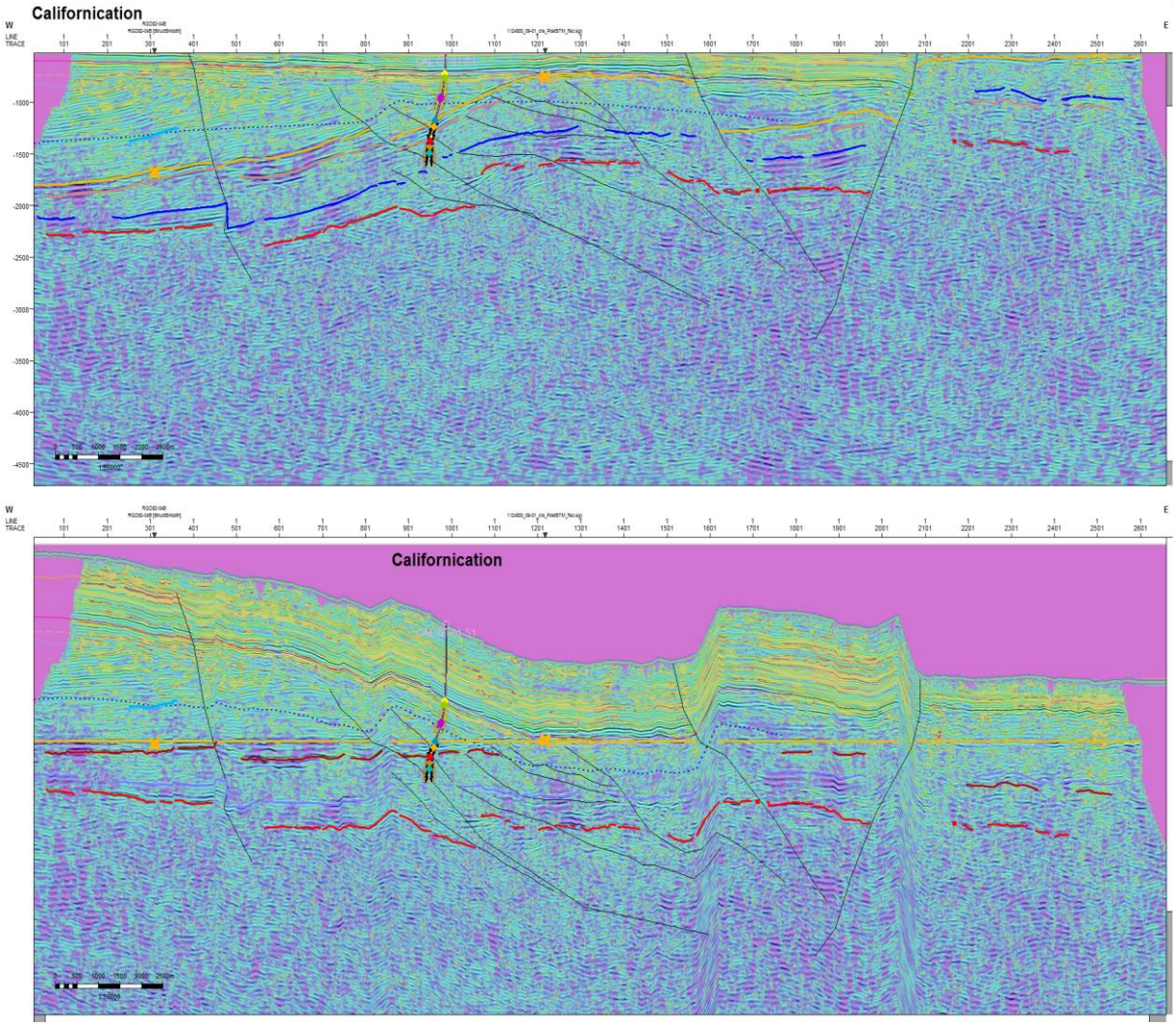

Figure 44: WE 2D seismic section crossing the well CAL-GT-01-S1 well. Data shown as B/W amplitudes with dominant frequency colour overlay. Section displayed both unflattened (above) and flattened on top Dinantian shown in yellow (below). Pink horizon represent base of the Dinantian carbonates, Dark blue reflector likely represents the base of the acoustically transparent Devonian, the red reflector could be top ?Basement, i.e., the top of a more chaotic and lower amplitude interval. Fault pattern is indicative of compressional reactivation of pre-existing Devonian half-grabens.

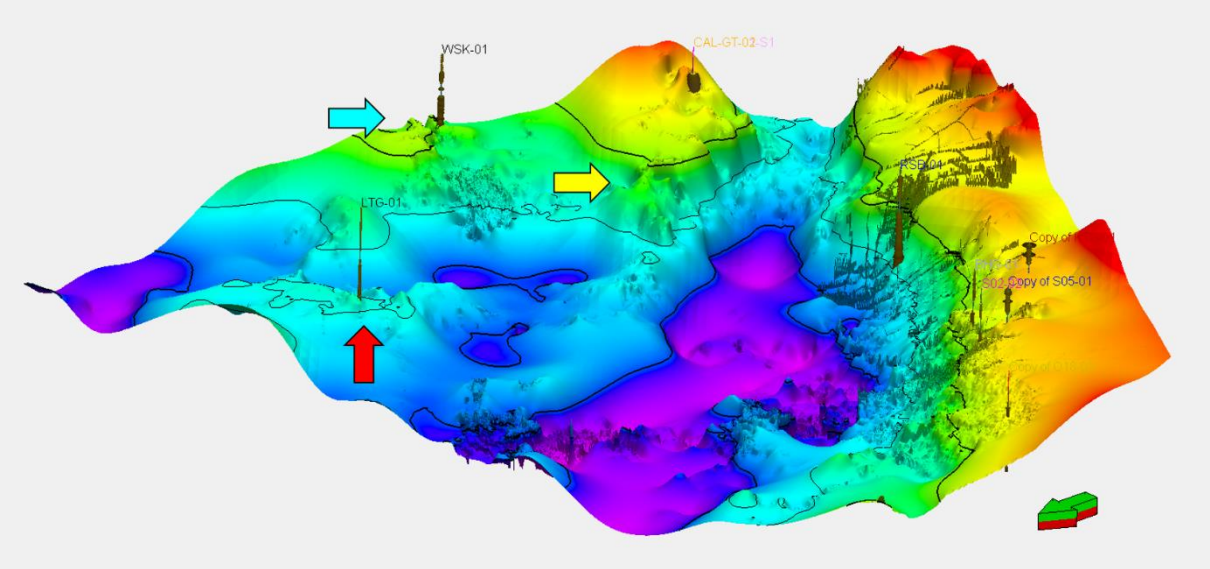

Figure 45: 3D view to the SE of the top Dinantian TWT surface showing the location of elevated Dinantian topography (?mounds) at Luttelgeest (red arrow), Winterswijk (blue arrow) and the Maasbommel High (yellow arrow).

6.1.7 Connecting the 2D data fringe along the Texel-IJselmeer High to Friesland

In a 2D seismic section connecting the northern 3D area around the Friesland carbonate platform to the central Netherlands faults zone it becomes clear that the topography of Dinantian carbonate structures diminishes to the south (Figure 46). The overall northward dip of the Dinantian substratum gives the impression of northward thickening wedge of Devonian and Dinantian strata that is structured in a tilt-block half graben arrangement (Figure 47). The larger fault blocks occur in the north and have higher uplifted fault crests. Smaller fault blocks occur in the south near Luttelgeest and Nagele.

6.1.8 3D covered area Northern Netherlands

In the northern part of the Netherlands, many 3D data exist, and the coverage of the seismic interpretation is dense (see Figure 1 and Appendix 9.5). In most areas it is possible to interpret the top of the Dinantian interval. It should be noted, however, that with limited well control this interpretation is not constrained everywhere. The distant UHM-02 and LTG-01 wells are the only wells in the northern 3D area that penetrate the Dinantian interval. However, both are positioned at carbonate platform localities and not one single well penetrates the intra platform domains. The well tie at UHM-02 (Figure 48) shows that the Namurian-Dinantian transition is very distinct in the logs as it is represented by a change to very low GR and high and constant velocity (low DT). This jump to a high velocity contributes to a huge acoustic impedance contrast and is seen as a low-frequency, high reflective seismic doublet. Where this doublet can be easily traced, it defines a platform geometry with considerable carbonate thickness (662 m in UHM-02).

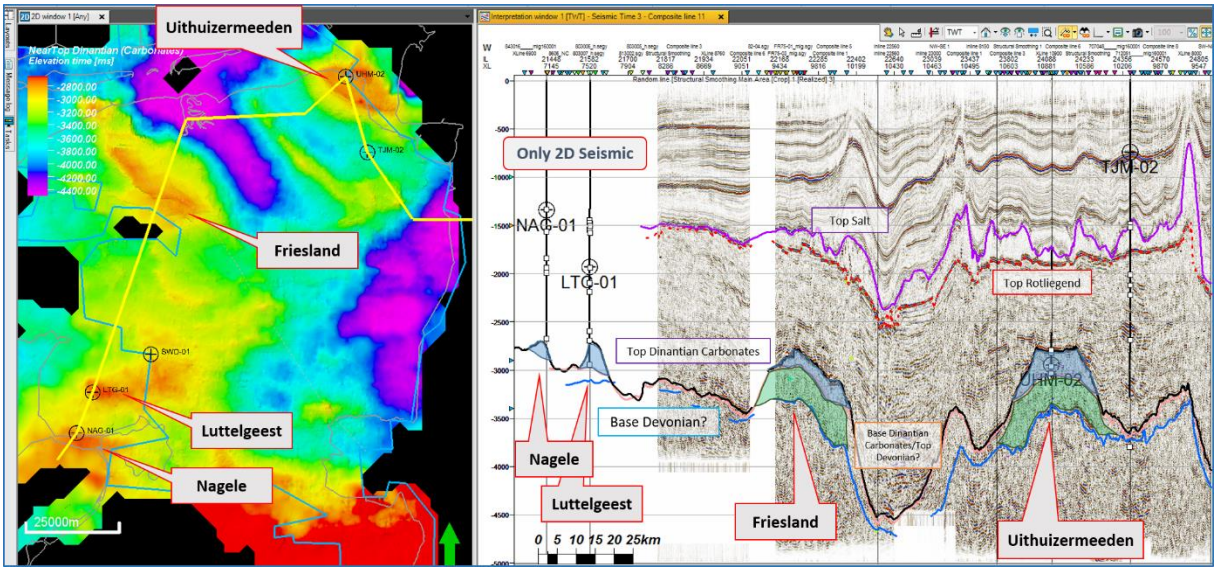

Figure 46: Right: SW-NE Random Line (approximately 175 km, highly vertically exaggerated), showing the relationship between the Carbonate build-ups and the Devonian sequence. This section suggests the northward tilt of individual fault blocks on which both the Dinantian (transparent blue) and Devonian (transparent green) are thicker developed. Left: TWT depth map of top Dinantian with trace of the random line shown.

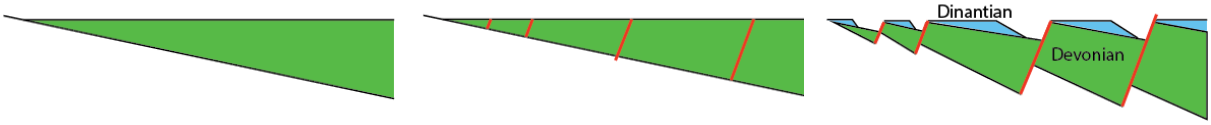

Figure 47: Conceptual model for the Devonian: Dinantian development of the northern part of the Netherlands

Where the Dinantian thickness diminishes, the doublet and high reflectivity vanishes, suggesting that either thickness is below the limit of separability or the carbonates are absent in the intra platform areas. The base of the Dinantian succession can be interpreted since the depth position is known from the well UHM-02. The impedance contrast at the base is low, however, and low amplitude reflections are to be expected. The top Devonian (base Dinantian) reflector can readily be interpreted since it is characterized as onlap surface. Here it shows (SW to NE) onlap of the Visean limestone against an inclined substratum with Devonian clastic of the Devonian Banjaard Group. The onlap geometry suggest that Dinantian stratigraphy older than that encountered in UHM-02 may onlap the tilted Devonian from the south. This notion is also based on the PaleoScan results presented in section 2.2.2 and Figure 30. This may imply that the Tournasian sequence, which is missing in the base of well UHM-02, might be present further downslope and caution should be taken when regarding the encountered well stratigraphy as representative for the larger area.

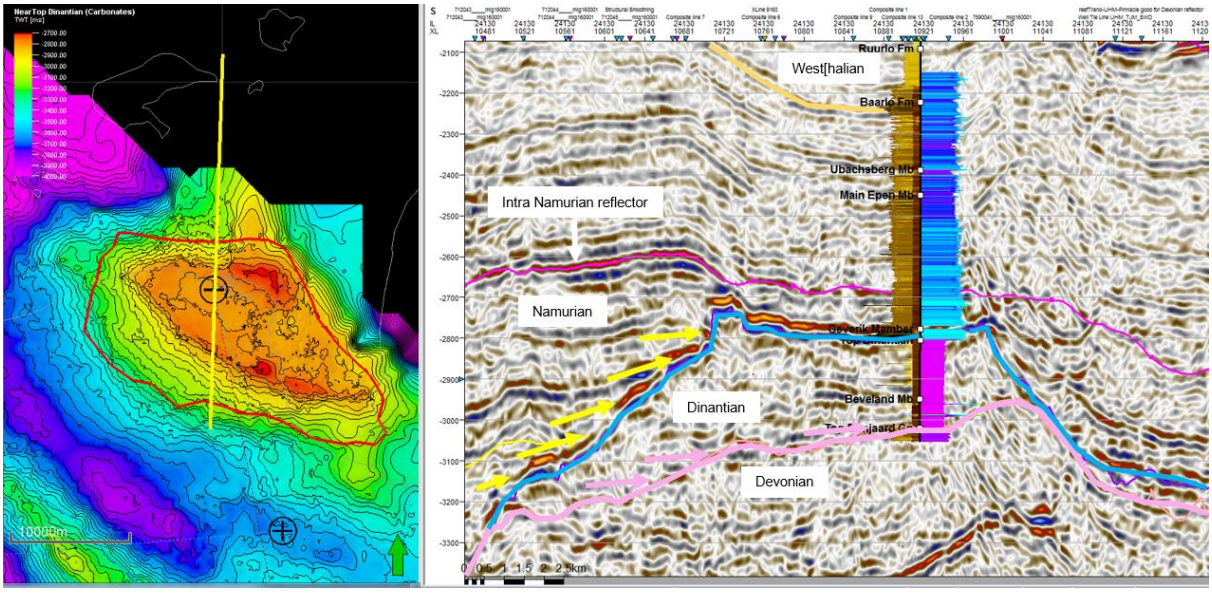

Figure 48: Platform geometry of the top Dinantian at and around well UHM-02. Left: map view of interpolated interpretation result, in yellow the position of the N-S section shown right. Right: seismic section through the UHM platform, with well logs of UHM-01 superposed. Here it shows onlap of the Dinantian limestone against an inclined substratum where Devonian clastic of the Devonian Banjaard Group are found (pink arrows). The platform top and slope are defined by LF-HR reflectors (doublets; blue line); the slope is further defined by the onlap of Namurian strata (yellow arrows)

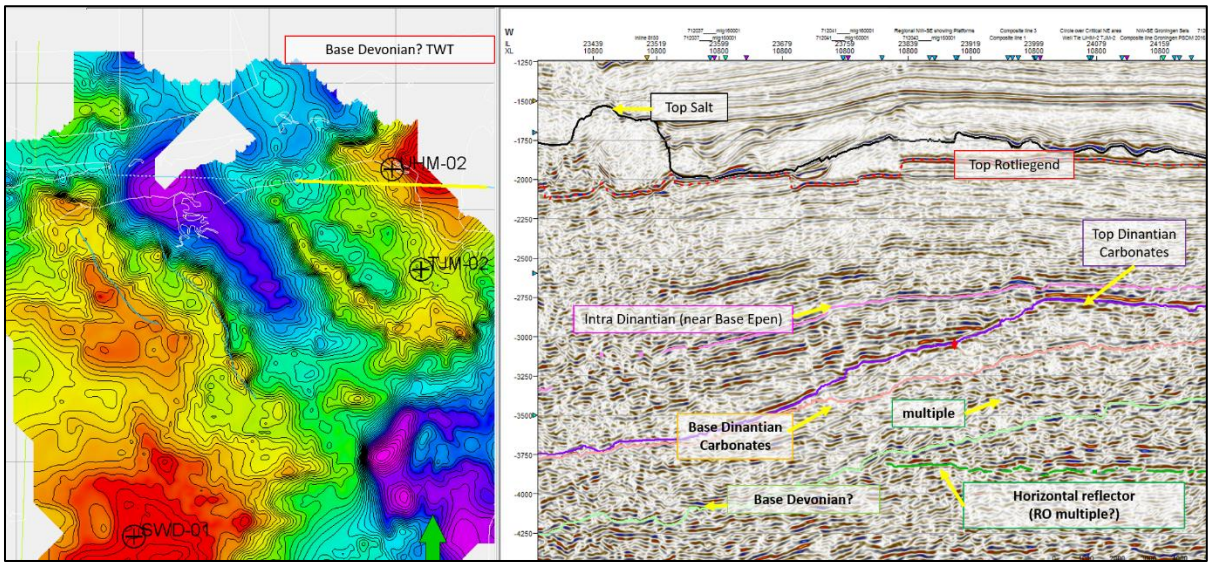

Figure 49: SSW dipping geometry of the top Devonian at and around well UHM-02. Left: map view of interpolated interpretation results, in yellow the position of the E-W section shown right. Right: seismic section through the UHM platform, showing top and base of the Dinantian. Here it also shows that the reflection amplitude is related the thickness of the carbonate interval as explained in the text. Horizontal reflectors cross-cutting the Devonian interval are either multiples or interbed multiples related to the top Rotliegend and/or dense lithologies (such as anhydrite stringers) in the Zechstein Group.

6.2 Seismic interpretation of other horizons

Other horizons were only interpreted within the northern 3D area in order to get a better hold on the structuration and thickness distribution of the Dinantian carbonates. These include:

6.2.1 (Near) Base Devonian

The Devonian interval is encountered in wells UHM-02, LTG-01, and WSK-01 in the northern part of the studied area. In seismic reflection data, the Devonian appears as a series of parallel reflectors with an angular conformity at its base. This unconformity is tentatively interpreted as the base Devonian (see also Figure 49)). The seismic imaging of this Devonian interval is hindered by multiples and reflection characteristics laterally vary quite dramatically. Notwithstanding these issues, the (near) base Devonian interpretation results in a consistent map view (Figure 50). The TWT thickness distribution of the Devonian interval (calculated from the base and top Devonian maps shows that the Devonian interval is thickest developed on structural highs and reaches minimum thickness in the intervening lows (Figure 51). Note the large thickness at the platform localities (red contours) and very limited thickness in intervening areas.

6.2.2 Intra Namurian (near base Epen Fm)

An intra Namurian reflector demarcates the top of a high reflective interval that onlap onto the Dinantian platform geometries (Figure 49). The interval above is more acoustically transparent and has an onlapping and draping geometry on top of the Dinantian platform topography. Locally this transition can be seen as a mild (angular) unconformity. This interval was interpreted (Figure 52) to allow thickness maps to be generated and for the purpose of structural restoration (Bouroullec et al., 2019). Based on seismic-to well tie of wells UHM-02 and TJM-02 it follows that this level closely corresponds to the Base Epen Formation.

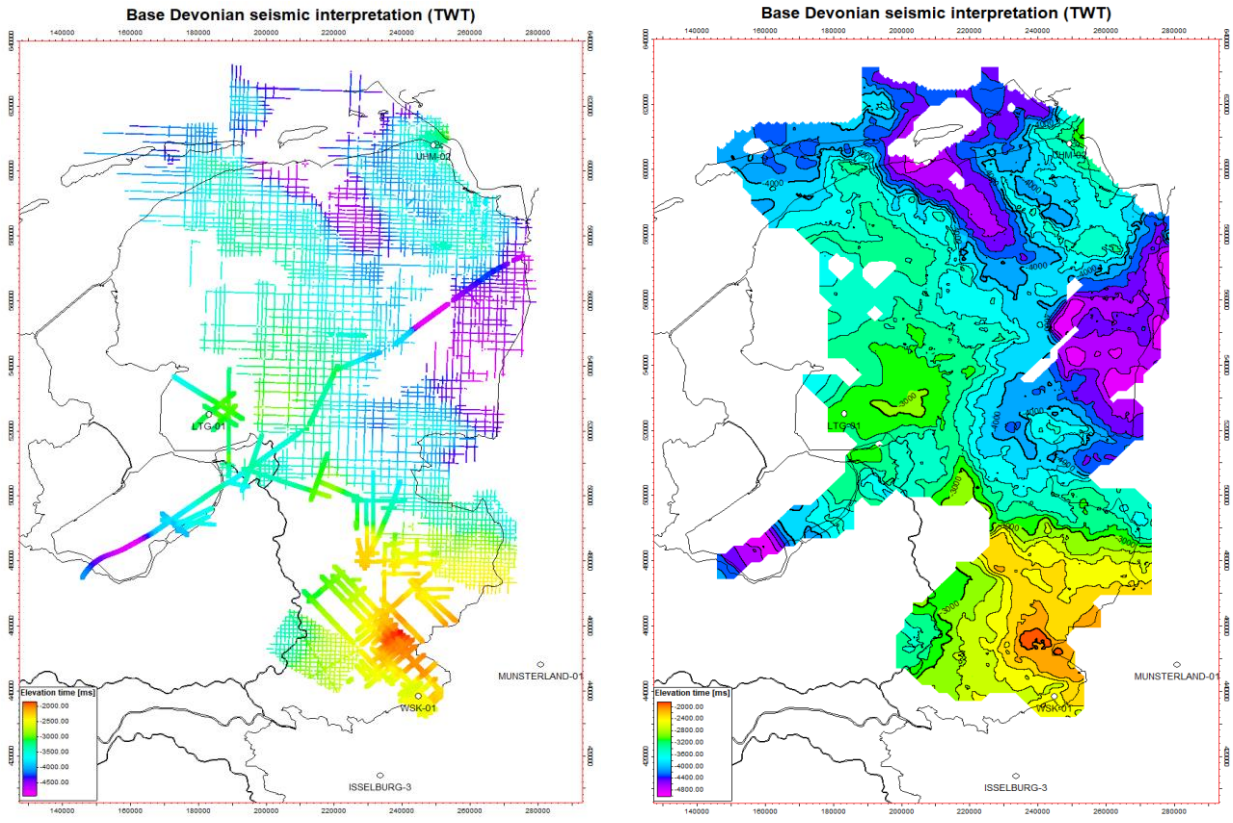

Figure 50: Interpretation (left) and TWT map of the (near) Base Devonian

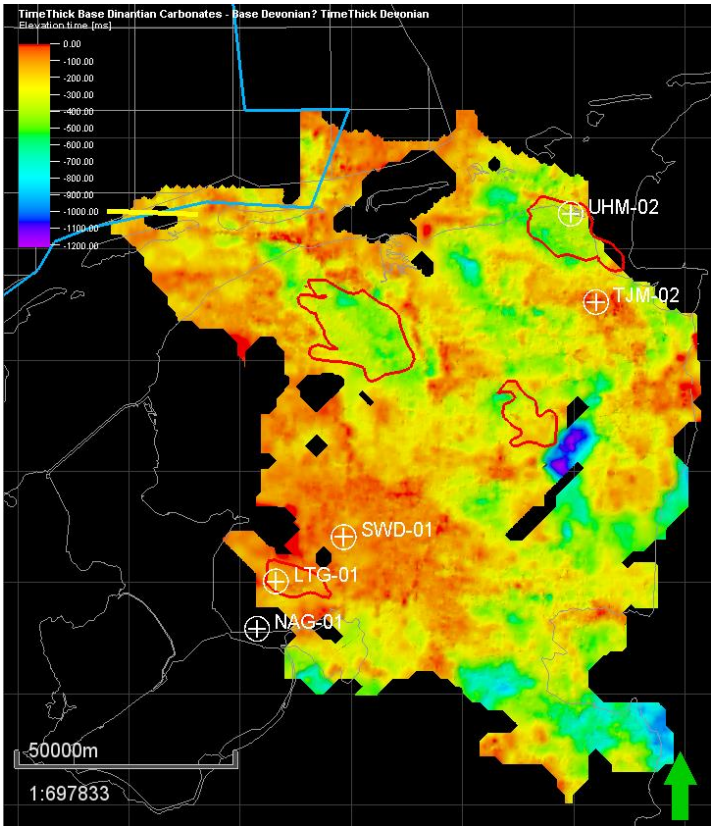

Figure 51: TWT thickness of the Devonian interval

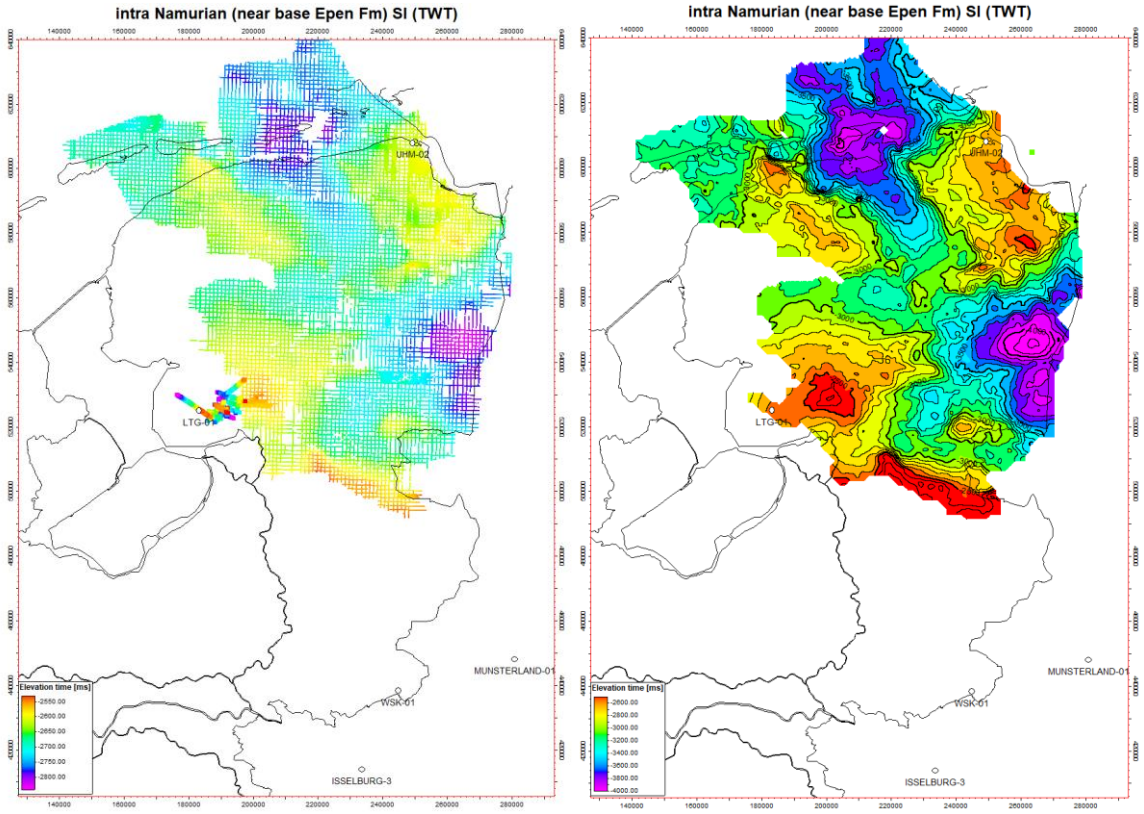

Figure 52: Interpretation (left) and TWT map of the (near) intra Namurian horizon

6.3 Interpretation uncertainties

The majority of the West and Central Netherlands basin 2D seismic is inadequate in quantity, quality and vertical reach to image the deeper levels of the Palaeozoic formations. Almost all 2D data is cropped at 4000 ms TWT, near absent in the central part of the Netherlands and poorly processed, with a focus on the Cenozoic and Mesozoic oil and gas targets.
The same problem holds for large parts of 3D seismic data, which is of very poor quality at deeper levels. The data is usually cropped at 5000 ms TWT, sometimes less (e.g. near Sloten and Assen). Stacking velocity models below the base Permian were usually flooded with oversimplified assumptions (constant velocity) or wrong gradients. Moreover, well data for the Lower Carboniferous levels are very sparse.
As a result of this lack of data constraints, various interpretations (different vintages, different interpreters) can diverge significantly in places. In such places, the choice of picking the right reflector often becomes more a matter of the model in mind, than a data driven, auto-track exercise with stringent controls. Faults at deeper levels are hard to pick up, fault planes can seldomly be mapped on 2D seismic data. This results in a risk of cycle-skipping into younger stratigraphic sequences that have better reflection characteristics.
It should be kept in mind that in the absence of more well control and until an overall image improvement has been achieved, each interpretation could be considered as a viable if not equiprobable realization of top Dinantian in TWT domain.
In an effort to indicate areas of divergence in interpretations, various polygons have been created that allow for clipping and selection of interpretation data. Generally, areas of low divergence exist in the better imaged parts of the MegaMerge 3D cube over the Groningen and Friesland highs, some parts of the Sloten 3D survey and over the 2D cover of Luttelgeest: Noordoost Polder and contiguous northern IJselmeer. The resulting merged interpretation data sets of the base and top Dinantian, to date, acts as the most probably representation (see Appendix 9.7 and 9.8). Areas without interpretation (white spots) are left intentionally blanked in the resulting depth maps.

6.4 Faults

Faults were interpreted on individual 2D lines where they significantly improved the understanding of tectonic movements. But given the sparseness of the 2D lines, and the lack of quality at target levels, these isolated fault observations could not be correlated and merged into a proper fault network. In the 3D areas faults have been interpreted. However, the expression of faults at depth is too variable to allow for connection of fault interpretations (i.e. fault sticks) between individual lines of the 3D surveys. The complexity of the fault zones leaves too much room for fault plane and -network construction at greater depths. To date, the existing fault interpretations only serve to illustrate the structuration of the Dinantian target level, rather than being the basis for a consistent and complete fault data set.

6.5 DTMS vs. Dinantian interpretation

The Depth to Magnetic source (DTMS) solution (Figure 53) shows a simple symmetrical basin-and-range configuration with NNW-SSE trending highs and lows. Most highs are delineated by margin/boundary faults that, based on seismic interpretation, can be also confirmed at the Dinantian level and possibly are of Palaeozoic origin. Early Palaeozoic subsidence has caused the backstepping of the Visean platform margins as inferred from seismics and facies analysis of wells O18-1 and P16-1 (see report WP facies). The suggested locations of mounds and platforms in the offshore WNB realm is an indication that carbonate deposition persisted very close to the ZH coast. The location of carbonate mounds and

platforms appear to line up with the location of structural highs supported by magnetic dykes as can be inferred from the magnetic modelling work (WP 2.1.3.).

6.6 Seismic interpretations in support of Dinantian carbonate facies distribution

Carbonate mounds and platforms occur mainly along the London Brabant Massif, the Luttelgeest and Maasbommel Highs. The mounds appear to occur only within the middle Dinantian Schouwen Member. Along the LBM the mound topography is levelled and filled in by the platform carbonates of the Goeree Member (e.g. Figure 6). The Luttelgeest mound appears to be of similar age but lacks the Goeree cover (pers. comm. Peter Gutteridge). Some mounds occur further north, i.e. at the foot of the LBM platform rim in the deeper paleo basin where they lack the drape of the Goeree Member. Most of these "toe-of slope mounds" are ill-defined on most seismic images, but reflection patterns give an impression of elevation.

In most of the West Netherlands and Roer-valley Basins as well as Schagen-Sloten area, the Dinantian appears to be a thin reflective unit where top and base can hardly be separated in seismic data.

Note that the Dinantian near Californië has the same appearance to the east of the well CAL-GT. The reflective sequence here gradually thickens (north)westward, perhaps towards what could be the core of a platform/build-up on the Maasbommel ridge at the midpoint of the line between WSK-1 and RSB-1 wells. The Maasbommel High has a platform character comparable to that offshore Zeeland and as seen in Luttelgeest. Thus, the Maasbommel High appears to extend via Utrecht into a 'Sloten' (edge of IJsselmeer High) and seems to represent an important Early Carboniferous basin boundary.

In most of the Zuid Holland, Noord Holland, Utrecht, Flevoland, Markermeer areas, there is no evidence of mounds or thick carbonates. Admittedly, seismic coverage is sparse here, but where a Dinantian image exists, it is represented as a thin (one or two loop) reflective sequence seen also to the east of the California wells and visible as the basal unit (Beveland Mb) that extents from the offshore Zeeland wells far into the West Netherlands Basin. This northward extension is much further than that of the middle Dinantian mound-prone Schouwen member and upper Dinantian Goeree Member.

Since seismic resolution did not allow to interpret individual sequences within the Dinantian interval, the facies distribution maps of Mozafari et al., (2019) can only be compared with the top geometry of the Dinantian. This does not withhold that the seismic image of some 2D and 3D surveys could be consulted for generating the facies map as they give a "feeling" of presence and distribution of facies types in relation with structure. Predominantly, Sequence 2 and 3 (Moliniacian-Livian and Warnantian) facies maps have been compared with, and were deemed necessary, amended by the seismic interpretation of the top Dinantian (Figure 54; Appendix 0). These amendments are specifically focusing on delineating areas with different types of carbonate structuration, i.e. platforms, slopes, mounds, basinal (deep), and basinal structural highs.

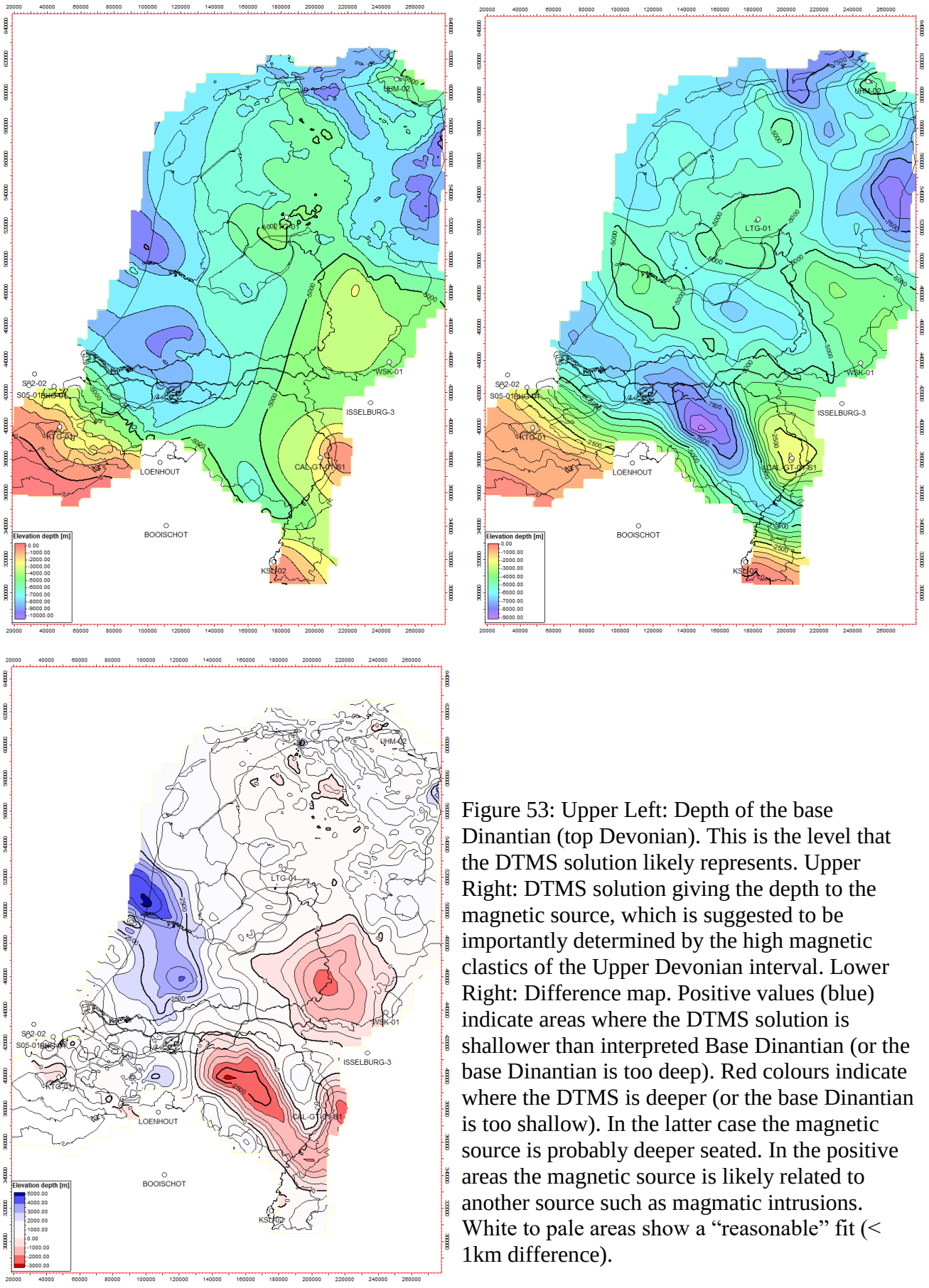

Figure 53: Upper Left: Depth of the base Dinantian (top Devonian). This is the level that the DTMS solution likely represents. Upper Right: DTMS solution giving the depth to the magnetic source, which is suggested to be importantly determined by the high magnetic clastics of the Upper Devonian interval. Lower Right: Difference map. Positive values (blue) indicate areas where the DTMS solution is shallower than interpreted Base Dinantian (or the base Dinantian is too deep). Red colours indicate where the DTMS is deeper (or the base Dinantian is too shallow). In the latter case the magnetic source is probably deeper seated. In the positive areas the magnetic source is likely related to another source such as magmatic intrusions. White to pale areas show a "reasonable" fit (< 1km difference).

6.7 Map representation of results

The results of the seismic interpretations of the areas described above are combined into two data sets of the top and base of the Dinantian carbonate sequence, respectively.
The seismic interpretation results where first converted to point data, then time-depth converted using the V0,k method (see page 58 and further). This sequence of seismic-interpretation data treatment was chosen to make sure that data density in the depth domain remains equal to that in the time domain, i.e. the interpolation procedure does not affect the intermediate TD conversion results. After obtaining the interpretations points in depth (TDV), surfaces where generated using Petrel's convergent gridding algorithm. The surfaces are tied to the respective data at well location (using a 3 km influence radius) to produce well-tied maps. Gridding was only performed within the limits of the interpretation. For this purpose, polygons were created for top and base of the Dinantian.
The interpretation of the top Dinantian is already challenging, but the coverage of the base interpretation is even smaller. This is not only due to the limited data quality at depth but is also due to the fact that in large parts of the study area, the Dinantian thickness is below the limit of separability, i.e., a the top and base are represented by one single reflector.
Note that thickness can only be calculated there where the base Dinantian was interpreted. Consequently, the thickness map has the same coverage as that of the Base Dinantian.
Additional polygons were constructed that are based on the experience of the seismic interpreter and serve to indicate data-poor areas or areas where the image of the Dinantian is poor. These polygons were only created for the top Dinantian, but also apply to deeper levels, and were used to blank the maps inside the interpretation polygons.

6.8 Conclusions

In a setting of low to moderate data quality and -coverage a rough and patchy picture has been painted of a possible Dinantian surface that, generally, provides a deeper interpretation than the pre-SCAN 2014 TNO map of the 'top Dinantian' (Figure 55; Appendix Difference top Dinantian TNO (2014) and SCAN (2019)9.9).
The new interpretation of the top Dinantian map in the SW Central Netherlands has been compared with, and where deemed correct, combined with existing on- and offshore interpretations. As the interpretation of the base Dinantian was of even greater challenge, the resulting information on the thickness distribution, to date, is limited. The presentation of the depth-converted interpretations in map view shows a simple symmetrical basin and range geometry with NNW-SSE trending margins/boundary faults, in places offset by a conjugate system of WNW-ESE trends. It combines the West Netherlands and Broad Fourteen Basin as well as the Roer Valley graben in one single graben domain and separated two structurally accentuated areas to the north and south. The paleogeographic image that has been painted in conjunction with analysis of well sedimentology suggests that features setting these subdomains apart must be of Mesozoic and younger origin.
A continuous and at stages rapid subsidence of this enhanced West Netherland Basin can be deducted from the backstepping of Dinantian carbonate formation members as seen on along the London-Brabant High. The localized presence of mounds in the now deeper part of the WNB offshore towards the Winterton High is associated with a predominant Low Frequency and thin seismic interval representing the Beveland member in most of the Basin. This would suggest that carbonates occur in most parts of the deep Early Carboniferous basin of West Netherlands, though thin and neither containing the full threefold sequence as developed on the Brabant High, nor the partial sequence as appears to characterize the Luttelgeest mound (Goeree Member missing) and UHM platform (Beveland Member missing).

The Central Netherlands High forms an important boundary between the thin basinal Dinantian interval and an area with more pronounced paleo-topography. Next to prominent

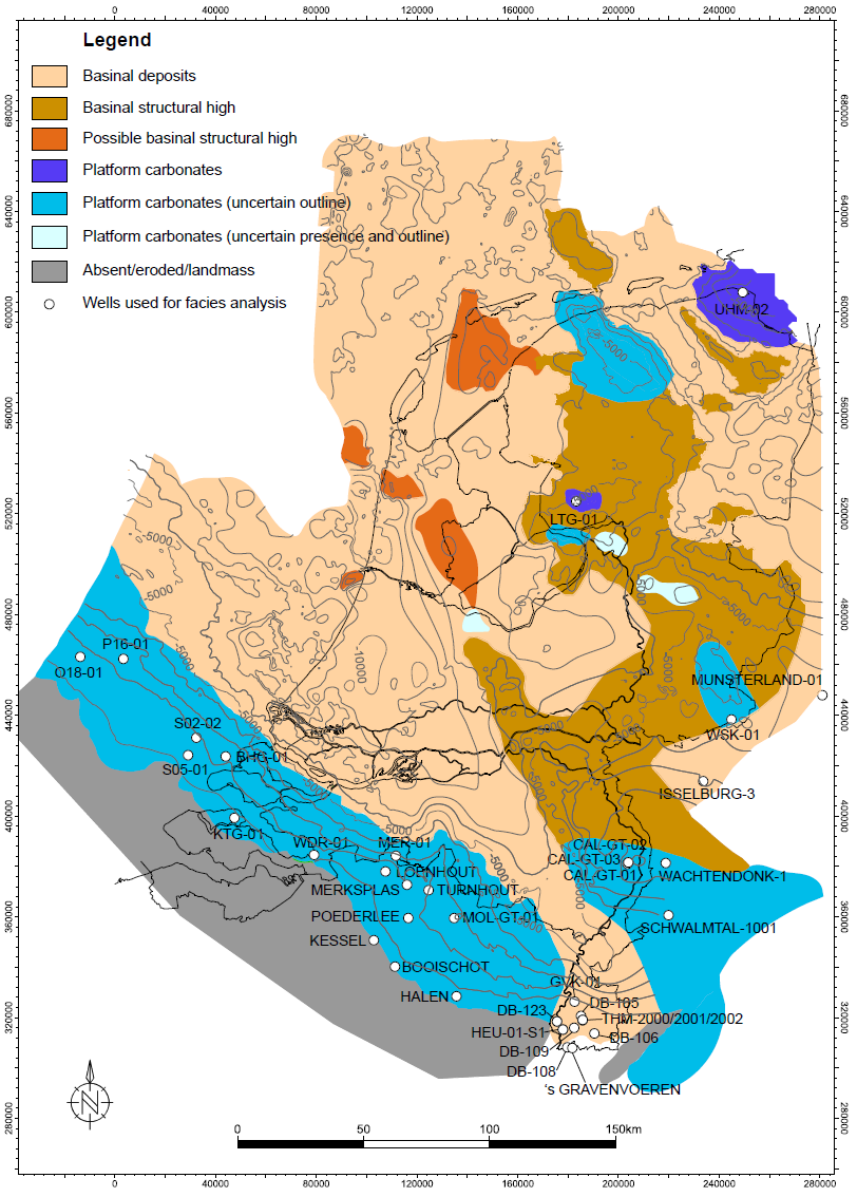

Figure 54: Facies distribution of the Dinantian sequence 2 and 3 combined (Moliniacian-Livian and Warnantian substages) overlain on the top of the Dinantian represented in contours. See legend for explanation of colours. Facies classes correspond to those described in Mozafari et al. (2019).

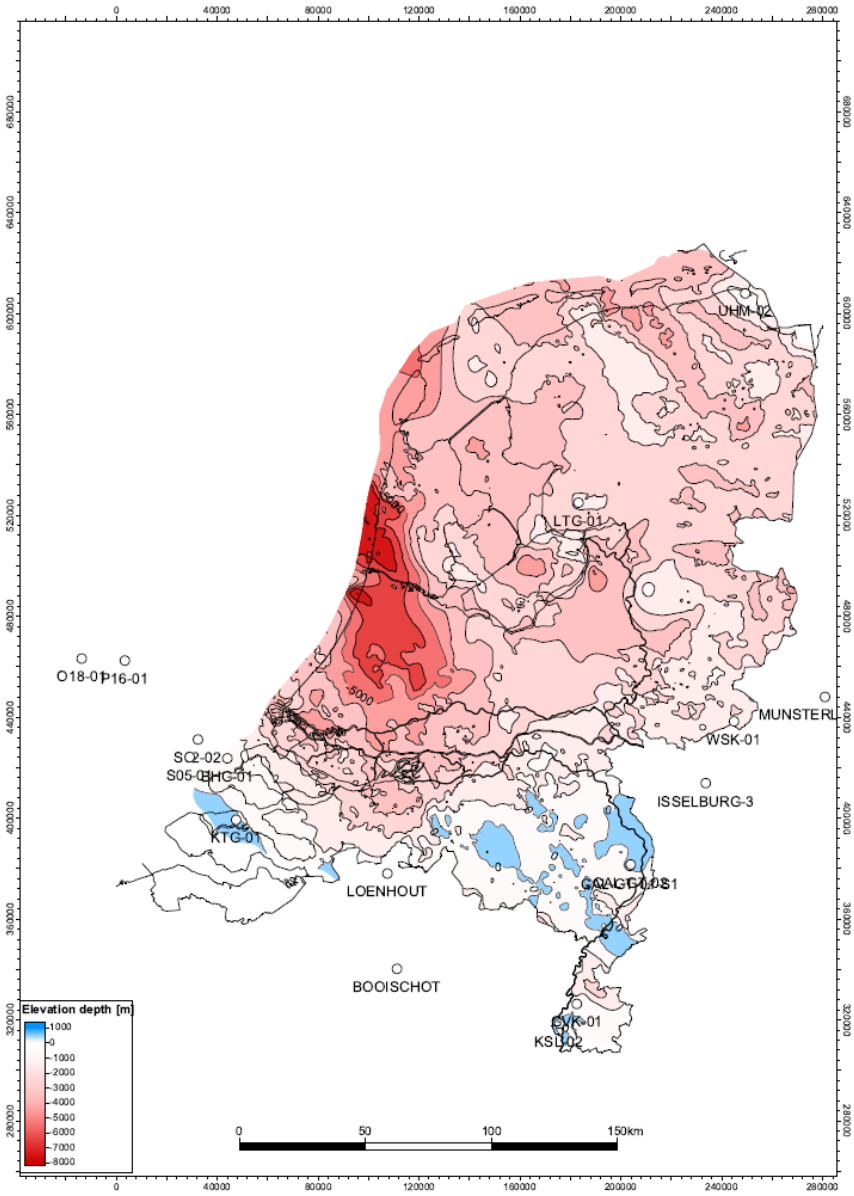

Figure 55: Difference between the previously constructed map of the top Dinantian carbonate level (TNO, 2014) and the results of the current interpretation and depth conversion. Red colours indicate areas where the new SCAN map is deeper than the pre-SCAN TNO version.

platform structures, which are not only inferred from seismic interpretation but locally also proven by the presence of slope carbonates (e.g. in WSK-01), several previously unknown mound-like structures appear from the top Dinantian interpretation. These gentle mounds appear in a strip from Nagele to the Schagen area but are also suggested to occur on the Maasbommel High.

Further improvement of the seismic interpretation of the Dinantian interval is only feasible after seismic data improvement (reprocessing and harmonization) but would also greatly benefit from the (to be) acquired long and deep 2D regional lines. This holds especially for the central part of the Netherland.

7. Recommendations for future work

7.1 Data Improvements for more efficient seismic workflows and play de-risking

7.1.1 Add contextual offshore and cross border data and interpretations

The poor data quality for deep interpretation and sparse data (wells and seismic) onshore in the Central and Southwestern Netherlands, require interpretations here to be corroborated via offshore data and interpretations. These should be (more) consistently loaded in the second phase UDG Petrel project.
For the same reason, also cross boundary -Germany, Belgium, Southern UK- information would be very useful to arrive at consistent map realizations. For those 'contextual' border regions of the study regional surfaces, seismic, wells and magnetic and gravity data should be made available.

7.1.2 Merge long regional line segments outside of Petrel

Almost all the long regional lines in the UDG Petrel project have been loaded in -many-segments. Post stack merge by a processing unit would greatly enhance interpretation efficiency in Petrel, which is poor in handling composite lines. For instance, memory leakage resulting in very low CPU/GPU performance, functionality failure with 2D conversion fails- and instability occurs often when dealing with multiple composite lines.

7.1.3 Create uniform dynamic scaling for all seismic in database

The seismic in the UDG Petrel project (and hence in the TNO EBN data base) suffers from inconsistencies in dynamic scaling between and -worse- even within surveys. Dynamic ranges vary with 6 orders of magnitude or more. A uniform scaling of all seismic will be extremely beneficial for the efficiency of the seismic interpretation workflow in Petrel. Once established, it would be no longer required to load seismic at 32-bit resolution but can be loaded at 8-bit. This would dramatically speed up performance of Petrel in large regional projects like SCAN-Dinantian.

7.1.4 Unravel the 'year group' NAM 2D surveys

The NAM surveys that are clustered in year groups, should be separated into acquisition survey vintages. This would greatly enhance efficiency and effectiveness of filter parameter and dynamic colour scale setting and will make quality control in general more straightforward.

7.1.5 Reprocess Central NL 2D seismic below present trace depth

In all of the synclinal axis of the West and Central Netherlands, the Dinantian sits at 4 seconds or deeper. When energy content, source strength and spread length allows so, migrated 2D vertical coverage should be extended to at least 5 seconds TWT.

7.1.6 Acquire accurate seismic tie lines at key wells

Almost all Dinantian Wells outside of the Groningen Friesland 3D cover, have inadequate seismic cover. To understand complex seismic response and de-risk future Geothermal drilling, it is essential to create better well ties for WSK, CAL, S05, S02, KTG, BHG, RSB with appropriately oriented and quality seismic.

7.2 Seismic Interpretation follow up

7.2.1 Extend depth and buy entire Rijnmond/Botlek 3D reprocessing

The Rijnmond and Botlek 3D surveys reprocessing should be extended to the maximum possible recording/processing TWT (7-8 seconds). This is of paramount importance to map the deep Dinantian from the Maasvlakte and allow a correlation with nearby wells in Zeeland (on- and offshore) and via the Biesbosch area north-eastward towards the Central Netherlands High (Maasbommel High). This would provide an essential complement to the ongoing 2D acquisition effort.

Ongoing reprocessing of the onshore West Netherlands Basin 3Ds ('Rijnmond' and 'Botlek') has resulted in dramatic image improvements compared to previous processing versions. Unfortunately, this data did not come available within the timeframe of this work. Note that also this reprocessed version is cropped at 5 seconds TWT, which isn't deep enough for the new Dinantian interpretation. A visual check revealed good quality coherent energy to be present below that 5 seconds cut off which warrants further reprocessing to extend the migrated vertical coverage to -at least- 7 seconds TWT.

7.2.2 Follow up with detailed Palaeozoic clastics horizon mapping

The workflow of interpretation on filtered 2D seismic lines and the resulting Dinantian interpretation should be extended to check the existing TNO 'top Namurian' map for consistency. This should be done in conjunction with well ties focused on the Palaeozoic clastics.

It may well be possible (as has been demonstrated herein for the northern part of the Netherlands) to locally interpret a number of other Namurian and Westphalian markers that would shed light on post Dinantian burial and exposure (karst!) of the Deeper Dinantian (and Devonian) carbonates.

7.2.3 Use of high-end interpretation tools: PaleoScan

Where reprocessing or acquisition seismic quality allows, an interpretation tool like PaleoScan would greatly add to the interpretation. Its relative age cube is valuable in unravelling basin subsidence in great detail, particularly for the Namurian-Westphalian sequence where this is at present poorly understood. Another use of the PaleoScan relative age cube would be to understand internal geometry of the Dinantian carbonate sequence.

8. References

Bouroullec, R., Nelskamp, S., Kloppenburg, A., Abdul Fattah, R., Foeken, J.P.T., ten Veen, J.H., Geel, C.R., Debacker, T., Smit, J. (2019) Burial and Structural Analysis of the Dinantian Carbonates in the Dutch Subsurface (SCAN). Report downloadable from www.nlog.nl/scan

Boxem, T.A.P., Veldkamp J.G. & van Wees J.D.A.M. (2016) Ultra-diepe geothermie: Overzicht, inzicht & to-do ondergrond, TNO 2016 R10803.

Brown, A. R. (2011). Interpretation of three-dimensional seismic data. Society of Exploration Geophysicists and American Association of Petroleum Geologists.

Hoornveld, N. (2013) Dinantian carbonate development and related prospectivity of the onshore. Master thesis, Vrije Universiteit Amsterdam (the Netherlands),142 pp.

Jaarsma, B., Brolsma, M.J., Hoetz, G. & Lutgert, J.E. (2013) Exploring Dinantian Carbonates in the SNS-New Data Offering New Insights, 75th EAGE Conference & Exhibition incorporating SPE EUROPEC 2013. EAGE, London.

Jaglan, H. (2017) Modelling Seismic Character of Dinantian Carbonates in the Dutch Subsurface dGB 2017: Final_Report_Presentation. Report presentation for EBN. Downloadable from www.nlog.nl/scan.

Klimchouk, A., Palmer, A., De Waele, J., Auler, A., Audra, Ph. (2017) Hypogene Karst Regions and Caves of the World. 10.1007/978-3-319-53348-3.

Kombrink, H., Doornenbal, J.C., Duin, E.J.T., Den Dulk, M., Van Gessel, S.F., Ten Veen, J.H., Witmans, N. (2012) The geological structure of the Netherlands Continental Shelf; results of a detailed mapping project. Neth. J. Geosci. 91 (4), 403-418.

Mozafari, M., Gutteridge, P., Riva, A., Geel, C. R., Garland, J., and Dewit, J. (2019) Facies analysis and diagenetic evolution of the Dinantian carbonates in the Dutch subsurface (SCAN). Report downloadable from www.nlog.nl/scan

Panterra (2012) Winterton Area Dinantian Prospectivity Review: Technical Summary and Concepts for Reservoir Models. Project G977. Report for EBN.

Reijmer, J., ten Veen, J.H., Jaarsma, B., and Boots., R. (2017) Seismic stratigraphy of the Dinantian carbonates in the Southern Netherlands. , Netherlands Journal of Geosciences, 96(4), 353-370.

Van Dalfsen, W., Mijnlieff, H.A. & Simmelink, E., (2005) Interval velocities of a Triassic claystone: key to burial history and velocity modeling. Poster 178 at EAGE 2005 Annual Meeting

9. Appendices

1. Depth Top Dinantian carbonates map
2. Depth Base Dinantian carbonates map
3. Thickness Dinantian carbonates map
4. Warnantian (Visean 2, Sequence 3) paleogeography with Dinantian thickness
5. Seismic Data Coverage
6. Listing of used 2D seismic data
7. Data density vs. interpretation density Top Dinantian carbonates map
8. Data density vs. interpretation density Base Dinantian carbonates map
9. Difference top Dinantian TNO (2014) and SCAN (2019)

9.1 Depth Top Dinantian carbonates map

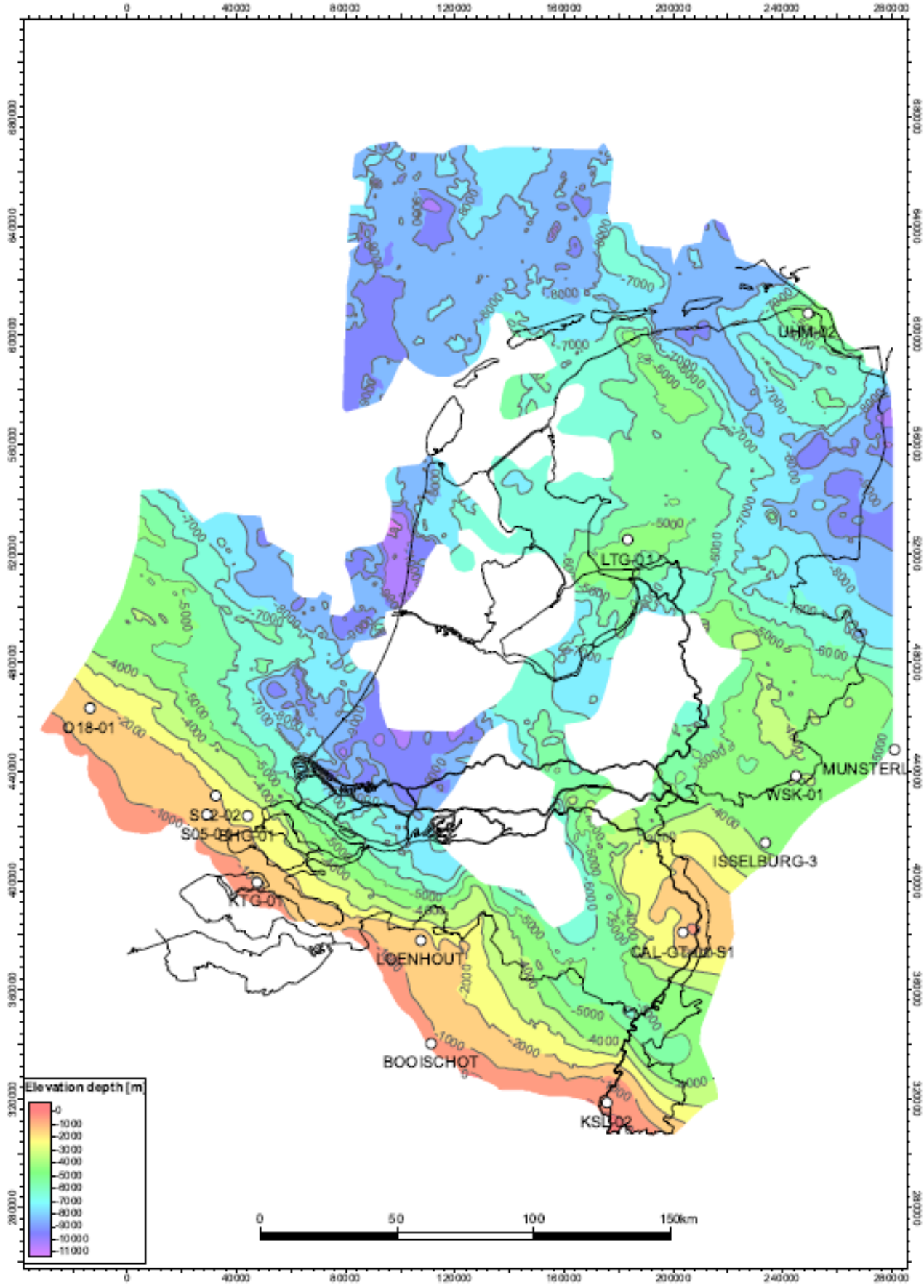

9.2 Depth Base Dinantian carbonates map

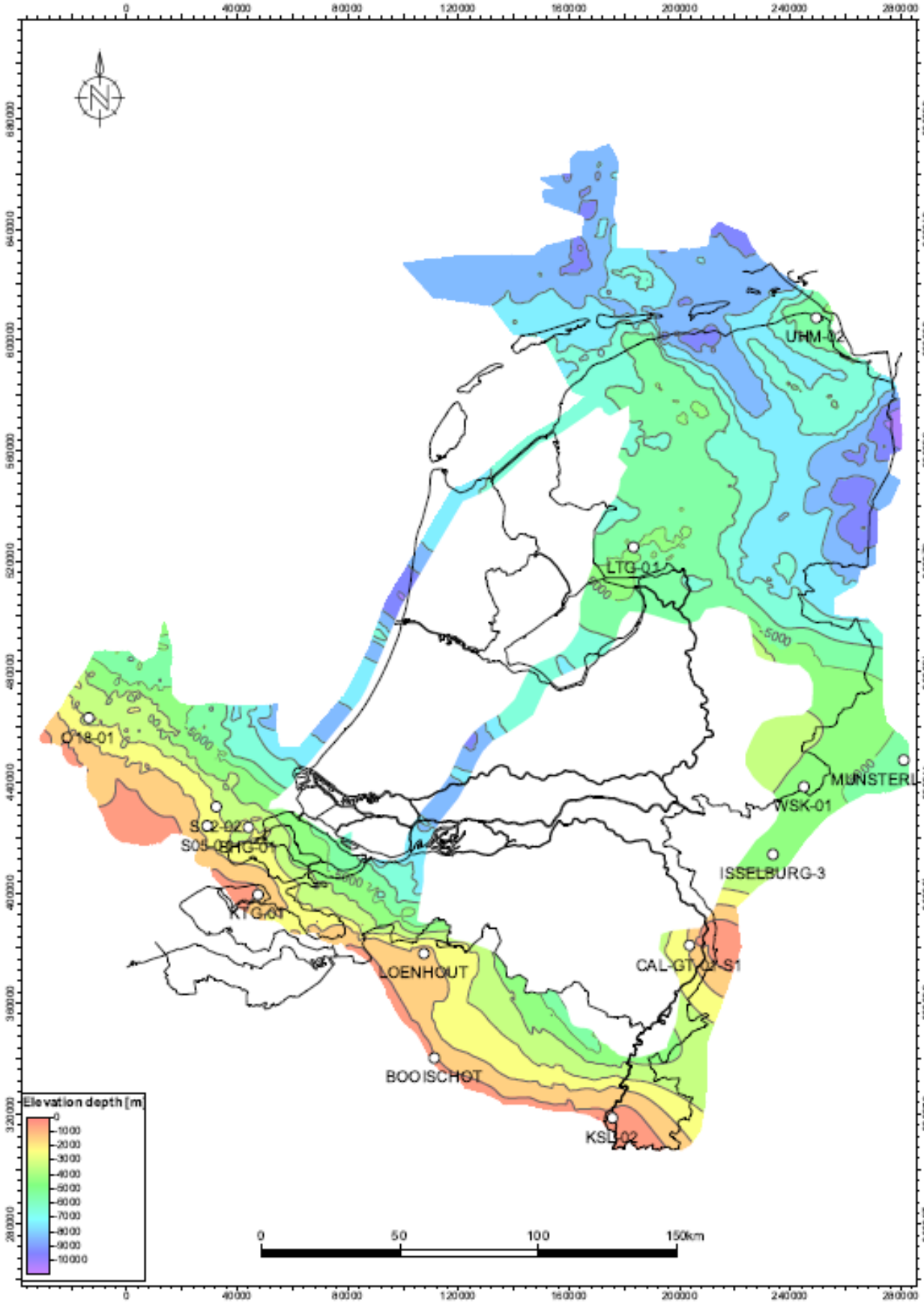

9.3 Thickness Dinantian carbonates map

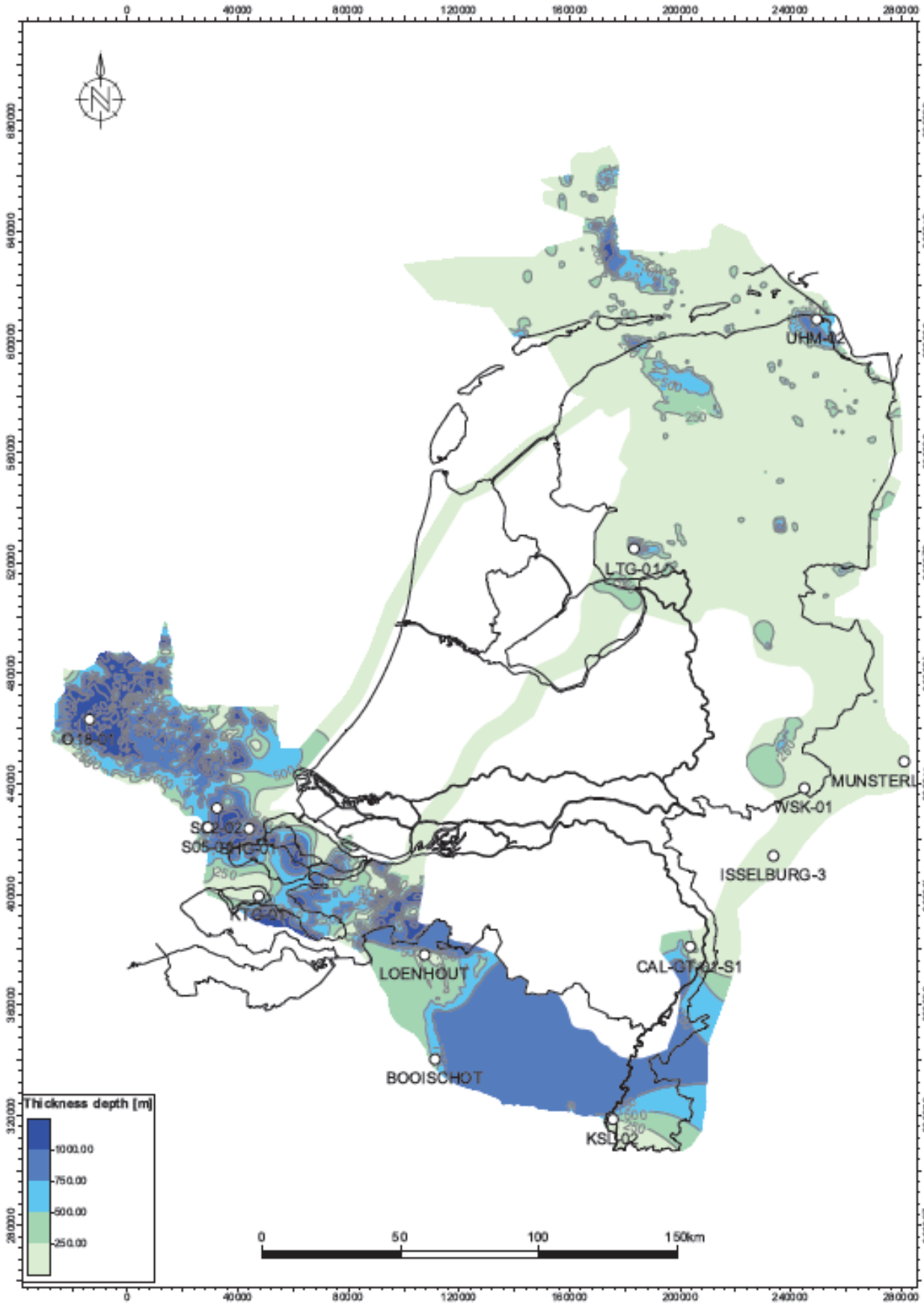

9.4 Livian- Moliniacian and Warnantian (Seq. 2 and 3) paleogeography on top Dinantian

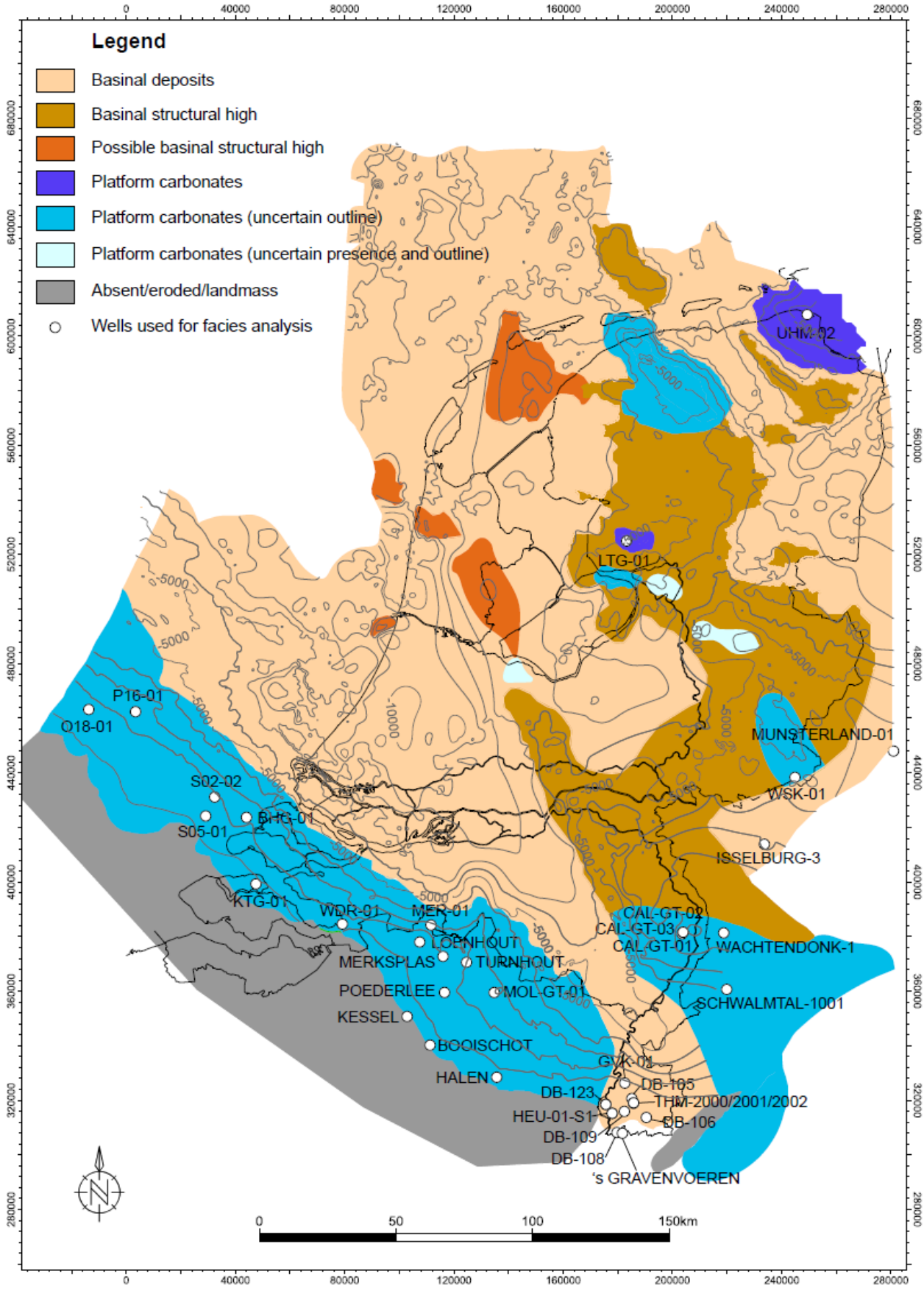

9.5 Seismic Data Coverage map

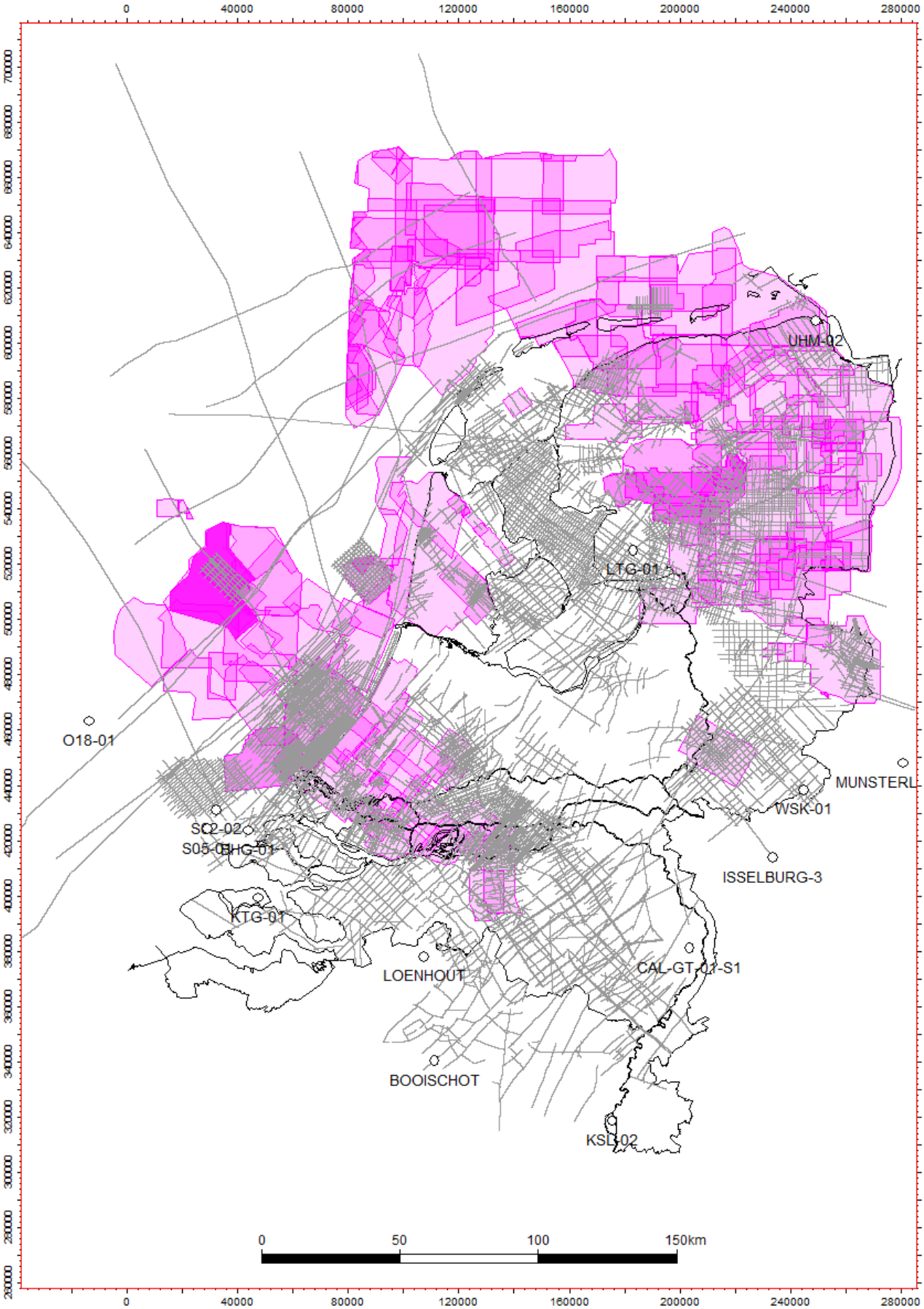

9.6 Listing of 2D Seismic Data

Naam survey	Aantal lijnen	Type	Onshore/Offshore	Locatie	Diepte [ms]
L2DGP1986A	6	.sgy	Onshore	2D_Seismiek	6000
L2DGP1986B	10	.sgy	Onshore	2D_Seismiek	4000/6000
L2DGP1988B	2	.sgy	Onshore	2D_Seismiek	6000
L2DGP1986C	11	.sgy	Onshore	2D_Seismiek	3250
Deep_NAM_1984N	1	.sgy	Onshore	2D_Seismiek	8000
L2NAM1984H			Onshore	2D_Seismiek	
Z2RGD1991A	2	.sgy	Offshore	2D_Seismiek	16000
L2AMC1980A	7	.sgy	Onshore	Carboon	4000
L2AMC1983A	13	.sgy	Onshore	Carboon	4000
L2CHE1982A	5	.sgy	Onshore	Carboon	3000
L2NAM1976C	1	.sgy	Onshore	Carboon	4000
L2NAM1979T	3	.sgy	Onshore	Carboon	3000
L2NAM1980C	8	.sgy	Onshore	Carboon	4000
L2NAM1981G	3	.sgy	Onshore	Carboon	5000
L2NAM1988B	8	.sgy	Onshore	Carboon	5000
L2NAM1989B	2	.sgy	Onshore	Carboon	5000
L2NAM1989C	11	.sgy	Onshore	Carboon	5000
L2NAM1994A	2	.sgy	Onshore	Carboon	5000
L2PET1975	40	.sgy	Onshore	Carboon	4000/5000
L2PET1976A	2	.sgy	Onshore	Carboon	4000
L2PET1988B	8	.sgy	Onshore	Carboon	4000
L2NAM1979H	3	.sgy	Onshore	NAM_2D_Offshore	4000
L2NAM1979N	18	.sgy	Onshore	NAM_2D_Offshore	4000
L2NAM1987J	31	.sgy	Onshore	NAM_2D_Offshore	4000
L2NAM1987M	15	.sgy	Onshore	NAM_2D_Offshore	4000
71	1	.sgy	Offshore	NAM_2D_Offshore	4000
83		.sgy	Offshore	NAM_2D_Offshore	4000/5000
85		.sgy	Offshore	NAM_2D_Offshore	4000
83A		.sgy	Offshore	NAM_2D_Offshore	4000
85H		.sgy	Offshore	NAM_2D_Offshore	4000
ANE79		.sgy	Offshore	NAM_2D_Offshore	4000
AO		.sgy	Offshore	NAM_2D_Offshore	4000
LN		.sgy	Offshore	NAM_2D_Offshore	3500
NNS		.sgy	Offshore	NAM_2D_Offshore	4000
NSW		.sgy	Offshore	NAM_2D_Offshore	4000
SNST83		.sgy	Offshore	NAM_2D_Offshore	4000/6000

UNSNS		.sgy	Offshore	NAM_2D_Offshore	4000
XL		.sgy	Offshore	NAM_2D_Offshore	3500
84		.sgy	Onshore	NAM_2D_Onshore	4000/8000
BPE1981A_Corrected		.sgy	Onshore	NAM_2D_Onshore	4000
L2NAM1965E		.sgy	Onshore	NAM_2D_Onshore	3000/4000/4500
L2NAM1969F		.sgy	Onshore	NAM_2D_Onshore	4000
L2NAM1971A		.sgy	Onshore	NAM_2D_Onshore	4000
L2NAM1976D		.sgy	Onshore	NAM_2D_Onshore	4000
L2NAM1987A		.sgy	Onshore	NAM_2D_Onshore	4000
L2NAM1987J		.sgy	Onshore	NAM_2D_Onshore	4000
L2NAM1989A	5	.sgy	Onshore	NAM_2D_Onshore	5000
NAM70		.sgy	Onshore	NAM_2D_Onshore	4000
NAM71		.sgy	Onshore	NAM_2D_Onshore	4000
NAM72		.sgy	Onshore	NAM_2D_Onshore	4000
NAM73		.sgy	Onshore	NAM_2D_Onshore	4000
NAM82		.sgy	Onshore	NAM_2D_Onshore	4000/8000/10000
NAM86H		.sgy	Onshore	NAM_2D_Onshore	4000
NAM85F	42	.sgy	Onshore	NAM_2D_Onshore	5000
NAM85	122	.sgy	Onshore	NAM_2D_Onshore	3000/4000/5000
L2NAM1989F	19	.sgy	Onshore	NAM_2D_Onshore	5000
L2PET1987A		.sgy	Onshore		4000
L2MOB1987A		.sgy	Onshore		4000/5000
L2PET1985G		.sgy	Onshore		4000
L2RGD1982A		.sgy	Onshore		2000
L2RGD1983D		.sgy	Onshore		2000
L2BPE1981A		.sgy	Onshore		4000
L2BPE1982A		.sgy	Onshore		4000
L2BPE1984A		.sgy	Onshore		4000
L2BPE1987A		.sgy	Onshore		4000
L2BPE1989A		.sgy	Onshore		5000
L2CHE1980A		.sgy	Onshore		4000
L2CLY1990A		.sgy	Onshore		5000
L2PET1984B	12	.sgy	Onshore		4000
L2PET1983D	7	.sgy	Onshore		4500
L2PET1989B	13	.sgy	Onshore		4000
L2PET1976B		.sgy	Onshore		4000
82-survey	4	.sgy	Onshore		2000
L2PET1992A	22	.sgy	Onshore		4000
L2PET1972A	24	.sgy	Onshore		4000
L2PET1984C	8	.sgy	Onshore		4000

9.7 Data density vs. interpretation coverage top Dinantian carbonates

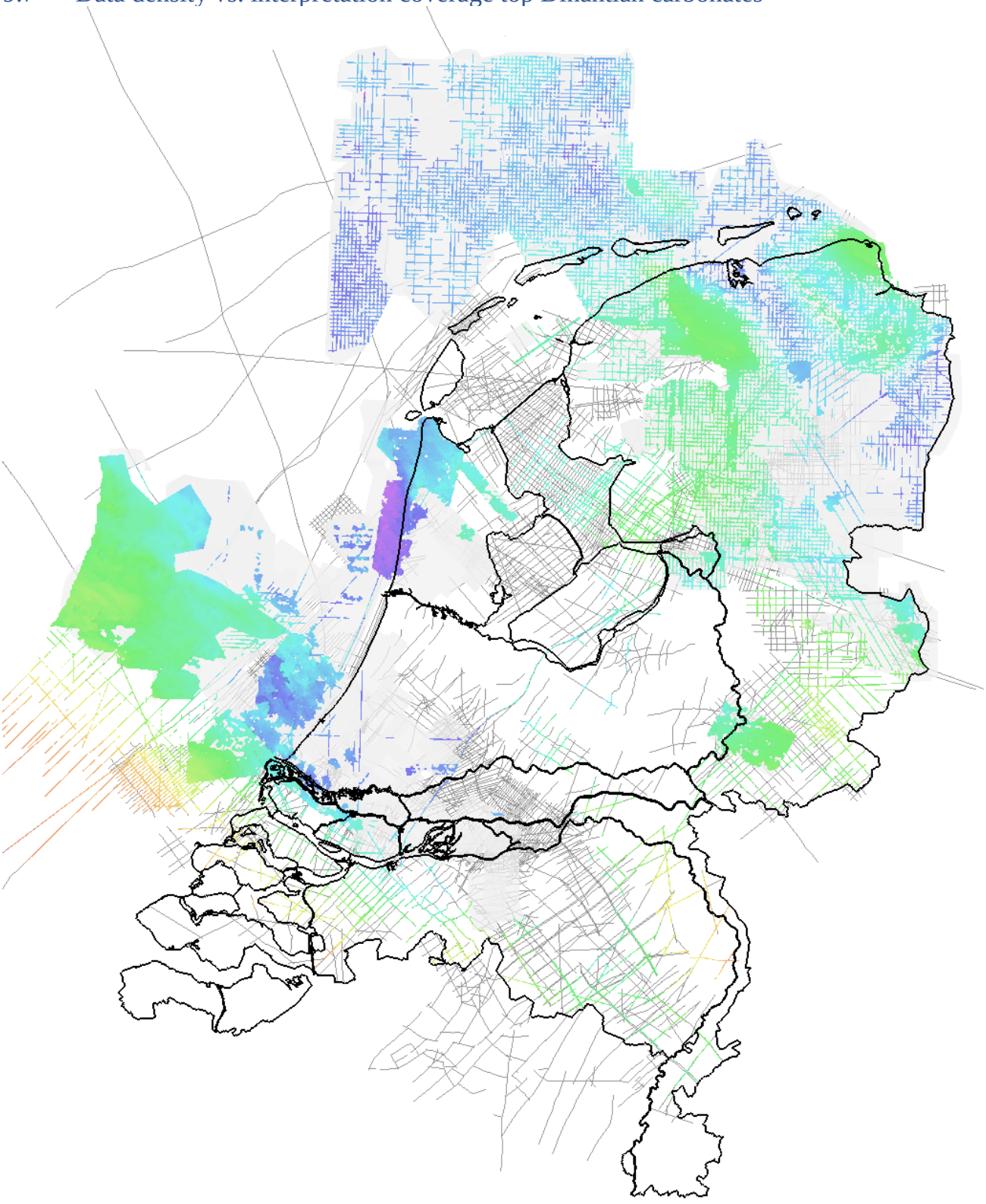

9.8 Data density vs. interpretation coverage Base Dinantian carbonates

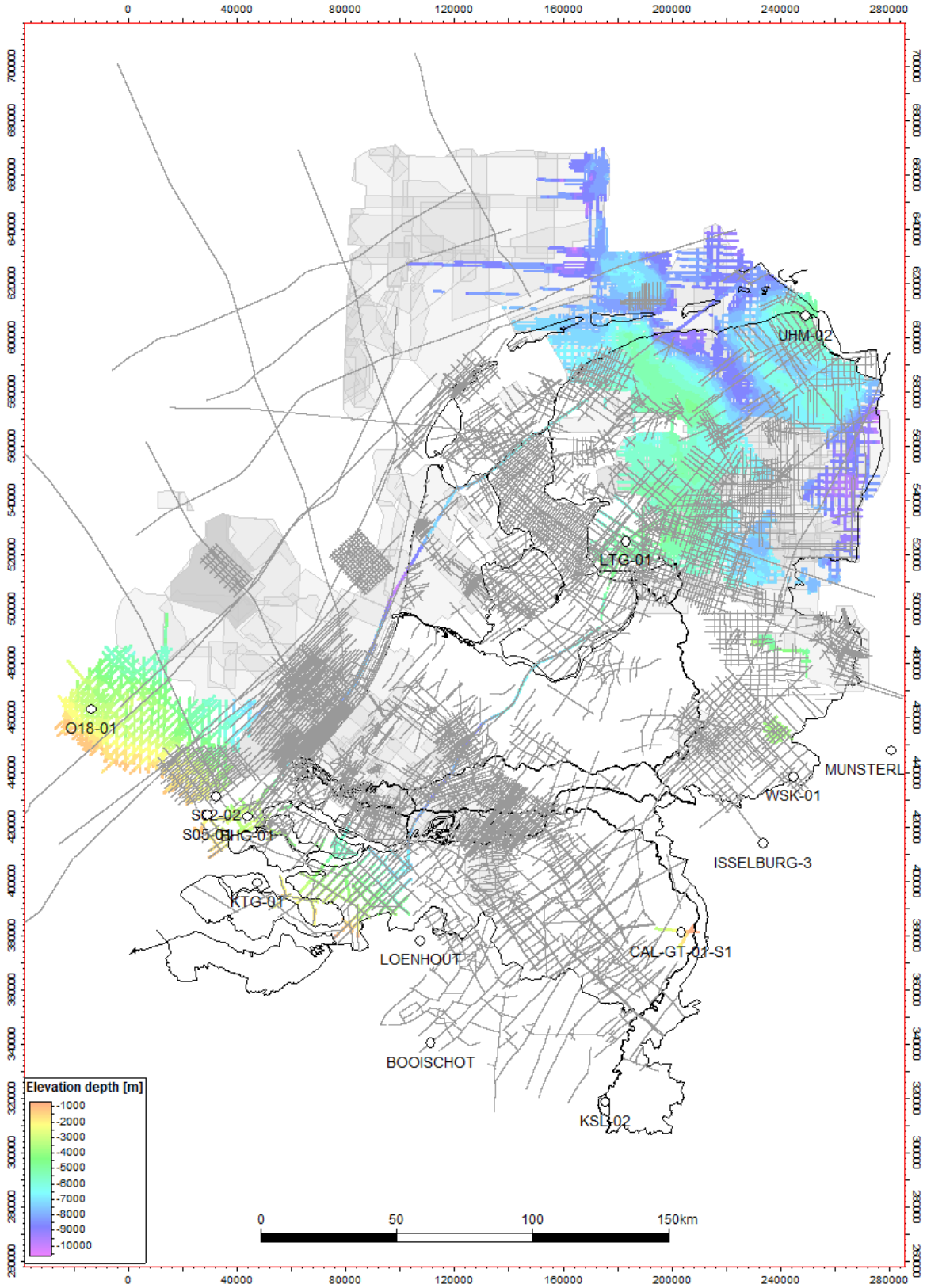

9.9 Difference top Dinantian TNO (2014) and SCAN (2019)

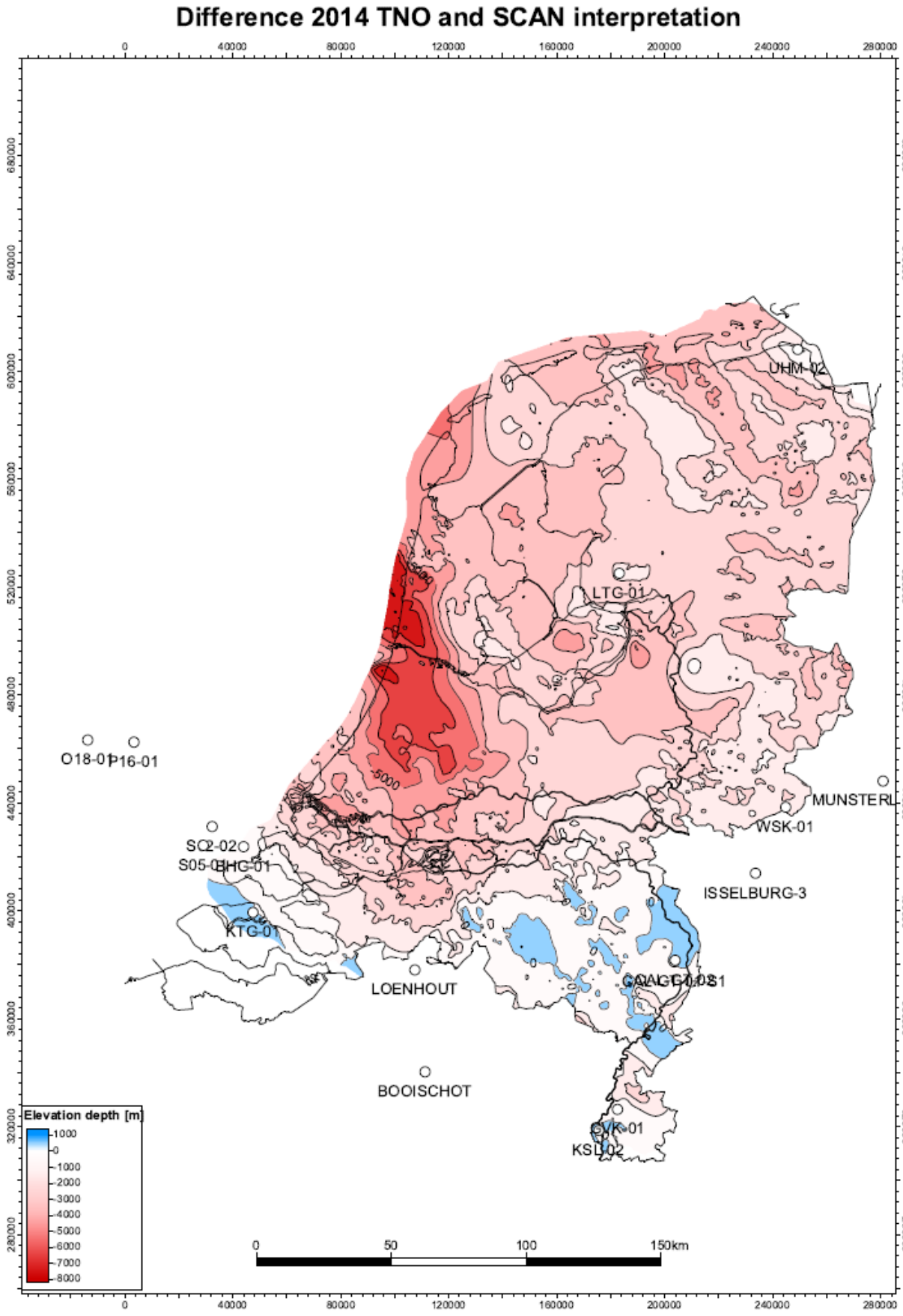

Daalsesingel 1
3511 SV Utrecht
scan@ebn.nl
www.scanaardwarmte.nl

Onderzoek in de ondergrond voor aardwarmte